Assessment of left ventricular volume and regional dysfunction based on 3D endocardial surfaces reconstructed from 2D ultrasound images of the heart

by

Jørgen Mæhle

A thesis submitted to the degree of Dr. Ing.

Report 96-26-W

Department of Engineering Cybernetics

and

Department Physiology and Biomedical Engineering

The Norwegian University of Science and Technology

Trondheim, June 1996

Summary

The aim of this work was to develop methods for quantitative analysis of heart function, based on three-dimensional reconstruction of the left ventricular endocardial surface from two-dimensional ultrasound images. In particular, the thesis addresses noninvasive determination of left ventricular cavity volumes, and quantitation and localization of regions with abnormal function due to coronary artery disease.

An algorithm for reconstruction of the endocardial surface from borders in apical echocardiographic views was developed. Different views were obtained by apical rotation of the imaging plane, and the borders were aligned by rotation angles and ventricular landmarks, whereas the endocardium was reconstructed by cubic spline interpolation, and subsequently represented in a finite number of points for further calculations and for display of three-dimensional dynamic geometry.

Determination of volume was evaluated in phantoms and in patient studies. Indices of global left ventricular function based on volumes and endocardial surface areas were developed and evaluated. Regional function was quantified and displayed in bull's eye maps by wall motion analysis comparing end-diastolic and end-systolic endocardial surfaces. Six different reference systems for regional wall motion calculation were studied in patients with recent myocardial infarction and control subjects. Finally, a study of how the accuracy of the algorithm depends on the number of imaging views used for reconstruction, was performed. The accuracy in volume, endocardial surface area and regional wall motion was assessed.

The results indicate that using 4 two-dimensional imaging views for reconstruction will give accurate determination of left ventricular volumes, surface areas and regional wall motion. Furthermore, using only 3 standard imaging views provided improved accuracy in volumes compared with conventional echocardiographic methods and identification of abnormal wall motion after myocardial infarction.

The present methodology is time-effective and can supplement routine echocardiography with display of 3D ventricular shape and quantitative indices of left ventricular function.

Acknowledgements

The present work has been carried out at the Department of Physiology and Biomedical Engineering over two active periods, from 1988 to 1992 and from 1994 to 1996. From 1988 to 1992 I was engaged by Sintef Unimed. Since 1992, and during completion of the present thesis, I have been employed by the School of Engineering and Food Science at the Sør-Trøndelag College.

I am indebted to many persons who have contributed in different ways through the work. In particular I will mention:

Professor Bjørn Angelsen, at the Dept. of Physiology and Biomedical Engineering, who has been my supervisor through the project. His great knowledge in the field has been a great source of inspiration, and his ideas and suggestions have been crucial for the progress of the present work.

Associate professor Hans Torp, at the Dept. of Physiology and Biomedical Engineering, who has continuously showed interest and contributed with ideas and solutions to problems through all parts of the project.

Svend Aakhus, MD, and Knut Bjørnstad, MD, at Section of Cardiology at the University hospital in Trondheim, who have been close collaborators through the present project. Besides nice social relations, this companionship has provided necessary insight in physiological problems and practice, important ideas and invaluable assistance with the text in the present thesis.

David Linker, MD, who contributed with fundamental ideas and fruitful suggestions in the initial phase of the project.

Wolfgang Fehske, MD, who has contributed with suggestions and inspiring discussions.

Olaf Normann , at Sintef Unimed , and Karl Arild Berg at Vingmed Sound A/S , who have been cooperating in programming and computer implementations.

Erik Kindseth, who has offered professional assistance in graphical layout. Furthermore, he and his colleagues at Audiovisual Dept., have provided relaxing conversations through lunchbreaks etc.

Olav Hole and Gerd Nybraaten, former and present leaders of Dept. of Food Technology at the Sør-Trøndelag College, who have given the opportunity and have encouraged me to complete the present thesis.

My colleagues during my years at Dept. of Physiology and Biomedical Engineering are thanked for a nice and interesting time. This work has also involved inspiring cooperation and discussions with many members of the staff of Vingmed Sound A/S.

The work of this thesis has been financially supported by grants from The Norwegian Research Council, Vingmed Sound A/S and the Sør-Trøndelag College.

CONTENTS

Papers:

A. Mæhle J, Bjørnstad K, Aakhus S, Torp HG, Angelsen BAJ:
Three-Dimensional Echocardiography for Quantitative Left Ventricular Wall Motion Analysis: A Method for Reconstruction of Endocardial Surface and Evaluation of Regional Dysfunction. Echocardiography 1994;11:397-408.

B. Aakhus S, Mæhle J, Bjørnstad K:
A New Method for Echocardiographic Computerized Three-Dimensional Reconstruction of Left Ventricular Endocardial Surface: In Vitro Accuracy and Clinical Repeatability of Volumes. J Am Soc Echocardiogr 1994;7:571-581.

C. Reconstruction and Analysis of Left Ventricular Surfaces by Three-Dimensional Echocardiography. I. Quantitation of the Endocardial Surface Area

D. Reconstruction and Analysis of Left Ventricular Surfaces by Three-Dimensional Echocardiography. II. New Indices for Global and Regional Systolic Function in Patients with Myocardial Infarction

E. Bjørnstad K, Mæhle J, Aakhus S, Torp HG, Hatle LK, Angelsen BAJ:
Evaluation of Reference Systems for Describing Regional Wall Motion From Three-Dimensional Endocardial Surface Reconstruction. An Echocardiographic Study in Subjects with and without Myocardial Infarction. (submitted)

F. Left Ventricular Dimensions and Shape by Three-dimensional Echocardiography: How Many Apical Imaging Views Should be Used for Reconstruction of Endocardial Short Axis Borders by Cubic Spline Interpolation ?

Introduction

1. Background - clinical

Imaging of human organs in vivo has developed through the last century and become important diagnostic tools in modern medicine. In cardiology, ultrasound imaging has been established during the last decades to become standard methodology for evaluation of cardiac chambers, valves and blood flow in everyday clinical practice. Today, ultrasound technology provides significant contributions to diagnosis in coronary artery disease, valve dysfunction and congenital heart disease. Compared to other imaging methods, e.g. contrast X-ray and MRI, ultrasound imaging is time and cost-effective. Furthermore, transthoracic ultrasound imaging is a noninvasive method, that can be applied safely in acute phases of cardiac diseases.

Real-time two-dimensional (2D) ultrasound imaging displays the dynamic geometry of the beating heart, and cardiac dimensions are illustrated. However, noninvasive determination of cardiac dimensions and indices are desired for accurate description of heart function. This need for objective information has been urged by the development of new medical and surgical procedures in cardiology, and is reflected in the high prevalence of coronary artery diseases in the modern society.

Coronary artery disease is a major cause of morbidity and mortality in Western societies. Acute coronary occlusion gives rise to myocardial infarction, with subsequent risk of sudden death or chronic myocardial dysfunction from tissue necrosis. Coronary X-ray angiography with contrast ejection provides visualization of the occluded artery, whereas ultrasound imaging is used to assess the functional status of the myocardium. The residual left ventricular contractile function is an important determinant for post-infarction prognosis. End-diastolic volumes, ejection fraction and the extent and location of regional myocardial dysfunction are important prognostic parameters in the follow-up of such patients. These parameters can be qualitatively assessed by 2D echocardiography, but quantitation is strongly desired for prognostic stratification after myocardial infarction in serial studies, and for evaluation of the benefit of invasive procedures for revascularization of myocardial tissue. Furthermore, by increasing the capacity for accurate quantitation of physiological parameters, novinvasive

echocardiography has the potential of substituting and excluding patients from expensive and potentially harmful invasive procedures.

The present thesis concentrates on the use of 2D ultrasound imaging of the left ventricle (LV) for quantitative analysis of the 3D ventricular geometry for diagnosis in coronary artery disease.

2. Background - echocardiography

Echocardiography comprises different diagnostic methods using backscattered ultrasound for imaging of tissue and blood flow in the beating heart. Standard modalities for tissue imaging are M-mode and 2D imaging based on amplitude in the reflected ultrasound wave, while Doppler techniques use the frequency shift in the reflected wave for measurement of velocity and imaging of blood flow. New trends making extensive use of computer science includes three-dimensional (3D) imaging, use of contrast agents, and tissue characterization from analysis of radio frequency ultrasound signals. Technology and clinical use of echocardiography are comprehensively covered in textbooks of Feigenbaum, Weyman and Hatle et. al. [1-3]. The physical and mathematical foundation of modern ultrasound imaging is thoroughly described in textbook of Angelsen [4].

Quantitative two-dimensional echocardiography

Diagnosis by 2D echocardiography is normally based on subjective assessment of the dynamic cardiac geometry. In the normal range of 25 - 60 frames pr. sec., the myocardium and valves are visualized in most patients in real-time or replay modes, however, still frames contain much noise and exact definition of borders is normally difficult. Two important reasons for this are the relative poor lateral resolution in ultrasound images, and edge drop-out in surfaces parallel to the ultrasound beam [4-6].

Edges representing tissue borders are, in addition to direct measurements of distances, the dominant basis for determination of quantitative indices from 2D echocardiography. Accurate and effective detection of edges is therefore a most crucial issue for the application of quantitative echocardiography. Accuracy is closely dependent upon image quality, and effectivity depends on computer environments and the availability of procedures for automatic edge detection. Recent developments in hardware and software for image enhancement seem promising in respect to delineation of edges, and the latest achievements in real-time edge

detection (DEQ, Vingmed sound) give prospects for quantitative measurements in routine 2D echocardiography in near future [7,8]. Additional accuracy can be gained by transesophageal imaging and use of contrast agents. However, these method can not be regarded as completely noninvasive, and are applied on the cost of effectivity compared to transthoracic imaging.

Determination of global ventricular dimensions.

Methods for echocardiographic determination of LV volume and mass are recommended by the The American Society of Echocardiography based on edges in one or two imaging planes [9]. Compared to cavity volumes based on endocardial borders, determination of mass is more difficult because the epicardial edges usually are less clearly defined by ultrasound imaging. Both volumes and masses can be accurately determined by these methods in normal and symmetrically shaped ventricles, however, the assumption of regular geometry (ellipsoid) used in these method does not apply to ventricles affected by e.g. severe myocardial infarction. Quantitation of the LV endocardial surface area (ESA) is of interest for the study of ventricular remodelling after myocardial infarction, and for quantitative assessment of regional dysfunction [10,11,2]. Accurate determination of ESA requires more than 2 imaging planes and a method for 3D reconstruction of the endocardial surface [12,13].

Quantitative wall motion analysis

Wall motion measurement between end-diastolic and end-systolic endocardial edges is the most common and simplest approach for quantitative assessment of regional ventricular function. Although many methods for this kind of analysis have been proposed and investigated [14-23], no standardized methodology is yet established. A most crucial question for the outcome of regional wall motion analysis seems to be if the method should include compensation for the translation and rotation of the ventricle through the cardiac cycle. The methods are classified as either using a fixed or floating reference. With a fixed reference, no correction is applied as the position of the edges are unchanged relative to a co-ordinate system defined by the ultrasound scan sector, whereas a floating reference applies realignment of the edges by landmarks geometrically defined from the edges themselves. Although unanimity does not exist for an optimal reference system, a fixed reference is recommended in general literature of echocardiography [1,2]. However, the results differ considerably and seem to depend both on which cross-sections are analyzed, and what type of disease that is examined. A floating system is recommended in patients undergoing cardiac surgery [20], and in stress echocardiography [14,24]. In short-axis views studied by Schnittger et. al. [19] a floating

system showed best results in the basal view, whereas a fixed system showed best results in the mid-ventricular short-axis view. Furthermore, if compensation by a floating reference is applied, what is the optimal method for alignment of the endocardial edges ? The most commonly applied reference for alignment is the center of area inside the edges for analyses. Whereas a fixed reference introduces error both in localization and quantitation due to translation and rotation of the ventricle, a floating reference with the alignment of area center will average the wall motion around the contour and thereby mask both reduced wall motion and potential hyperkinesia. In long-axis view both these references are recommended, but have shortcomings with different types of dysfunction [19,20,22]. The problem of underestimation of dysfunction by area center alignment can partially be avoided by using other references for alignment, e.g. in long-axis views by center of the mitral valve [14], or center of major axis [20]. Although applied in special situations, both these reference are recommended compared to the fixed reference.

In addition to problems of translation and rotation related to reference system (fixed or floating), translation of the ventricle perpendicular to the imaging plane and rotation out of the plane will cause problems as different sections of ventricle will be imaged in end-diastole and end-systole [25]. To some extent these problems can be compensated for by performing wall motion analysis on 3D reconstructed endocardial surfaces [26, A]. A 3D reconstruction can also produce new, and hopefully more robust, geometrical centroids for alignment when using floating references for wall motion analysis.

Regional dysfunction with coronary artery disease is not always revealed by analysis of end-diastolic and end-systolic frames only [1]. Improved outcome from wall motion analysis could be gained if a sequence of edges are used for calculations. Correlation analysis of systolic wall motion as described of Gillam and co-workers [21] was more sensitive than methods using only two frames, whereas analysis of phase and relaxation and contraction parameters can be applied if edges from the entire cardiac cycle are available [27]. The present work introduces and evaluates 6 different reference system for 3D wall motion analysis [A,D,E], and a framework for phase analysis applied to 3D wall motion is presented and illustrated in clinical examples [A].

Regional wall thickening.

With analysis of wall thickening, the problem of reference systems is avoided, and this method is considered to be more sensitive than wall motion analysis [1,16]. By visual

assessment of contraction abnormalities in 2D images, wall thickening is an important part of the analysis, whereas quantitative measurements are difficult because epicardial borders are needed in addition to the endocardial borders [26].

Regional curvature and wall stress analysis

Diagnosis through direct analysis of regional LV shape has been performed by curvature analysis displaying the variation in the radius of curvature along endocardial border [28,29]. These analysis have the advantages that only endocardial borders are required, and that the problems with reference systems are avoided. In comparative studies, curvature analysis has shown better ability than both quantitative wall motion and wall thickening analysis to identify regions with abnormal function due to coronary artery disease [30-32].

Regional wall stress should directly reflect the state of myocardium locally [33-35]. However, both endocardial and epicardial borders are required, and assumptions of material properties introduce a high degree of inaccuracy in the estimates.

Three- and four-dimensional echocardiography

By 2D echocardiography cross-sections of cardiac geometry are visualized. Thus, interpretation involves mental 3D reconstruction for appreciation of the real shape of the beating heart. Furthermore, accurate determination of physiological dimensions, such as LV volumes and masses, requires a spatial description of the object in 3 dimensions. The extension from 2D to 3D echocardiography is therefore an active area of research, in order to simplify the evaluation of cardiac structures by ultrasound imaging and to improve accuracy in the estimates of global and regional indices. Four-dimensional (4D) echocardiography is here an actual description, due to visualization of dynamic 3D geometry with time as the fourth dimension Although, work on 3D echocardiography was first reported in 1974 [36], no methodology has yet been accepted for clinical practice.

Several factors cause problems in performance of 3D or 4D echocardiography, whereas the speed of sound in tissue (approx. 1540 m/s) represents an absolute physical limit for acquisition of spatial and temporal data at sufficient resolution [37]. Data acquisition for 3D echocardiography, e.g. the entire LV in adults, has to comprise several cardiac cycles for reconstruction. This introduces serious error sources due to respiration, motion of the subject and beat to beat variations in the cardiac cycle.

Transthoracic access to imaging by ultrasound is limited because interfering ribs and lungs are restricting the positioning of the transducer. Acquisition of 3D data is therefore normally

performed with the transducer in a fixed position (illustrated in paper A, Fig. 1): by controlled tilting of the 2D imaging plane in a parasternal position [38-40], or by rotating the imaging plane in the apical position [41-44]. Other approaches are more or less arbitrary positioning of the imaging plane with registration of the imaging plane's positions [45-47], or linear displacement of the imaging plane using transesophageal imaging [48]. Linear displacement is advantageous because an almost equal density of spatial data is achieved, however, it can not be applied with transthoracic imaging.

For 3D reconstruction of the left ventricle, the apical rotation method offers the advantage that a complete long-axis view including ventricular landmarks, apex and mitral valve annulus, can be obtained in each imaging plane, and that rotation of the imaging plane can be performed accurately with a minimum of extra instrumentation. In addition, by transthoracic 2D echocardiography, ventricular dysfunction due to coronary artery disease is normally best visualized from the apical window [1]. A disadvantage is that the spatial resolution of 3D samples diminishes radially from the axis of rotation. However, a priori knowledge of ventricular geometry can be utilized in reconstruction procedures.

More recently, 3D and 4D echocardiography have developed in two directions: surface reconstruction based on edges from a limited number of 2D images, and volume reconstruction based on incremental motion of the imaging plane in small steps (see Fig. next page). The first approach will supply quantitative measurements and display of reconstructed surfaces, while the latter primarily is a qualitative approach with potential for visualizing details of cardiac structures as valve leaflets etc. In general, volume reconstruction demands high computer capacity for processing and storage of high resolution 3D volumetric data ("voxels"), and computerized display of voxel data is today an active area of research [49-51]. Realtime voxel-based 3D echocardiography utilizing new technology with high 2D frame-rate or dedicated transducers have been reported [52,53]. However, these modalities are limited to imaging of small volumes in relative short distance from the ultrasound crystals. To obtain volumetric data covering the beating left ventricle at sufficient spatial and temporal resolution requires great efforts in data acquisition and subsequent processing. This technology is rapidly developing, but volume representation of the LV is still not practical for use outside the research laboratory.

This thesis follows an almost opposite approach compared to full volume reconstruction, aiming at the description of ventricular surfaces at adequate accuracy for quantitation and display, as a minimal number of imaging plane should be used for the surface reconstruction.

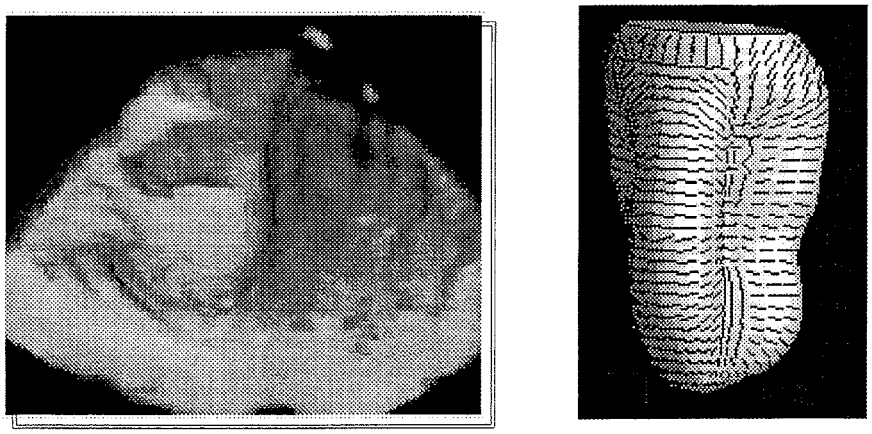

Left ventricular shape by 3D echocardiography. Left panel: volume rendering of LV voxel-data (obtained from Reidar Bjørnerheim, The National Hospital, Oslo, and Hans J Alker, Vingmed Sound A/S). Right panel: reconstructed endocardial surface displayed by shading, regional surface curvature has been estimated and the maximal curvature direction is displayed.

3. Aims of study

- To develop and implement an algorithm for 3D reconstruction of the endocardial surface using 2D ultrasound images. The algorithm should be applicable with transthoracic echocardiographic recordings, and provide rendering of 3D dynamic LV shape and quantitative indices of LV function.

- To develop and evaluate indices of global and regional LV function based on calculation of cavity volume, endocardial surface area and 3D wall motion.

- To study the potential of the algorithm when only 3 standard apical imaging views are used for reconstruction of the endocardial surface; with respect to accuracy of LV volumes, surface areas and assessment of regional wall motion.

- To evaluate different reference systems used for quantitative wall motion analysis and localization of regional dysfunction due to myocardial infarction.

- To study how the accuracy of the algorithm depends on the number of apical imaging views used for reconstruction by cubic spline interpolation. Furthermore, to give recommendations for the minimal number of apical views that should be used for determination of LV cavity volume, endocardial surface area and regional wall motion.

4. Summary of papers

Paper A: This study presents a new algorithm for reconstruction of the endocardial surface using a limited number of echocardiographic apical views. The algorithm represents a simple approach to 3D reconstruction by being applicable to 3 imaging planes from routine 2D echocardiography, and furthermore, it is flexible by using an arbitrary number (range 3-12) of imaging planes. By using long-axis endocardial borders as input data the algorithm reconstructs short-axis endocardial geometry by cubic spline interpolation. The study includes a detailed description of the algorithm, and it's potential use for evaluation of LV function is discussed and illustrated with clinical examples.

The algorithm produces a quantitative description of the endocardial surface from which the cavity volume and the endocardial surface area can be determined, and further application for LV mass calculation is presented. Different surface rendering techniques are presented, as the reconstructed endocardium is displayed simultaneously in different projections for the appreciation of dynamic LV geometry.

A main issue for this study was to propose new methodology for quantitative 3D wall motion analysis. Calculations based on end-diastolic and end-systolic endocadial surfaces and phase analysis based on the whole cardiac cycle are presented. The methods include estimation of the size of regions with abnormal wall motion, whereas location and extent of the abnormalities are displayed in bull's-eye maps. Application of quantitative 3D wall motion analysis methods in stress-echo and for assessment of myocardial infarction are discussed and illustrated.

The algorithm performs well with standard ultrasound equipment without accessory devices. By using 3 standard apical views and predefined angles for reconstruction, quantitation and display of 3D ventricular geometry are obtained with a minimum of extra time and efforts.

Paper B: The aim of this study was to assess the accuracy of the algorithm introduced in paper A, used for determination of left ventricular volumes.

In vitro accuracy was tested in phantoms (waterfilled latex balloons) with or without rotational symmetry around the midcavitary long axis using 3 and 4 imaging planes for 3D surface reconstruction. In vivo repeatability of volumes was studied in human subjects with

myocardial infarction and healthy controls using 3 standard echocardiographic apical views for reconstruction of the endocardial surface. The influence of deviation from assumed angular position (± 15 degrees) of the standard apical views (4-chamber, 2-chamber and long-axis), was studied in 2D short-axis views. These short-axis were generated by cubic spline interpolation in the same manner as within the reconstruction algorithm.

Estimated phantom volumes, obtained from 4 (3) image planes, were close to true volumes with a mean difference±SD of 0±2 (2±3) cm^3 in symmetrical and 1±3 (4±4) cm^3 in asymmetrical objects. Volume estimates obtained with conventional echocardiographic methods, single plane and biplane disk summation, were less accurate. Inter- and intra-observer repeatability of 3D left ventricular volumes was good for analysis (coefficients of variation: 3.5 to 6.2 %), and lower for recording (coefficients of variation: 7.4 to 10.9 %). Angular deviations from the assumed plane positions caused only small errors (0.3 ± 3.2 %) in short-axis areas (used for volume calculation by disk summation in the reconstruction algorithm).

In conclusion, the present algorithm reproduces volumes of symmetrical and deformed in vitro objects accurately over a wide range of size and shape, and produces repeatable left ventricular volumes in the clinical situation. Furthermore, volume estimates based on 3D reconstruction have less bias and are more repeatable than those of conventional biplane and single plane methods.

Paper C: The aim of this study was to evaluate the accuracy of the present algorithm for 3D reconstruction with respect to determination surface areas, and to study validity of endocardial surface areas (ESA) obtained from 3 standard LV long-axis apical ultrasound views. The text presents in details the mathematical description of reconstructed geometry provided by the algorithm, and methods used for surface rendering and surface area calculations are described.

Accuracy in estimation of surface area was assessed in predefined objects with rotational symmetry, by using drawings of their cross-sectional geometry for 3D reconstruction. Furthermore, the influence of selected resolution in the description of the reconstructed surfaces was studied with respect to accuracy of surface areas and volumes. Accuracy in calculations of endocardial surface area obtained from 3 standard apical views and predefined angles for reconstruction, was evaluated. The same short-axis material and similar methods as presented in

paper B were applied. Instead of cross-sectional area the accuracy in reconstructed circumference was assessed (accuracy in cross-sectional circumference will be a major determinant for the final accuracy in endocardial surface areas).

Using a resolution of 32x32 points in the reconstructed surface, the mean ± SD differences between values from 3D reconstruction and true values of symmetric objects were -0.46 ± 0.84 % for surface areas and -0.25 ±1.5 % for volumes. Increasing the resolution had minor influence on surface area estimates, whereas volumes were not affected. Angular deviations from the assumed plane positions caused only small errors (0.0 ± 1.6 %) in short-axis circumferences.

The results of this study indicate that endocardial surface areas can be determined at higher precision than volumes based on 3 apical views, and that surface area estimations are less sensitive to angular deviations from the assumed plane positions. In conclusion, this study suggests the present 3D reconstruction algorithm as a simple method for accurate quantitation of endocardial surface areas in clinical practice.

Paper D: The aim of this study was to develop new indices of systolic left ventricular function based on the quantitative description of the endocardial surfaces presented in paper C. Furthermore, their usefulness was tested for identification of global and regional dysfunction after myocardial infarction.

Left ventricular cavity volumes and endocardial surface areas from 3D reconstruction at end-diastole and end-systole were used for calculation of indices of global function. Besides volume ejection fraction, the fractional change in endocardial surface area (FCESA) was calculated, and a 3D shape index (3DSI) expressing sphericality of object was calculated based upon volume and surface area of the LV. Six different floating reference systems for 3D wall motion analysis were described. Regional wall motion was combined with area calculations for statistical parameters characterizing systolic contraction, and bull's eye maps were used for display of location and extent of dysfunction. The area representing abnormal wall motion (AWM) was estimated using a threshold value set at 50 % of mean regional wall motion. The indices were studied in 15 subjects (10 with recent MI, and 5 healthy subjects) based on 3D reconstruction from 3 apical imaging planes, and compared to visual 2D echocardiographic analysis by wall motion score index (WMSI).

Location of regional dysfunction from 3D wall motion analysis agreed well with those from

more conventional 2D visual analysis, and area of abnormal function (% AMW) from 3D computerized analysis correlated well to calculations of WMSI based on visual assessment. The global index for change in surface area, FCESA, differentiated between normals and MI patients ($p<0.0001$) and correlated well to WMSI ($r = 0.93$). Although comparable results were obtained by volume ejection fraction, the FCESA was superior in the present study. The shape index, 3DSI, did not differentiate between normal and abnormal systolic function.

Indices expressing systolic function, presented in this work, are available from noninvasive transthoracic ultrasound, and may supplement routine echocardiography with quantitative parameters describing LV dysfunction after MI.

Paper E: The aim of this study was to evaluate the clinical potential of the six reference systems presented in paper D for 3D quantitative assessment of left ventricular wall motion abnormalities. Each reference system was applied to the same patients and controls as in paper D, and the results were compared with visual wall motion analysis of 2D images. The localization of abnormal wall motion was displayed in bull´s-eye maps, and the area of abnormality was determined as a percentage of total endocardial area. For each reference system, the segmental concordance between 3D computerized and visual assessment was determined.

The best agreement between computerized and visual analysis was obtained with a reference system based on wall motion towards the major ventricular axis. Correlation between the estimated area of wall motion abnormality and visually determined wall motion score index (WMSI) was best using the aligned center of mitral valve plane as reference ($r = 0.92$). The reference system based on wall motion towards the midpoint of the major ventricular axis showed the best ability to differentiate between healthy subjects and patients with myocardial infarction. Poorest results were obtained when the center of left ventricular cavity (center of mass) was used as reference. The other references show potential, alone or in combination, for use in 3D wall motion analysis as a quantitative supplement to routine echocardiography.

Paper F: The aim of this study was to evaluate how accuracy of the algorithm described in paper A, depends on the number of apical imaging views used for reconstruction of endocardial surfaces. Accuracy in determination of LV volumes, endocardial surface area and regional wall motion was studied on the basis of reconstruction of endocardial short axis

borders by cubic spline interpolation. These short-axis borders were hence reconstructed in the same manner as those reconstructed within the 3D algorithm.

Manually drawn end-diastolic and end-systolic midventricular short axis endocardial borders from 10 subjects (with and without myocardial infarction) were analyzed. Endocardial borders were reconstructed by use of cubic spline interpolation through points (4-24) on the original borders. These points were positioned on radial lines mimicking the intersection of (2-12) apical imaging planes. Cross-sectional area and length of circumference of reconstructed and original borders were compared for assessment of accuracy in volume and endocardial surface area, respectively. Accuracy in wall motion analysis was assessed from calculations of global shape difference and maximal local distance between reconstructed and original borders.

For short axis borders the mean±SD of percent error for all indices was significantly reduced when the number of points for interpolation was increased from 4 to 6, and from 6 to 8. When 8 points were used, the 95 % confidence limits for the difference between reconstructed and original borders were -2.2 to 0.7 % for area, -2.1 to 0.1 % for circumference, and 3.4 to 8.4 % for the maximal local distance.

Applied to 3D reconstruction using cubic spline interpolation, these results indicate that regional shape analysis and calculation of dimensions can be performed accurately from 4 apical views. Detection of minor abnormalities in shape improved when the number of views increased, whereas dimensions can be determined with sufficient accuracy from 3 apical views.

5. Concluding remarks

The collection of papers in the present thesis, presents and evaluates a new algorithm for 3D reconstruction of endocardial surfaces for quantitative assessment of LV function. The algorithm has been implemented in commercial programs for processing ultrasound data (EchoLoops and EchoPac, Vingmed Sound), performing LV volume calculation and 4D display of reconstructed endocardial surfaces. Determination of volumes has been studied [B, 54-62], and results have shown considerable improvement in accuracy compared to conventional echocardiographic methods [54, B, F]. Recent studies have compared the present algorithm using 3 imaging planes with 3D voxel reconstruction from 90 rotated imaging planes, and the methods scored equally with respect to accuracy in LV volumes in vitro [56]. Furthermore, the

use of predefined angles for the 3 standard apical views seems to have minor effect on volumes [B, 55], thus, volumes can by determined accurately from routine echocardiographic examinations.

The computer programs provide a rapid and feasible method for superimposing 2D ultrasound data for compuerized display of 3D dynamic geometry. The moving endocardial surface displays size and shape of the ventricle, and reveals normal and abnormal 3D wall motion as torsion and axial rotation that can not be seen in 2D imaging [A,37, 59-62 ,63,64].

Methods for quantitation of global LV function and regional wall motion abnormalities are introduced in the present work, and clinical potential has been demonstrated for indices based upon calculation of regional wall motion and endocardial surface area [C,D,E].

Future perspectives

This thesis presents a simple and feasible method for quantitation of 3D LV geometry. The algorithm is limited to reconstruction of dominantly convex objects, thus, it is not directly applicable to the right ventricle. A modified algorithm for the left atrium has been developed and is at present time used in clinical studies.

A general data structure for description of LV geometry is presented. Thus, analysis and indices proposed in this thesis can easily be adapted to various methods of reconstruction and imaging. Several more or less sophisticated analysis can be performed based on this description. Preliminary procedures for phase analysis of wall motion and estimation and analysis of local curvature in endocardial surfaces have been developed (Fig. 10 paper A, and Fig. page 7), but have so far not been clinically tested. Improvements in ultrasound imaging and automatic edge detection give prospects of inclusion of epicardial surfaces in analysis for accurate assessment of LV masses, and furthermore, feasible methods for quantitative 3D wall thickening and regional wall stress analysis can be realized.

By using the most recent generation of desktop computers the present computer software provides 3D reconstruction, display and quantitative indices of LV function almost instantly. However, detection of edges limits both accuracy and effectivity of the present methodology. New development in real-time edge detection (DEQ, Vingmed Sound) are promising with respect to overcome these problems. Thus, quantitative echocardiography by 3D reconstruction has the potentiality of considerable clinical usefulness by providing objective measurements noninvasively at sufficient effectivity and accuracy.

6. References

Articles included in the present thesis are referred with their capital letter.

1 Feigenbaum H. Echocardiography, 5. ed. Lea & Febiger, Philadelphia, 1994.

2 Weyman AE. Principles and Practice of Echocardiography, 2. ed. Lea & Febiger, Philadelphia, 1994.

3 Hatle L, Angelsen B. Doppler ultrasound in cardiology, physical principles and clinical applications, 2. ed. Lea & Febiger, Philadelphia, 1985.

4 Angelsen B. Waves, signals and signal processing in medical ultrasound,Volume I and II, Department Physiology and Biomedical Engineering, The Norwegian University of Science and Technology, Trondheim, April 1996.

5 Roelandt J, van Dorp WB, Bom N, Laird JD, Hugenholtz PG. Resolution Problems in Echocardiography: a Source of Interpretation Errors. Am J Cardiol 1976;27:256-262.

6 Joynt L, Popp RL. The Concept of Three Dimensional Resolution in Echocardiographic Imaging. Ultrasound Med Biol 1982;8:237-247.

7 Olstad B. Automatic wall motion detection in the left ventricle using ultrasound images. Proc of SPIE/SPSE 1991;1450:243-254.

8 Olstad B. Real-time image processing based on nonlinear models with applications to image enhancement, area detection and volume visualization. Ultraschall in der Medizin 1993;14:210-213.

9 Schiller NB, Shah PM, Crawford M, et. al. Recommendations for quantitation of the left ventricle by two-dimensional echocardiography. J Am Soc Echocardiogr 1989;2:358-67.

10 Picard MH, Wilkins GT, Ray PA, Weyman AE. Natural history of left ventricular size and function after acute myocardial infarction - assessment and prediction by echocardiographic endocardial surface mapping. Circulation 1990;82:484-494.

11 Picard MH, Wilkins GT, Ray PA, Weyman AE. Progressive changes in ventricular structure and function during the year after acute myocardial infarction. Am Heart J 1992;124:24-31.

12 Guyer DE, Gibson TC, Gillam LD, et. al. A new echocardiographic model for quantifying three-dimensional endocardial surface area. J Am Coll Cardiol 1986;8:819-29.

13 King DL, Gopal AS, King Jr. DL, Shao MY. Three-dimensional echocardiography: In vitro validiation of quantitative measurement of total and"infarct" surface area. J Am Soc Echocardiogr 1993;6:69-76.

14 Ginzton LE, Conant R, Brizendine M, Thigpen T, Laks M. Quantitative analysis of segmental wall motion during maximal upright dynamic exercise: variability in normal adults. Circulation 1986;73:268-75.

15 Zoghbi WA, Charlat ML, Bolli R, Zhu W, Hartley CJ, Quinones MA. Quantitative assessment of left ventricular wall motion by two-dimensional echocardiography: validation during reversible ischemia in the conscious dog. J Am Coll Cardiol 1988;11:851-60.

16 McGillem MJ, Mancini GBJ, DeBoe SF, Buda AJ. Modification of the centerline method for assessment of echocardiographic wall thickening and motion: A comparison with area of risk. J Am Coll Cardiol 1988;11:861-866.

17 Moynihan PF, Parisi AF, Feldman CL. Quantitative detection of regional left ventricular contraction abnormalities by two-dimensional echocardiography. I. Analysis of methods. Circulation 1981;63:752-60.

18 Parisi AF, Moynihan PF, Folland ED, Feldman CL. Quantitative detection of regional left ventricular contraction abnormalities by two-dimensional echocardiography. II. Accuracy in coronary artery disease. Circulation 1981;63:761-67.

19 Schnittger I, Fitzgerald PJ, Gordon EP, Alderman EP, Popp RL. Computerized quantitative analysis of left ventricular wall motion by two-dimensional echocardiography. Circulation 1984;70:242-54.

20 Force T, Bloomfield P, O'Boyle JE, Khuri S, Josa M, Parisi A. Quantitative two-dimensional echocardiographic analysis of regional wall motion in patients with perioperative myocardial infarction. Circulation 1984;70:233-241.

21 Gillam LD, Hogan RD, Foale RA, Franklin TD, Newell JB, Guyer DE, Weyman AE. A comparison of quantitative echocardiographic methods for delineating infarct-induced abnormal wall motion. Circulation 1984;70;113-22.

22 Assmann PE, Slager CJ, van der Borden S, Sutherland GR, Roelandt JR. Reference system in echocardiographic quantitative wall motion analysis with registration of respiration. J Am Soc Echocardiogr 1991;4:224-34.

23 Assmann PE, Slager CJ, van der Borden SG, et. al. Comparison of models for quantitative left ventricular wall motion analysis from two-dimensional echocardiograms during acute moycardial infarction. Am J Cardiol 1993;71:1262-69

24 Shapiro SM, Ginzton LE. Quantitative stress echocardiography. Echocardiography 1992;9:85-96.

25 Mann DL, Gillam LD, Weyman AE. Cross-sectional echocardiographic assessment of regional left ventricular performance and myocardial perfusion. Progress in Cardiovascular Diseases 1986;XXIX:1-52.

26 Bjoernstad K, Maehle J, Aakhus S. Quantitative computerized analysis of left ventricular wall motion. In Domenicucci S, Roelandt J, Pezzano A. (Eds.), Computerized Echocardiography, Centro Scientifico Editore, Torino,1993;41-55.

27 Melchior JP, Doriot PA, Chatelain P. et al. Impovement of left ventricular contraction and relaxation synchronism after recanalization of chronic total coronary occlusion by angioplasty. J Am Coll Cardiol 1987;9:763-768.

28 Marcus E, Harzahav Y, Lorente P, et. al. Characterization of regional left-ventricular contraction by curvature difference analysis. Basic research in cardiology 1988;A:486-500.

29 Mancini GBJ, Deboe SF, Anselmo E, Simon SB, LeFree MT, Vogel RA. Quantitative regional curvature analysis: an application of shape determination for the assessment of segmental left ventricular function in man. Am Heart J 1987;113:326-334.

30 Mancini GBJ, Deboe SF, Anselmo E, LeFree MT. A comparison of traditional wall motion assessment and quantitative shape analysis: a new method for characterizing left ventricular function in humans. Am Heart J 1987;114:1183-1191.

31 Mancini GBJ, Bates ER, Deboe SF, McGillem MJ. Quantitative regional curvature analysis - a prospective evaluation of ventricular shape of ventricular shape and wall motion measurements. Am Heart J 1988;116:1616-21.

32 Takata H, Sawada H, Okabe A, et. al. Treadmill exercise echocardiography: Quantitative analysis of regional left ventricular wall motion by computer graphics.Journal of Cardiology;18: 629-637(in japanese).

33 Janz RF. Estimation of local myocardial stress. Am J Physiol 1982; 242:H875-81.

34 Lobodzinski SM,Janz RF, Ginzton LE, Gjerve K, Laks M. Computer implementation of an algorithm for the quantitative assessment of left ventricular wall stress. Computers in Cardiology 1987; 623-626.

35 Ginzton LE, Lobodzinski SM, Laks M. Identification of coronary artery obstructions by analysis of regional left ventricular function: exercise segmental wall motion vs. end-systolic regional wall stress.Computers in Cardiology 1987;1119-122.

36 Dekker DL, Piziali RL, Dong E. A system for ultrasonically imaging the human heart in three dimensions. Computers and Biomedical Research 1974;7:544-553.

37 Angelsen BAJ, Dørum S, Hoem J, et. al. Annular array TEE probe allowing 3D reconstruction of cineloops of the heart. - in Cardiovascular Imaging by Ultrasound. P. Hanrath, R. Uebis and W. Krebs eds. Kluwer academic Publishers, Dordrecht, 1993;287-296.

38 Nixon J, Saffer SI, Lipscomb K, et al: Three-dimensional echoventriculography. Am Heart J 1983;106:435.

39 Fine DG, Sapoznikov D, Mosseri M, Gotsman MS. Three-dimensional echocardiographic reconstruction: qualitative and quantitative evaluation of ventricular function. Computer Methods and Programs in Biomedicine 1988;26:33-44.

40 Zoghbi WA, Buckey JC, Massey MA, Blomqvist CG. Determination of left ventricular volumes with use of a new nongeometric echocardiographic method: vlinical validation and potential application. J Am Coll Cardiol 1990;15:610-17.

41 Eiho S, Kuwahara M, Asada N, Yamashita K. Reconstruction of 3-D images of pulsating left ventricle from two-dimensional sector scan echocardiograms of apical long axis view. Computers in Cardiology 1981;19-24.

42 Ghosh A, Nanda NC, Maurer G. Three-dimensional reconstruction of echocardiographic images using the rotation method. Ultrasound Med Biol 1982;8:655-661.

43 Fazzalari NL, Davidson JA, Mazumdar J, Mahar LJ, DeNardi E. Three dimensional reconstruction of the left ventricle from four anatomically defined apical two-dimensional echocardiographic views. Acta Cardiologica 1984;XXXIX(6):409-436.

44 McCann HA, McEwan CN, Sharp JC, Kinter TM, Greenleaf JF, Barillot C. Multidimensional ultrasonic imaging for cardiology. Proc IEEE 1988;76;1063-1073.

45 Geiser EA, Lupkiewicz SM, Christie LG,et al: Framework for Three-Dimensional Time-Varying Reconstruction of the Human Left Ventricle: Sources of Error and Estimation of Their Magnitude. Computers and Biomedical Research 1980;13: 225.

46 Moritz WE, McCabe DH, Pearlman AS, et al. Computer generatedthree dimensional ventricular imaging from a series of two-dimensional ultrasonic scans. Computers in Cardiology 1982;119.

47 Nikravesh PE, Skorton DJ, Chandran KB, Atterwala YM, Pandian N, Kerber RE. Computerized three-dimensional finite element reconstruction of the left ventricle from cross-sectional echocardiograms. Ultrasonic Imaging 1984;6:48-59.

48 Pandian NG, Nanda NC, Schwartz SL, et al: Three-dimensional and four-dimensional transoesophageal echocardiographic imaging of the heart and aorta in humans using a computed tomographic imaging probe. Echocardiography 1992:9;677.

49 Pandian NG, Roelandt J, Nanda N, et. al. Dynamic three-dimensional echocardiography: methods and clinical potential. Echocardiography 1994;11:237-59.

50 Salustri A, Roelandt J. Three dimensional reconstruction of the heart with rotational acquisition: methods and clinical applications. Br Heart J 1995;73 (Supplement 2);10-15.

51 Steen E, Olstad B. Volume rendering of 3D medical ultrasound data using direct feature mapping, IEEE Transactions on Medical Imaging 1994;13:517-525.

52 Sheikh KH, Smith SW, Ramm O. Real-time, three-dimensional echocardiography: feasibility and initial use. Echocardiography 1991; 8;119-125.

53 Torp H, Dørum S, Holm E, Steen E, Kristoffersen K, Berg KA, Alker HJ, Olstad B. Real-time three dimensional echocardiography for assessment of valvular function, Abstracts of the 11th Symposium in Echocardiology, Rotterdam, 1995;141.

54 Mele D, Pratola C, Pedini I, Alboni P, Levine RA. Validation and application in patients of a new system for three-dimensional echocardiographic reconstruction of the left ventricle. Circulation 1994;90:I-337 (abstract).

55 Mele D, Mæhle J, Pratola C, et al. Application in patient of a new simplified system for 3D-echo reconstruction of the left ventricle. J Am Soc Echocardiogr 1995;8:343 (abstract).

56 Rødevand O, Bjørnerheim R, Kjekshus J. Assessment of left ventricular volumes by three dimensional echocardiography using three different methods. Abstract accepted for the congress of the European Society of Cardiology, Birmingham, August 1996.

57 Azevedo J, Garcia-Fernandez MA, Moreno M, et. al. Dynamic three-dimensional echocardiographic reconstruction of the left ventricle, calculation of ventricular volumes and ejection fraction: an animal study of functional changes induced by experimental ischemia. Eur Heart J 1995;16:207(abstract).

58 Fehske W, Mæhle J, Olstad B, et. al. Frame-by frame threedimensional echocardiographic reconstruction of the left ventricle. J Am Coll Cardiol 1993;19:4A(abstract).

59 Iwase M, Kondo T, Hasegawa, et. al. Three-dimensional echocardiography and semi-automatic border detection to assess left ventricular volume and function: comparison with MRI measurements. Circulation1994;90:I-337(abstract).

60 Hsieh KS, Chang CK, Chen FL,Liu WS. A new semi-automatic four dimensional reconstruction system using digital real-time two-dimensional echocardiography to determine left ventricular volume. J Am Soc Echocardiogr 1994;7:S44(abstract).

61 Tardif JC, Cao QL, Pandian NG, Azevedo J, Schwartz S, Rastegar H. Dynamic three-dimensional echocardiographic evaluation of the impact of ventricular endoaneurysmorrhaphy on regional and global left ventricular size, shape and function in patients with left ventricular aneurysm. J Am Soc Echocardiogr 1994;7:S33(abstract).

62 Vannan M, Cao QL, Freire M, Azevedo J, Pandian NG. Utility of serial three-dimensional echocardiography in the study of ventricular remodeling and function in patients after first anterior myocardial infarction. J Am Soc Echocardiogr 1994;7:S34 (abstract).

63 Fehske W, Mæhle J, Olstad B, et. al. Serial three-dimensional reconstruction of the left ventricle from multiple apical echocardiographic planes. Eur Heart J 1991;12:175 (abstract)

64 Fehske W, Schippper K, Torp H, et. al. The clinical impact of computer assisted evaluation of ultrasound tissue and flow data. - in Cardiovascular Imaging by Ultrasound. P. Hanrath, R. Uebis and W. Krebs eds. Kluwer academic Publishers, Dordrecht, 1993;435-451.

7. List of abbreviations

2D	two-dimensional
3D	three-dimensional
4D	four-dimensional (space+time)
3DSI	three-dimensional shape index
AWM	area representing abnormal wall motion
% AWM	AWM in percent of end-diastolic endocardial surface area
CoV	coefficient of variation (of wall motion)
EF	volume ejection fraction
ESA	endocardial surface area
FCESA	fractional change in endocardial surface area from end-diastole to end-systole
LV	left ventricular (or left ventricle)
MI	myocardial infarction
SD	standard deviation
WMSI	wall motion score index

Three-Dimensional Echocardiography for Quantitative Left Ventricular Wall Motion Analysis:

A Method for Reconstruction of Endocardial Surface and Evaluation of Regional Dysfunction

JØRGEN MÆHLE, M.S., KNUT BJOERNSTAD,* M.D., SVEND AAKHUS,* M.D., HANS G. TORP, DR. TECHN., BJØRN A.J. ANGELSEN, DR. TECHN.
Department of Biomedical Engineering, University of Trondheim, and *Section of Cardiology, Department of Medicine, Regional Hospital of Trondheim, Trondheim, Norway

A method for quantitative LV wall motion analysis based on 3-D reconstruction of the LV endocardial surface is presented. The reconstruction is based on a minimum of three transthoracic apical 2-D cineloops of the LV, digitally transferred from the ultrasound scanner to a computer. Images are obtained by rotating the transducer around the LV long axis. Endocardial borders are traced with an automatic edge detection algorithm with manual correction. These borders are used with a specially designed computer algorithm for reconstruction of LV cavity 3-D shape, and LV volumes, ejection fraction, and endocardial surface area can be determined. The end-diastolic and end-systolic endocardial surfaces are compared for analysis of regional wall motion. A threshold value is selected to discriminate between normal and abnormal wall motion. Regional wall motion abnormalities are displayed in a bull's eye plot, and the corresponding endocardial surface area is expressed in percent of the total endocardial area. Phase analysis is performed from reconstruction of the endocardial surface throughout the cardiac cycle, and displays regions with abnormal wall motion as being out of phase with LV volume variation. Thus, LV 3-D reconstruction performed by this method can be used for quantitative analysis of wall motion in several clinical situations, and due to the simplicity of processing the data, can be useful outside the research laboratory. (ECHOCARDIOGRAPHY, Volume 11, July 1994)

three-dimensional reconstruction, wall motion analysis, left ventricular dysfunction

Two-dimensional (2-D) echocardiography is a widely used method for evaluation of left ventricular (LV) function. LV chamber dimensions, volumes, and ejection fraction can be assessed on a beat-to-beat basis. In addition, regional wall motion analysis can be used for diagnosis of myocardial infarction or evaluation of coronary perfusion during cardiac stress testing.[1,2] However, methods for quantitative LV wall motion analysis, such as the centerline or radial wall motion method, have limited clinical value.[3] This is due both to methodological problems and to the fact that the information obtained from these methods is restricted to one image view. Wall motion score index is a semi-quantitative method for describing LV segmental wall motion from qualitative analysis of 2-D images. Quantitative analysis of LV wall motion has become important as the use of cardiac interventions is increasing. By three-dimensional (3-D) reconstruction of the LV, wall motion abnormalities can be localized and quantitated more accurately. With recent developments in computer technology, such 3-

Address for correspondence and reprints: Jørgen Mæhle, Department of Biomedical Engineering, University of Trondheim, 7005 Trondheim, Norway. Fax: 47-73598613.

D reconstruction of the cardiac chambers can be performed from 2-D images. To obtain sufficient density of samples for 3-D reconstruction of the contracting LV, both temporal and spatial variation of this object must be taken into account. A 3-D reconstruction is assembled from data of several cardiac cycles, synchronized by the electrocardiographic signals.

LV 3-D reconstruction using B-mode technology was first reported in 1974.[4] More recently, real-time 3-D imaging from simultaneous processing of 16 ultrasound scan-lines has been reported, using a dedicated 3-D probe.[5] However, most studies on 3-D echocardiography are based on 2-D imaging with controlled positioning of the transducer scan-plane. There are three principal methods for such controlled motion of 2-D scan-plane for 3-D data collection:

1) rotation of scan-plane around the center axis of the transducer (Fig. 1a);
2) tilting of the scan-plane (Fig. 1b); and
3) linear displacement of the scan-plane.

LV 3-D reconstruction has been performed from the apical position during transthoracic imaging by rotation of the scan-plane,[6–8] and from the parasternal position by tilting of scan-plane.[9–11] Due to costal interference, parallel short axis images are not possible to obtain with transthoracic imaging, but this method has recently been reported with transesophageal echocardiography.[12] 3-D reconstruction of the LV has also been performed with data from arbitrary positioning of the transducer, using mechanical or acoustic devices for measuring the spatial position of the scan-planes.[13–15]

In this study, a new algorithm for 3-D reconstruction of the LV is presented. The method is based on transthoracic apical imaging with transducer rotation around the LV major axis. By this method, reliable estimates of LV volumes can be obtained, and wall motion abnormalities can be localized and quantitated. The mathematical basis for the method, the reconstruction algorithm, and the use of this method for quantitative LV wall motion analysis are discussed.

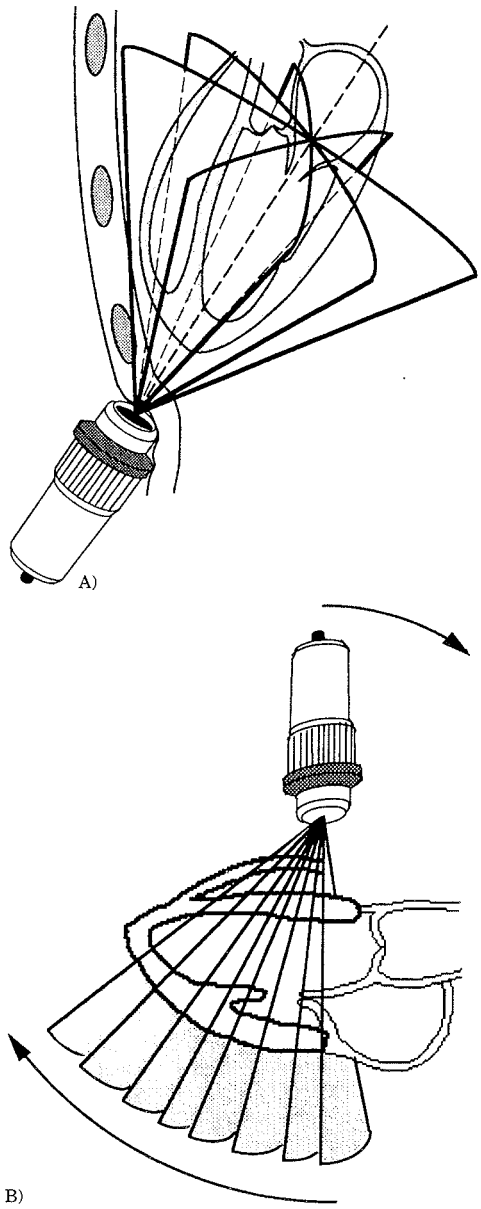

Figure 1. *Controlled motion of 2-D scan-plane for acquisition of ultrasound data for 3-D reconstruction: A) rotation of the scan-plane from the apical position; B) tilting of the scan-plane from parasternal position.*

Methods

Data Acquisition

We have used an ultrasound scanner (CFM 750, Vingmed Sound A/S, Horten, Norway) with a 3.25 MHz annular array transducer. The scanner is interfaced to a personal computer (Macintosh II, Apple Computers, Cupertino, CA, USA) for transfer of digital 2-D cineloops. Three standard apical image views of the LV can be used: apical four-chamber, two-chamber, and long-axis. More accurate reconstruction has also been obtained by using an electrical device for probe rotation which rotates the transducer scan-plane in steps from 2°–60° (Fig. 2). The cineloops comprise the total cardiac cycle, and have a frame-rate of 47 frames per second with 60° sector angle. All cineloops are previewed on the scanner screen before transfer to the computer. Subsequent processing and analysis are performed using a specially designed computer program operating under a general software for display and handling of digital ultrasound data (EchoPrograms, Vingmed Sound, Norway).

LV 3-D Reconstruction Procedure

An automatic edge detection algorithm is used for endocardial edge tracing, with manual correction when necessary. All frames of the cineloops are traced at the endocardial border,

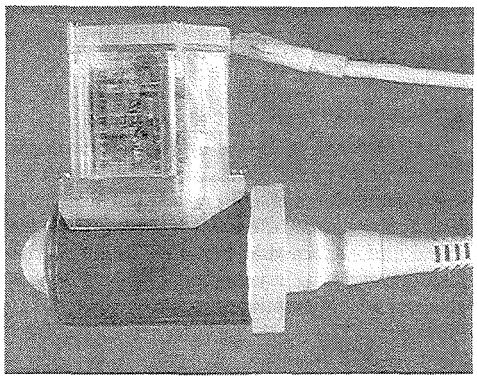

Figure 2. *This electrical device rotates the scan-plane in predetermined angular steps for accurate LV 3-D reconstruction.*

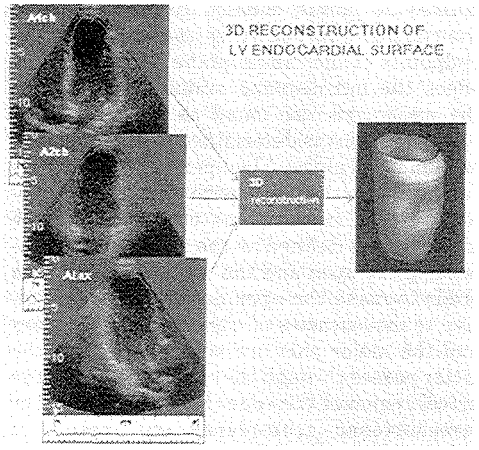

Figure 3. *3-D reconstruction of LV endocardial surface from edges drawn on 2-D ultrasound images. In this example, the reconstruction is based on apical four-chamber, two-chamber and long axis views, and on the rotational angles between scan-planes.*

excluding the papillary muscles, and starting from the left endpoint of the mitral plane line. In the apical long axis view, the LV outflow tract is traced to the level of the aortic valve.

The endocardial edges from the LV long axis views and the angles of rotation between the respective scan-planes comprise the input data to the algorithm for reconstruction of the endocardial surface. These edges have the same temporal position in the cardiac cycle relative to the electrocardiographic trace. The views are given angles corresponding to counter-clockwise rotation of the transducer around its center axis, starting at zero angle for the apical four-chamber view. When the three standard apical views are used for reconstruction (Fig. 3), the angles used in the reconstruction algorithm for apical two chamber and long-axis views are predefined as 62° and 101°, respectively.[16]

Each edge is represented by a polygon description, with the mitral plane as the longest segment in the polygon. All edges are then redefined to continuous smooth curves by cubic spline interpolation. The curve inter-

polates 30 points equally distributed along the original edge, starting and ending at the endpoints of the mitral plane. In each of the edges the mitral-plane midpoint, apex, and the major axis are found as follows: Mitral plane midpoint is determined as the midpoint of the mitral plane. The apex is first found as the point in the edge with the longest distance to the mitral plane midpoint, and the major axis is defined as the straight line connecting the apex and the mitral midpoint. In order to make the apex definition less sensitive to inaccuracies of edge tracing, the apex and the major axis are adjusted so that the latter passes through the center of area in the apical region of the edge (Fig. 4A). Skewed or foreshortened scan-planes will result in under-estimation in volume and also error in reconstructed endocardial surface. The algorithm compensates for skewed scan-planes by stretching the edges in their major axes direction so that all major axes equal the longest (Fig. 4B). The endocardial edges are placed in a 3-D space, a Cartesian xyz-system, according to the input angles, and are aligned by a common apex in origo, and a common direction of the major axes along the y-axis (Fig. 4C).

In the 3-D space, we now assume that the mitral valve root reside in one plane. The coefficients a, b, and c in the plane equation $y = ax + bz + c$ are found by the method of least squares, as the best fit to the mitral-plane endpoints in the edges. The edges are again redefined by projecting the endpoints into this plane. This plane is then displaced in a parallel manner along the major axis. At each level, a closed cubic spline curve interpolating the intersection points between the edges and the plane, is constructed. These curves will represent short-axis cross-sections of the endocardium. The number of cross-sections corresponds to the desired resolution in axial direction. The output of the algorithm provides 3-D coordinates of points residing on these cross-sections, equally distributed around the major axis (Fig. 4D). The points are stored in a matrix according to their respective angular and axial positions. According to the reconstruction method, these points are positioned on a bicubic spline surface, which is the surface of minimum variation of curvature interpolating the input edges in the 3-D space. The LV cavity volume is calculated by summation of areas inside the reconstructed cross-sections. In addition, the reconstruction algorithm provides the length of LV major axis and the spatial position of the center of mass inside the LV cavity.

Area Calculation

Both total and regional areas of the endocardial surface can be calculated from the 3-D shape description. The reconstructed surface is divided into small regions surrounding each point, and the areas of each of these regions are calculated. Regions with wall motion abnormalities are quantitated by summation of areas belonging to points in the actual regions, and the result is expressed in percent of the total endocardial surface area.

Display of 3-D Geometry

LV surfaces are displayed on the computer screen by shadowing, wire-frame, or drawing of cross-sectional contours. The 3-D shape can be rotated and translated by the computer software. In the actual implementation, the user can choose between six different projections of the endocardial surface (Fig. 5). For studies of dynamic 3-D geometry, the cyclic motion of the reconstructed surface is displayed on the computer screen. The geometry is displayed with the center of mass at fixed position in space, and by a constant major axis direction.

LV Mass Calculation

Total LV volume including the myocardium is determined by 3-D reconstruction from epicardial edge tracings. LV myocardial volume is calculated as the difference between the epicardial and endocardial volumes. Knowing the specific weight of myocardial tissue, the LV mass can be determined (Fig. 6).

Wall Motion Analysis

To determine regional LV wall motion, the end-systolic and end-diastolic surfaces are superimposed. Wall motion is calculated at

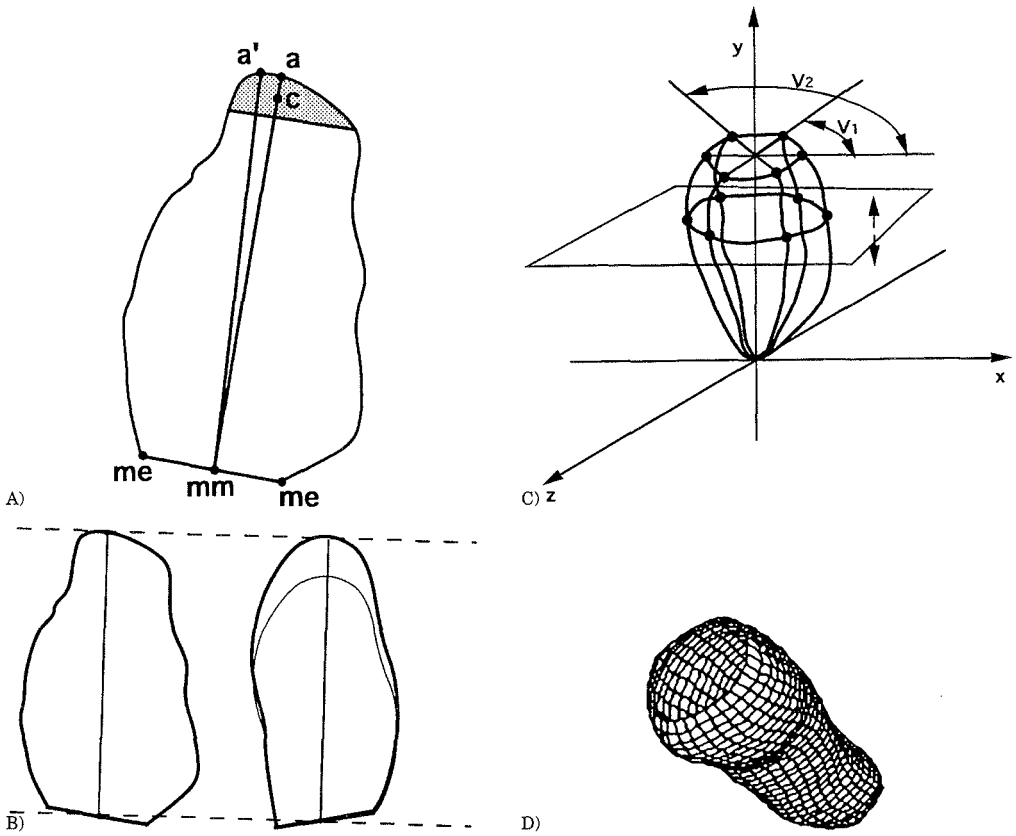

Figure 4. *3-D reconstruction procedure. A) Definition of landmarks, apex (a), mitral plane endpoints (me), and mitral plane midpoint (mm). Point (a') is apex, found as the point on the edge with longest distance from the mitral plane midpoint. The point (c) is the center of area inside the dotted region bounded by the endocardial edge and a normal to the line connecting (mm) and (a'). The normal crosses this line at 90% of the length from (mm) to (a'). B) Edge correction. The endocardial edge at the left represents the image view with the longest major axis. At the right, the thin line represents a different image view with shorter major axis, the thick line represents the edge after correction. C) Edges in a 3-D xyz-system aligned by the apex in origo and the major axis along the y-axis. The edges are rotated respective to the angles between the scan-planes obtained from 2-D image data. The mitral plane endpoints and the reconstructed mitral valve plane is shown. A cross-section border is generated through the intersection points between the edges and a plane parallel to the mitral plane. Several cross-sections are generated as this plane is parallel to the reconstructed LV major axis. D) Wire-frame representation of the reconstructed endocardial surface. The surface is described by 1,024 points in 3-D space, according to the resolution selected to be 32 both in angular and axial direction. The surface is transformed to present a view from the superior position.*

each point in the 3-D LV shape description. The resolution is chosen to 1,024 points on the surface in order to obtain sufficient density of local wall motion estimates within acceptable time.

We have implemented six different methods in the computer software. Three of these methods may be regarded as extensions of 2-D radial wall motion methods to three dimensions (Fig.

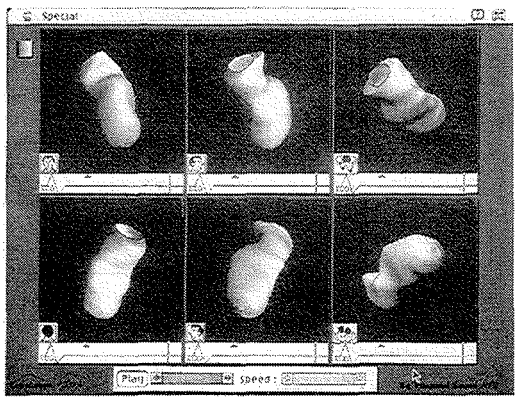

Figure 5. *Six different projections of the reconstructed LV endocardium are displayed simultaneously in a cineloop for qualitative assessment of 3-D wall motion. The figure shows the endocardial surface at end-systole in a patient with an apical myocardial infarction. The resolution chosen is 4,096 points, 64 points both in angular and axial direction, producing a smooth looking surface displayed by shadowing.*

7).[17,18] In these methods, regional wall motion is measured as the percent shortening of the distance from the points in the reconstructed endocardial surface to a chosen center or axis. The LV major axis, the center of the major axis, or the center of mass are used, respectively. The other methods may be regarded as extensions of the 2-D centerline method to three dimensions and regional wall motion is calculated in millimeters as the actual displacement of the point during systole (Fig. 8). These methods differ in the way the surfaces are aligned. The center of mass, the center of the mitral

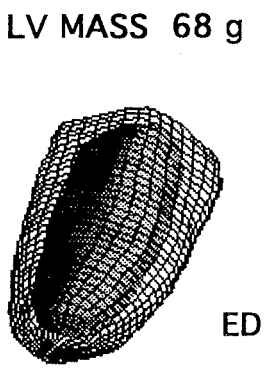

Figure 6. *Calculation of LV myocardial mass in open-chest pig model. Four apical views with rotational angles of 45° between the scan-planes were used for 3-D reconstruction. Both epicardial and endocardial borders are manually traced at end-diastole, and the LV myocardial mass is determined as the difference between epicardial and endocardial volumes corrected for the specific weight of myocardial tissue. The measured weight of the excised LV excluding the papillary muscles was 67.6 g, while the estimated weight from 3-D reconstruction was 68.1 g.*

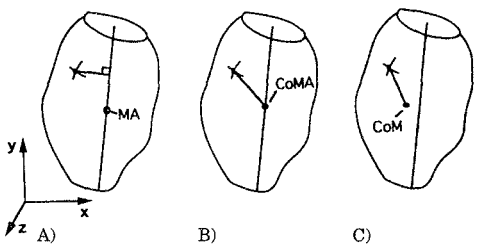

Figure 7. *Reference systems used for quantitation of regional wall motion. The panels show, from left to right, how radial shortening during contraction can be determined from: A) the distances along normals to the LV major axis (MA); B) the distances to the center of the LV major axis (CoMa); and C) the distances to the center of mass (CoM) inside the reconstructed cavity volume.*

plane, or the center of the major axis are used, respectively. The implementation of the methods is simplified as compared to the 2-D centerline method originally described,[19] as the algorithm measures distances along normals to the end-systolic surface.

The mean value and standard deviation for the distribution of regional wall motion in percent shortening or in mm displacement are calculated. Normal LV function has a narrow range of wall motion with small standard deviation, whereas LV with regional dysfunction have a wider range. The investigator decides a threshold value to discriminate between normal and abnormal wall motion. The location and extent of the wall motion abnormality are displayed in a bull's eye plot (Fig. 9). The total end-diastolic surface area, and the surface area of the region with wall motion below the selected threshold value is calculated in cm^2. From this, the absolute and the percent of endocardial area with reduced systolic motion may be determined.

Regional Phase Analysis

With phase analysis, the wall motion throughout the cardiac cycle is analyzed for each of the points in the 3-D reconstructed endocardial surface. By Fourier analysis of the radial wall motion, amplitude and phase of the first harmonic component for all 3-D points and the LV volume variation through the cycle are determined. The phase angle for wall motion and volume variation are compared for each point. The difference in phase angle is assigned a color in a continuous spectrum from −180° to +180°, and the result is displayed in a bull's eye map (Fig. 10). LV regions with normal contraction have small differences in phase angle, while dysfunctional regions have larger differences, due to delayed contraction and relaxation. The product of the amplitude and cosine to the phase difference is displayed

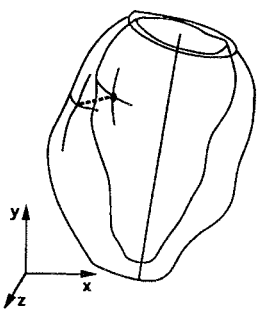

Figure 8. *Wall motion analysis from displacement of points in the endocardial surface during contraction. The endocardial surfaces at end-systole and end-diastole are aligned by geometrically defined landmarks. In the figure, these are chosen as the midpoint of the mitral plane and a common major axis direction. Wall motion is measured between the surfaces along normals to the end-systolic surface.*

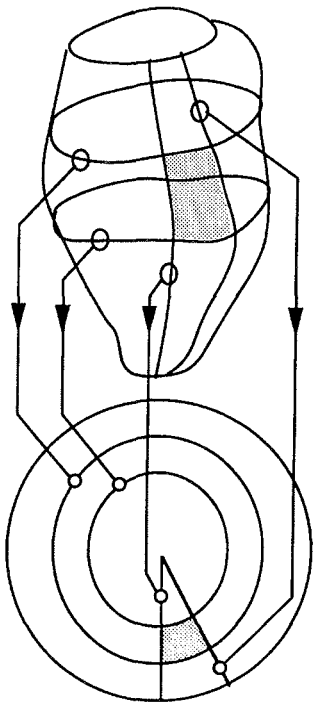

Figure 9. *A bull's eye plot gives a continuous representation of the 3-D endocardial surface into the 2-D plane. Curves in major axis direction in the surface are mapped into radial lines, and short-axis cross-sections are mapped into concentric circles. Note that relations between area of regions in the surface are not preserved in the bull's eye plot.*

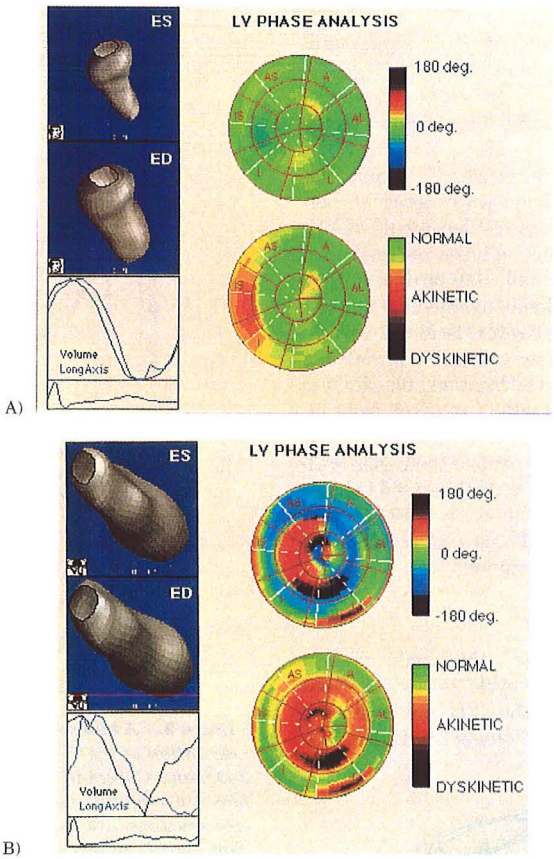

Figure 10. *Regional wall motion from phase analysis: A) Normal wall motion. The upper bull's eye shows the phase analysis input (see text), which is the basis for the display of amplitude and phase of regional wall motion in the lower bull's eye. The green color indicates uniform LV contraction. The yellow and red colored inferior segments indicate small wall motion amplitude in basal LV regions. B) LV apical aneurysm: phase analysis shows a large apical area out of phase (upper bull's eye), displayed as a region with akinesia or dyskinesia (lower bull's eye).*

in the bull's eye map. Normal regions are assigned a green color. Akinetic regions, with no contribution to blood ejection, will be given the outcome of zero (red color) according to 90° phase difference or zero amplitude. Dyskinetic regions will give negative outcome due to more than 90° phase difference, corresponding to negative contribution to blood ejection (dark red to black color).

Discussion

Methodological Considerations

Compared to other methods for 3-D echocardiographic data collection, rotation of the transducer in the apical position is easy to perform and requires a minimum of instrumentation for control of scan-plane position. A major

advantage with this method is the simplicity of the reconstruction procedure, which can be performed within clinical examinations. The postprocessing of data for 3-D reconstruction requires 15–30 minutes, depending on image quality. The reconstruction is performed with a personal computer system, and the data can be stored digitally for easy access to review.

Instead of using the axis defined by the center axis of the transducer, we identify the major LV axis as a reference for 3-D reconstruction. The problems caused by motion of the heart is thus minimized, and the image plane orientation may be adjusted in order to obtain optimal imaging. The reconstruction algorithm allows determination of parameters not readily available with 2-D echocardiography. In addition to the interest in 3-D dynamic geometry of the ventricle, the calculation of ventricular volumes and ejection fraction has considerable clinical interest.

The method presented allows the endocardial area exhibiting reduced wall motion to be quantified as the percent of total endocardial surface. This is made possible by the 3-D description of endocardial surface, and the use of a reference system for alignment of the end-diastolic and end-systolic surfaces. The optimal threshold value, and the most appropriate reference system for wall motion analysis is still under investigation in our laboratory. This method may be the first step in the process of echocardiographic quantitation of myocardial wall motion abnormalities after myocardial infarction or during stress echocardiography. The bull's eye display for regional wall motion abnormalities is easy to interprete, and provides information on both the location and the extent of the wall motion abnormality. With this algorithm, the bull's eye display of wall motion is implemented both for myocardial infarctions, for stress echocardiography, as well as for phase analysis.

The limitations of the method include difficulties with image quality in some patients, making edge detection and hence the 3-D reconstruction inaccurate. The definition of endocardial edges is the most crucial issue of quantitative echocardiography. The evolution of intravenous contrast agents is promising for this purpose, but the clinical value of these agents is so far not established. New technology using transesophageal multiplane imaging gives high-quality data that may be used for 3-D reconstruction. In disfavor of 3-D as compared with 2-D echocardiography is the loss of real-time investigation and errors due to beat-to-beat variations. LV reconstruction is difficult to perform in patients with cardiac arrhythmias. This is due to the variation of systolic duration, and to the variability in LV filling dynamics and ejection. All LV wall motion analysis methods are influenced by the loading conditions, and both global and regional parameters of LV myocardial performance must be related to ventricular preload and afterload. Furthermore, respiratory movement of the heart should be eliminated by recording the cineloops at the same stage of the respiratory cycle. Using the standard three apical planes, with the recognition of landmarks defining each view, the angulations between the image planes may show some individual variation. However, small variations in angulation have only minor influence on the reconstructed LV geometry.

We have used a threshold value of 50% of the mean overall wall motion for the identification of regional dysfunction. A lower threshold value will increase the specificity, but tends to underestimate the area of dysfunction as compared to visual analysis. In normal subjects, wall motion in the basal LV regions is usually less pronounced than in the more distal or apical regions. Thus, a graded threshold based on wall motion determined from a database of a normal population would be preferable. With wall motion analysis during stress echocardiography, the patient can act as his own control; i.e. the wall motion in each endocardial point during stress can be compared to the value at rest. This is an attractive approach, eliminating the need for comparing with a database for normal regional wall motion. The ventricular region outlined as exhibiting reduced wall motion usually overestimates the size of myocardial infarction. This is primarily due to the phenomenon of myocardial tethering, which is also observed with 2-D echocardiographic imaging.[20]

Clinical Applications

LV volume and ejection fraction are important parameters for prognostic stratification after myocardial infarction. However, these parameters are difficult to quantitate with two-dimensional echocardiography in patients with regional LV dysfunction. Nuclear isotope studies are most commonly used for such quantitative procedures. Radiation exposure, costs, and time consumption associated with these methods make them inappropriate for routine follow-up. Unlike recent techniques such as ultra-fast CT or magnetic resonance, 2-D echocardiography has widespread availability. We have found that 3-D reconstruction from three apical views accurately determined shapes and volumes of deformed and normal balloons over a large range of sizes. Interobserver variation on volumes determined with 3-D reconstruction were in the range of 2%–3%, when using manual tracing of the edges. 3-D LV reconstruction may display details on ventricular geometry and morphology.[21] This can only be achieved if the sampling of data is accurate, both with respect to time and to space. With this method, sampling of ultrasonic raw data provides cineloops with the same high frame rate as the ultrasound scanner itself. However, the spatial resolution obtained with three apical image views is not sufficient for detailed studies on LV morphology.

Calculation of LV mass would be of interest for evaluation of patients with hypertensive disease or various myocardial disorders. Traditionally, the LV wall thickness has been measured with M-mode techniques, or with tracing of the endocardial and epicardial contours in LV short axis views. These methods assume a homogeneous wall thickness, which may not be appropriate in patients with coronary artery disease. With a 3-D reconstruction of the endocardial and epicardial surface, this simplification is not necessary, and more accurate measures of LV mass can be performed.

Echocardiographic quantitation of regional LV wall motion has been a difficult task, due to the movements of the heart during systole and respiration. Despite substantial clinical impact, reliable quantitation of LV wall motion has not been available with any noninvasive method, and remains the goal of all LV reconstruction methods. Our method may be used for assessment of regional wall motion abnormalities in patients with myocardial infarctions or in patients undergoing stress echocardiography. We have found that reconstruction from three apical image planes can localize myocardial infarctions of medium and large size (Fig. 11). Detection of smaller infarctions, and more accurate area quantitation, may require more than three imaging planes. Quantitative wall motion analysis can also be applied to stress echocardiographic examinations (Fig. 12). By tracing the endocardial contours of the three standard apical images in end-diastole and end-systole at

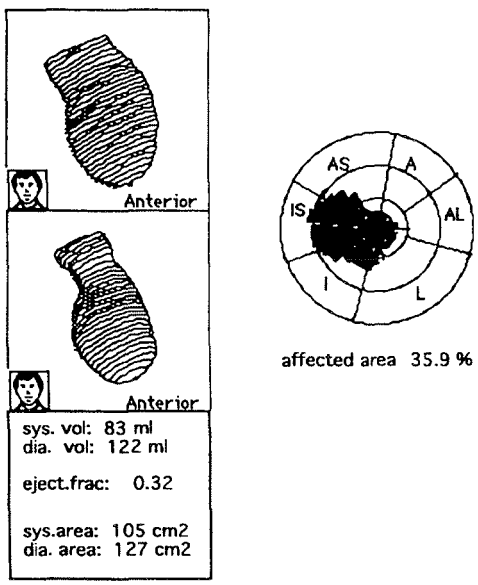

Figure 11. *3-D reconstruction of a left ventricle with regional wall motion abnormality. Left panel: The reconstructed end-diastolic and end-systolic LV endocardial surface shapes and dimensions are displayed from the anterior view. Right panel: Bull's eye plot of the regional wall motion abnormality, located in the septal and apical part of the left ventricle. The darkened area of the bull's eye plot is defined by the endocardial area with wall motion <50% of the mean endocardial motion. A = anterior; AL = anterolateral; AS = anteroseptal; I = inferior; IS = inferoseptal; L = lateral.*

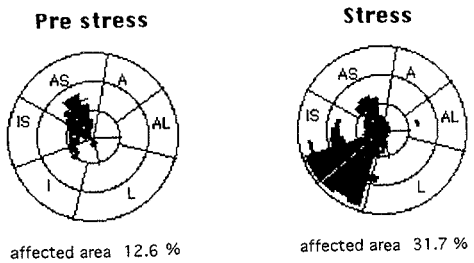

Figure 12. *Bull's eye plots for 3-D quantitation of wall motion abnormalities during stress echocardiography. Left panel: At rest, a wall motion abnormality in the anterior part of the septum and apex is shown. Right panel: During stress, the patient developed a new wall motion abnormality in the inferior region of the LV, indicating the presence of multivessel coronary artery disease.*

rest and during stress, regional wall motion of the corresponding 3-D reconstructions can be displayed as bull's eye plots. The two plots identify the location and extent of wall motion abnormalities at rest and during stress, and the change associated with stress can be displayed.

Regional phase analysis is an interesting new application of this method, although it requires edge tracing of all frames through the cardiac cycle. An aneurysmal region with systolic bulging will give a negative contribution to the reduction in LV volume during systole, and will be easily identified within the phase analysis plot.

As a conclusion, 3-D LV reconstruction provides a new interesting field of echocardiography, in which quantitative wall motion is a particularly important, and challenging, issue. At present, the major limitation for quantitative wall motion analysis, is suboptimal image quality in some patients. However, during the last years, technical improvements in ultrasound imaging have been achieved, and quantitative wall motion analysis may thus become a valuable clinical tool in the near future.

References

1. Sabia P, Afrookteh A, Touchstone DA, et al: Value of regional wall motion abnormality in the emergency room diagnosis of acute myocardial infarction. *Circulation* 1991;84(Suppl I):I-85.
2. Feigenbaum H: Evolution of stress echocardiography. *Echocardiography* 1992;9:73.
3. Shapiro SM, Ginzton LE: Quantitative stress echocardiography. *Echocardiography* 1992;9:85.
4. Dekker DL, Piziali RL, Dong E: A system for ultrasonically imaging the human heart in three dimensions. *Comput Biomed Res* 1974;7:544.
5. Sheikh KH, Smith SW, Ramm O: Real-time, three-dimensional echocardiography: Feasibility and initial use. *Echocardiography* 1991;8:119.
6. Ghosh A, Nanda NC, Maurer G: Three dimensional reconstruction of echocardiographic images using the rotation method. *Ultrasound Med Biol* 1982;8:655.
7. Fazzalari NL, Davidson JA, Mazumdar J, et al: Three dimensional reconstruction of the left ventricle from four anatomically defined apical two-dimensional echocardiographic views. *Acta Cardiologica* 1984;XXXIX:409.
8. McCann HA, Sharp JC, Kinter TM, et al: Multidimensional ultrasonic imaging for cardiology. *Proc IEEE* 1988;76:1063.
9. Nixon J, Saffer SI, Lipscomb K, et al: Three-dimensional echoventriculography. *Am Heart J* 1983;106:435.
10. Fine DG, Sapoznikov D, Mosseri M, et al: Three-dimensional echocardiographic reconstruction: Qualitative and quantitative evaluation of ventricular function. *Comput Methods Programs Biomed* 1988;26:33.
11. Zoghbi WA, Buckey JC, Massey MA, et al: Determination of left ventricular volumes with use of a new nongeometric echocardiographic method: Clinical validation and potential application. *JACC* 1990;15:610.
12. Pandian NG, Nanda NC, Schwartz SL, et al: Three-dimensional and four-dimensional transoesophageal echocardiographic imaging of the heart and aorta in humans using a computed tomographic imaging probe. *Echocardiography* 1992;9:677.
13. Geiser EA, Lupkiewicz SM, Christie LG, et al: Framework for three-dimensional time-varying reconstruction of the human left ventricle: Sources of error and estimation of their magnitude. *Comput Biomed Res* 1980;13:225.
14. Moritz WE, McCabe DH, Pearlman AS, et al: Computer generated three dimensional ventricular imaging from a series of two-dimensional ultrasonic scans. *Comput Cardiol* 1982;1982:19.
15. Nikravesh PE, Skorton DJ, Chandran B, et al: Computerized three-dimensional finite element reconstruction of the left ventricle from cross-

sectional echocardiograms. *Ultrason Imaging* 1984;6:48.
16. Henry WL, DeMaria A, Feigenbaum H, et al: Identification of myocardial wall segments. *The American Society of Echocardiography Committee on Nomenclature and Standards 1982.*
17. Moynihan PF, Parisi AF, Feldman CL: Quantitative detection of regional left ventricular contraction abnormalities by two-dimensional echocardiography. I. Analysis of methods. *Circulation* 1981;63:752.
18. Schnittger I, Fitzgerald PJ, Gordon EP, et al: Computerized quantitative analysis of left ventricular wall motion by two-dimensional echocardiography. *Circulation* 1984;70:242.
19. Bolson EL, Kliman S, Sheehan F, et al: Left ventricular segmental wall motion—A new method using local direction information. *Comput Cardiol* 1980;1980:245.
20. Force T, Kemper A, Perkins L, et al: Overestimation of infarct size by quantitative two-dimensional echocardiography: The role of tethering and of analytic procedures. *Circulation* 1986;73:1360.
21. Levine RA, Handschumacher MD, Sanfilippo AJ, et al: Three-dimensional echocardiographic reconstruction of the mitral valve, with implications for the diagnosis of mitral valve prolapse. *Circulation* 1989;80:589.

A New Method for Echocardiographic Computerized Three-dimensional Reconstruction of Left Ventricular Endocardial Surface: In Vitro Accuracy and Clinical Repeatability of Volumes

Svend Aakhus, MD, Jørgen Mæhle, MSc, and Knut Bjoernstad, MD, *Trondheim, Norway*

This study evaluates the in vitro accuracy and clinical repeatability of volumes derived by a new algorithm for three-dimensional reconstruction of cavity surfaces based on echocardiographic apical images obtained by probe rotation. The accuracy of the method was tested in latex phantoms (true volumes, 32 to 349 cm^3) with (n = 9) or without (n = 9) rotational symmetry around the midcavitary long axis. Repeatability of left ventricular volumes was assessed in subjects without (n = 5) or with (n = 10) myocardial disease. Estimated phantom volumes obtained from four (three) imaging planes were close to true volumes with a mean difference ± SD of 0 ± 2 (2 ± 3) cm^3 in symmetric and 1 ± 3 (4 ± 4) cm^3 in asymmetric objects. Biplane and single-plane volume estimates were less accurate. Interobserver and intraobserver repeatability of three-dimensional left ventricular volumes was good for analysis (coefficients of variation: 3.5% to 6.2%) and was lower for recording (coefficients of variation: 7.4% to 10.9%). Hence the present algorithm reproduces volumes of symmetric and deformed in vitro objects accurately over a wide range of size and shape, and it produces repeatable left ventricular volumes in the clinical situation. (J Am Soc Echocardiogr 1994;7:571-81.)

Cardiac dimensions are important for prognosis in patients with heart disease. Serial assessment of left ventricular dimensions and geometry is conventionally performed by two-dimensional (2D) echocardiography with the use of apical four-chamber and long-axis (two-chamber) imaging planes to obtain left ventricular volume by the biplane disk summation method.[1] Because this method is limited by geometric assumptions of ventricular shape and is not very accurate when the ventricle is regionally diseased, methods for measurement of left ventricular volume by three-dimensional (3D) echocardiography have gained increasing attention.[2] Cavity volumes can be derived from 3D reconstructions of the left ventricle based on defined endocardial borders on multiple 2D echocardiograms.[3-16] Different methods for image acquisition and processing have been reported, with either the parasternal position for short axis imaging[3-8] or the apical position for long axis imaging, obtained by parallel probe displacement[9] or rotation.[10,11,17] The spatial position of transducer and imaging planes can accurately be registered by use of mechanical arms[4,12] or acoustic systems,[8,13-15] which, however, cannot be used in all clinical situations.[2]

It is recognized that 3D echocardiography produces more accurate and repeatable left ventricular volume estimates than does conventional 2D imaging.[8,16] However, 3D echocardiography is not regarded as feasible in the everyday clinical practice because of the complexity of image acquisition and data processing. We have developed a new algorithm for 3D reconstruction of cavity surfaces[18] based on apical imaging planes obtained by probe rotation.

From the Department of Medicine, Section of Cardiology, and the Department of Biomedical Engineering, University of Trondheim.

Supported by grants from the Norwegian Council on Cardiovascular Diseases (Oslo, Norway) and Norwegian Technical Research Council (NTNF).

Reprint requests: Svend Aakhus, MD, Department of Medicine, Section of Cardiology, University Hospital, N-7006 Trondheim, Norway.

0894-7317/94/$3.00 + 0 27/1/57579

Journal of the American Society of Echocardiography
November-December 1994

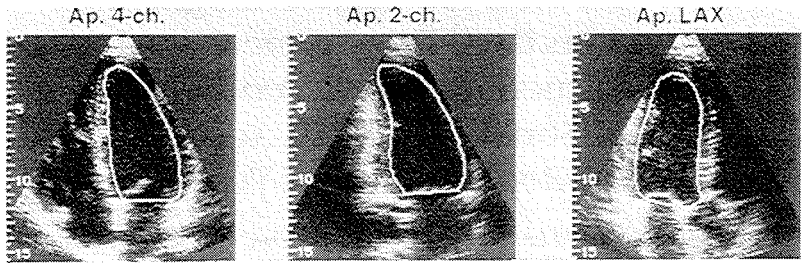

Figure 1 Two-dimensional ultrasound images of left ventricle in end-diastole obtained from apical position. *From left to right:* apical four-chamber, long-axis (two-chamber), and long-axis imaging planes. Endocardial traces are shown as *white continuous lines.* Numbers indicate distance from transducer in centimeters.

Table 1 Interobserver variability for three-dimensional estimates of left ventricular volumes, recording

	Average by two observers	Recording 1-2	CR	CV (%)
LV EDV (cm^3)	125 (83, 246)	−7 ± 9 (−50, 16)	18	7.4
LV ESV (cm^3)	70 (30, 203)	0 ± 8 (−39, 23)	16	10.9
LV SV (cm^3)	55 (36, 74)	−6 ± 6 (−25, 8)	12	11.8
LV EF (%)	47 (17, 64)	−3 ± 4 (−13, 16)	8	8.7

Mean values (± SD), range in parentheses, of two independent observers' recordings in 15 subjects.
LV, Left ventricular; *EDV,* end-diastolic volumes; *ESV,* end-systolic volume; *SV,* stroke volume; *EF,* ejection fraction; *CR,* coefficient of repeatability; *CV,* coefficient of variation.

This algorithm was designed to be fast and simple to use and to be operable with commercially available ultrasound and computer equipment. The algorithm accepts any number of imaging planes from 3 to 12, and in this study we assessed the accuracy of volume estimation in vitro by using three or four imaging planes and the clinical repeatability by using apical imaging planes identified by anatomic landmarks.

METHODS

In Vitro Accuracy

An ultrasound scanner (Vingmed 750, Vingmed Sound, Horten, Norway) with a 3.25 MHz annular array transducer was used for all ultrasound imaging. Nine thin-walled latex balloons were filled with 20% ethanol solution to obtain objects with a clinically relevant range of cardiac volumes (i.e., 32 to 349 cm^3) and with rotational symmetry around the midcavitary long axis. Ultrasound imaging was performed with the phantoms immersed in this solution, where ultrasound velocity is 1540 m/sec and similar to that in blood and soft tissue. The probe was mounted in a hull with angle guide around the circumference. Four long-axis ultrasonic images were obtained by subsequent probe rotation in increments of 45 degrees around the midcavitary long axis (0, 45, 90, and 135 degrees). The imaging planes were adjusted to avoid foreshortening without altering the angle of rotation. The images were transferred as digital scanline data (Echolink 3.0, Vingmed Sound), to a computer (Macintosh series II, Apple Computers, Cupertino, Calif.) for analysis in specially designed software operating under a general program for handling of digital ultrasound data (EchoDisp 3.0, Vingmed Sound). Subsequently the phantoms were deformed by application of adhesive tape to obtain rotational asymmetry around the long axis, comparable to that of regionally diseased left ventricles. The imaging procedure was then repeated, thus a total of 18 phantoms were studied. The thin phantom wall border was defined at peak ultrasound backscatter intensity (i.e., at midline of the wall echoes) and was manually traced on the computer on all four images, allowing a short "mitral-plane" at basis. Cavity volume was then determined by use of the algorithm for 3D reconstruction as described below, first by use of all four border traces and subsequently by use of three border traces (i.e., 0, 90, and 135 degrees). Conventional biplane and single-plane volumes were obtained by the disk summation method[1]

with the 0 and 90 degree images and the 0 degree image only, respectively. With this procedure the in vitro accuracy of the methods could be compared without redrawing the wall contours. The procedure was repeated in a blinded fashion at least 4 weeks later, and the average volume estimate was calculated for comparison with true volume. True volumes were determined as the difference between total and dry phantom weight divided by 0.96 to correct for the solution density.

Clinical Repeatability of Left Ventricular Volumes by 3D

Fifteen subjects, 13 men and two women who ranged in age from 28 to 75 years and had a representative range of cardiac dimensions (Table 1), gave informed consent to participate in the study. Five subjects were healthy, seven had previous myocardial infarction, and three had dilated left ventricles caused by congestive cardiomyopathy (two patients) or coronary artery disease (one patient). All patients were in sinus rhythm; one had first-degree atrioventricular block, and one had left bundle branch block. Medication was continued through the investigation. All subjects were examined in the left lateral decubitus position after at least 5 minutes supine rest, and all had readable echocardiograms, although they were not specifically selected for echogenicity. Ultrasound images were obtained independently and in immediate and random succession by two experienced investigators using apical access to the four-chamber, long-axis (two-chamber), and long-axis imaging planes (Figure 1), which were identified by anatomic landmarks.[1,19] The four-chamber plane was assigned 0 degrees, and the angular deviations of long axis (two-chamber) and long axis from this plane were assumed to be 62 and 101 degrees counterclockwise, respectively.[20] For each imaging plane sequential images from one cardiac cycle (cineloop) were sampled, usually at 47 frames/sec, during held end-expiration and transferred as digital scanline data to the computer. An electrocardiogram (lead III) was recorded with the ultrasound data. The two assessments of each subject were completed within 1 hour.

The duplicate set of images from each subject (two recordings) was analyzed in a blinded fashion by two independent observers on two occasions more than 14 days apart. On the computer endocardial border definition was optimized by adequate contrast setting, and the endocardial borders of all three imaging planes were manually traced in end-diastole (defined at the R-peak on the electrocardiogram) and end-systole (defined at the frame before mitral valve opening). Endocardium was traced at the echogenic transition zone between left ventricular cavity and myocardial wall, excluding the papillary muscles and including the left ventricular outflow tract up to the aortic valve in the long-axis plane (Figure 1). Mitral valve plane was traced as the straight line between mitral annulus echo boundaries (i.e., at insertion of the mitral valve leaflets). The traces on the freeze-frame images (end-diastole and end-systole) were repeatedly evaluated against the moving endocardium and mitral annulus by use of the cineloop replay function. The endocardial edges from these three apical long-axis views of the left ventricle and their assumed rotation-angles made up input data to the surface reconstruction algorithm.

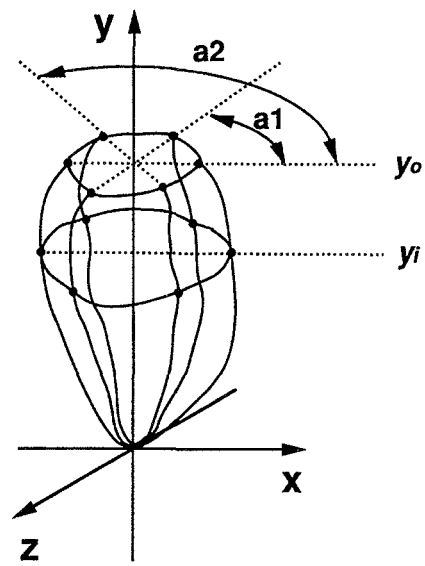

Figure 2 Principle for three-dimensional reconstruction of left ventricular endocardial surface from multiple apical long axis ultrasound images. Endocardial border trace from each image (three traces shown) are reassembled in Cartesian xyz–system according to their relative angles (a1, a2), common position of apex in origo, and common mitral plane midpoint. Mitral valve annulus is determined by (1) finding the plane $y = ax + bz + y_o$ as best fit to border trace endpoints (least squares method), (2) projecting these endpoints into this plane, and (3) reconstructing annulus by cubic spline interpolation on these projected points. Multiple planes in parallel with mitral plane, y_o, are then positioned between apex and mitral midpoint. At each plane, y_i, a closed curve is generated by cubic spline interpolation through points of intersection between plane and apical border traces. Endocardial surface is then reconstructed from the cubic spline interpolated multiple apical and cross-sectional borders (see text).

Journal of the American Society of Echocardiography
November-December 1994

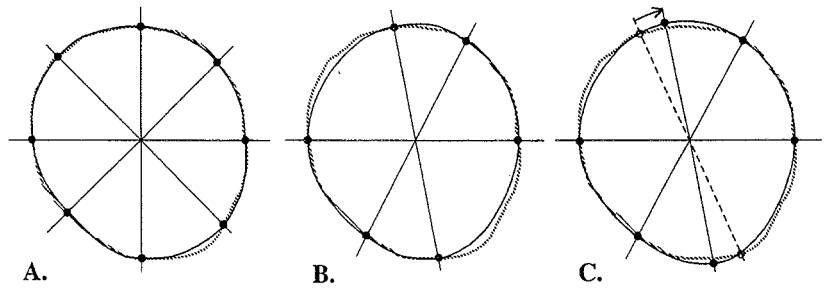

Figure 3 Reconstruction of left ventricular cross-sectional border. Closed cubic spline curve *(continuous line)* as compared with true endocardial border *(broken line)* in regionally diseased left ventricle at end-diastole imaged in cross-section from parasternal position. *A* and *B* show cubic spline curves interpolated on eight and six points *(closed circles)* corresponding to four (0, 45, 90, and 135 degrees) and three (0, 62, and 101 degrees) apical long-axis imaging planes *(straight lines)*. Difference between areas within true and interpolated cavity borders was −1.2% in *A* and −2.8% in *B*. *C* shows deviation of apical long axis 15 degrees *(dashed line)* from assumed angular position. Cubic spline interpolation was performed as if deviating endocardial point *(open circle)* was located at assumed imaging plane position *(closed circle)*. Difference between area within this curve and that obtained from correctly positioned imaging planes was 2.5%.

Algorithm for 3D Reconstruction of Cavity Surface

As the cavity border traces and their measured or assumed spatial positions are entered into the specially designed software, the present 3D algorithm performs the following steps automatically. First 30 points are equally distributed on each of the original border traces, which then are redefined to continuous smooth curves by cubic spline interpolation on these points. In each imaging plane the mitral plane midpoint is defined as the midpoint of the straight line between mitral annulus echo boundaries. The border's apex is defined as the border point furthest away from the mitral plane midpoint, and the major axis is defined as the straight line between this apex and mitral plane midpoint. To make the apex definition less sensitive to inaccuracies of endocardial border tracing, apex and major axis are automatically adjusted so that the latter passes through the center of area in the apical region of the border. Because the apical probe position does not always correspond to the cardiac apex, the imaging planes may occasionally be foreshortened and lead to underestimation of volume. Assuming that the longest major axis is the most correct, the present algorithm compensates automatically for foreshortening by elongating the endocardial border traces in major axes direction so that all major axes equal the longest. The border traces are then reassembled in a xyz–space according to their measured or assumed input angles, with apex and the mitral midpoint of each border positioned in origo and at the y-axis, respectively, so that the common major axis coincides with the y-axis (Figure 2). The reconstruction of the cavity border surface is now performed as follows. A plane is found as best fit to the endpoints of the border traces (least squares method) and is defined to be the mitral plane. The endpoints are then projected into this plane, and the mitral valve annulus is approximated by a planar curve generated by cubic spline interpolation on these projected points. New equidistant planes parallel to the mitral plane are then positioned between apex and mitral midpoint. At each plane a cross-sectional closed curve is generated by cubic spline interpolation through the points of intersection between the plane and apical border traces. The number of reconstructed cross-sections corresponds to the selected axial resolution. With this procedure the cavity surface is reconstructed as a bicubic surface that interpolates the borders reassembled in the xyz–space. The cavity volume is calculated by disk summation (Simpson's rule). The area of each cross-sectional disk is obtained from the mathematic description of the cubic spline curve, and disk volume is calculated as the product of disk area and height where the latter is given as the major long axis length divided by the selected axial resolution. Stroke volume was calculated as end-diastolic minus end-systolic volume, and ejection fraction was calculated as stroke volume over end-diastolic volume.

Table 2 In vitro accuracy of echocardiographic volume estimates

Method	Shape	Imaging planes	Echo-TRUE (cm^3)	95% LA (cm^3)		CV (%)
				Lower	Upper	
3-D	Symmetric	4	0 ± 2 (−3, 6)	−4	3	1.3
3-D	Symmetric	3	−2 ± 3 (−6, 5)	−7	3	1.9
Biplane	Symmetric	2	−2 ± 3 (−8, 1)	−7	3	1.9
Single plane	Symmetric	1	−3 ± 4 (−13, 2)	−10	4	2.6
3-D	Asymmetric	4	−1 ± 3 (−7, 6)	−7	4	2.0
3-D	Asymmetric	3	−4 ± 4 (−9, 3)	−11	4	2.7
Biplane	Asymmetric	2	−5 ± 5 (−12, 3)	−15	5	3.8
Single plane	Asymmetric	1	−6 ± 6 (−24, 1)	−18	6	4.6

Mean values ± SD (range) from nine symmetric and nine asymmetric phantoms.
3-D, The present three-dimensional method; *Echo-TRUE*, difference between echocardiographically determined and true phantom volume; *LA*, limits of agreement; *CV*, coefficient of variation.

Validity of Reconstructed Left Ventricular Cross-Sectional Area

The present algorithm reconstructs the borders of cross-sectional disks from a limited number of apical imaging planes and calculates cavity volume from area and height of these disks. The accuracy of the disk area estimate depends on the agreement between true and reconstructed cavity border and the influence of deviations from the assumed spatial position of the imaging planes. This accuracy was tested in 10 subjects (eight men and two women) aged 24 to 66 years, with (n = 6, all with previous myocardial infarction) or without (n = 4) left ventricular regional wall motion abnormalities at rest. All were in sinus rhythm. Cineloops of the midventricular short axis were recorded by imaging from parasternal position and were transferred to the computer. The endocardial borders were traced in end-diastole and end-systole, excluding the papillary muscles. On these borders we used the eight or six points corresponding to the four (0, 45, 90, and 135 degrees) or three (0, 62, and 101 degrees) apical imaging planes, respectively, to generate a closed cubic spline curve (Figure 3). The end-diastolic and end-systolic areas within the true endocardial border trace and the corresponding spline curves were obtained for all 10 subjects, and the respective differences were calculated in percent of the former.

The apical four-chamber, long-axis (two-chamber), and long-axis imaging planes may deviate up to 15 degrees from their assumed spatial position.[20] To test how this deviation influences the disk area estimates and thus volume estimates, we generated new cubic spline curves corresponding to an angular deviation of ± 15 degrees in any of the three imaging planes. We used the six points on the traced endocardial border corresponding to the assumed position of the three apical imaging planes (i.e., 0, 62, and 101 degrees). Each point's position is defined by its distance to the major axis (i.e., center of area within the border) and by the rotation angle of the corresponding imaging plane. The distance between point and major axis was identified along the deviating imaging plane. The reconstruction was performed with the point relocated to the correctly positioned plane with the identified distance to major axis (Figure 3, *C*). The difference between the areas within the new curve and that with correct position of the imaging planes was calculated in percent of the latter. In each patient this procedure was performed for end-diastolic and end-systolic borders according to 0, 15, and −15 degrees deviation in the three apical imaging planes (54 combinations).

Statistical Analysis

Values are presented as mean ± standard deviation (SD). Coefficient of variance and the 95% limits of agreement were obtained by standard methods.[21] Coefficient of repeatability was determined as 1.96 SD of the differences between the observers.[22] The relation between variables was also assessed by simple linear regression, where the squared correlation coefficient (R^2) and residual standard deviation (s_{rcs}) were used for assessing goodness of fit of the regression line.

RESULTS

In Vitro Accuracy

The estimated volumes agreed well with true volumes both in symmetric and deformed phantoms and when either four or three imaging planes were used

Journal of the American Society of Echocardiography
November-December 1994

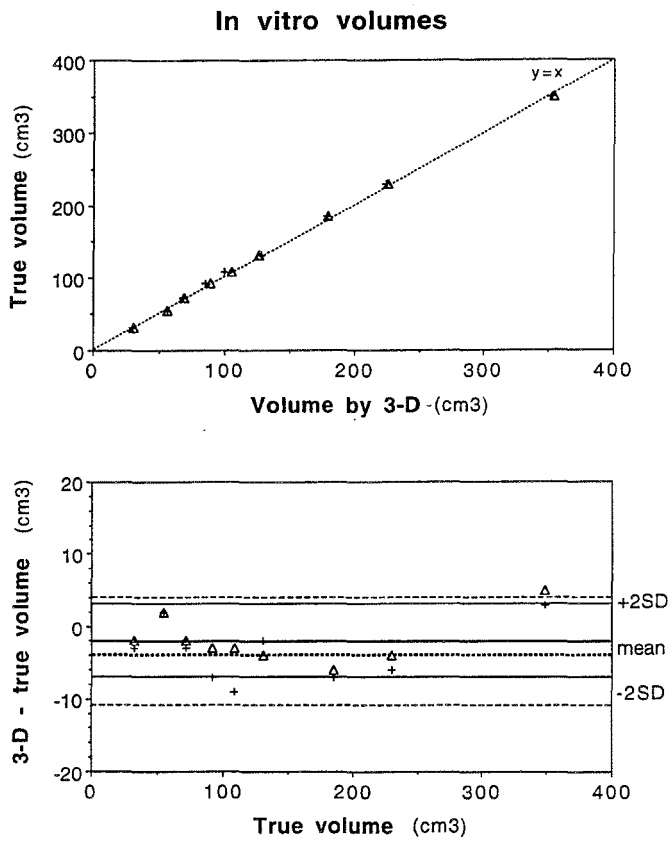

Figure 4 In vitro accuracy of volumes by three-dimensional method. Cavity surface of nine symmetric *(open triangles)* and nine asymmetric *(crosses)* fluid-filled latex phantoms were reconstructed by present algorithm from three long-axis imaging planes and volumes determined from this reconstruction (see text). *Upper panel,* plot of volumes by three-dimensional method, at abscissa, against true volumes, at ordinate. Line of identity (y = x) hides linear regression line for all phantoms (R^2 = 0.999, residual standard deviation 3.7 cm^3, $p < 0.001$). *Lower panel,* plot of difference between volumes by three-dimensional and true volumes, at ordinate, against true volumes, at abscissa. Mean ± 2 SD for symmetric phantoms is indicated by *continuous lines* and for asymmetric phantoms by *dashed lines.*

for surface reconstruction (Table 2, Figure 4). The estimated volumes tended to be slightly lower than true volumes for all methods except when four imaging planes were used on symmetric objects, and the underestimation was greater on deformed objects. The regression lines between estimated and true volumes were close to the line of identity when both four or three imaging planes were used. Although the in vitro accuracy of volume estimation was best when four imaging planes were used, it was adequate when three were used as well, where 95% limits of agreement indicates that any volume estimate in an asymmetric object would be less than 11 cm^3 less than and 4 cm^3 greater than true volume. Bias and variability were smallest with the 3D method, slightly greater for biplane method, and greatest for single plane method (Table 2). Intraobserver repeatability for analysis of phantom volumes by 3D method was good with coefficients of variation between 2.2% and 3.0% for both symmetric and deformed phantoms when reconstructed from either four or three imaging planes, whereas the repeatability was lower for biplane and single plane methods with coefficients of variation ranging from 3.3%

Table 3 Interobserver variability for three-dimensional estimates of left ventricular volumes, analysis

	Analysis 1-2	CR	CV (%)
LV EDV (cm^3)	1 ± 4 (−10, 17)	8	3.5
LV ESV (cm^3)	−4 ± 4 (−15, 12)	8	6.2
LV SV (cm^3)	4 ± 4 (−7, 17)	8	7.5
LV EF (%)	4 ± 3 (−3, 10)	6	7.0

Mean values (±SD), range in parentheses, of two independent observers' analysis of data from 15 subjects.
Abbreviations as in Table 1.

Table 4 Intraobserver variability for three-dimensional estimates of left ventricular volumes, analysis

	Analysis 1-2	CR	CV (%)
LV EDV (cm^3)	3 ± 5 (−16, 16)	10	4.1
LV ESV (cm^3)	4 ± 4 (−9, 20)	8	6.1
LV SV (cm^3)	−2 ± 4 (−23, 11)	8	8.5
LV EF (%)	−2 ± 3 (−9, 9)	6	5.8

Mean values (±SD), range in parentheses, of one observer's two independent analysis sessions on data from 15 subjects.
Abbreviations as in Table 1.

(with the biplane method) to 7.8% (with the single plane method).

Clinical Repeatability

Interobserver repeatability for recording (Table 1) was best for end-diastolic left ventricular volume with a coefficient of variation of 7.4% and was lower for end-systolic volume and stroke volume. The coefficient of repeatability indicates that any difference in recorded end-diastolic or end-systolic volume less than 18 or 16 cm^3, respectively, may be due to variation in recording technique alone. The differences between the observers were, however, evenly distributed over the range of measurements. Interobserver repeatability for analysis (Table 3) was better than that for recording, with coefficients of variation ranging from 3.5% for end-diastolic volume to 7.5% for stroke volume. Variation in analysis technique can explain only a difference less than 8 cm^3 for serial left ventricular volumes analysis by 2 different observers. The differences between the observers were evenly distributed over the range of measurements. Intraobserver repeatability for analysis (Table 4) was at similar level with coefficients of variation ranging from 4.1% for end-diastolic volume to 8.5% for stroke volumes. The differences between the observers were evenly distributed over the range of measurements.

Reconstructed Left Ventricular Cross-Sectional Area

The average difference between the area within the mid-ventricular short axis endocardial border and that within the corresponding closed spline curve generated through eight or six border points (i.e., four or three apical imaging planes) were 0.8% ± 0.7% (95% limits of agreement: −0.3% to 1.9%) and 1.2% ± 1.6% (95% limits of agreement: −1.9% to 4.3%), respectively. The results were similar for end-systolic and end-diastolic area (Figure 5). The average difference between the reconstructed area generated from the six points that were allowed to deviate ±15 degrees from their assumed position on the endocardial border trace and that within the curve with correctly positioned points was 0.3% ± 3.2% (95% limits of agreement: −6.0% to 6.9%).

DISCUSSION

In this study we have presented a new algorithm for 3D surface reconstruction based on conventional 2D ultrasound apical imaging, and we have evaluated the accuracy in vitro and the repeatability of left ventricular volume determination in the clinical situation. The time needed for recording of three apical imaging planes depends on image quality and investigator experience, but it is usually less than 15 minutes. The endocardial borders of the three imaging planes can be traced in end-diastole and end-systole within 10 to 15 minutes. Once the traces are input to the special purpose software, surface reconstruction and volume calculation are completed within a few seconds with the described setup. We used the apical position for obtaining an image, because in

Journal of the American Society of Echocardiography
November-December 1994

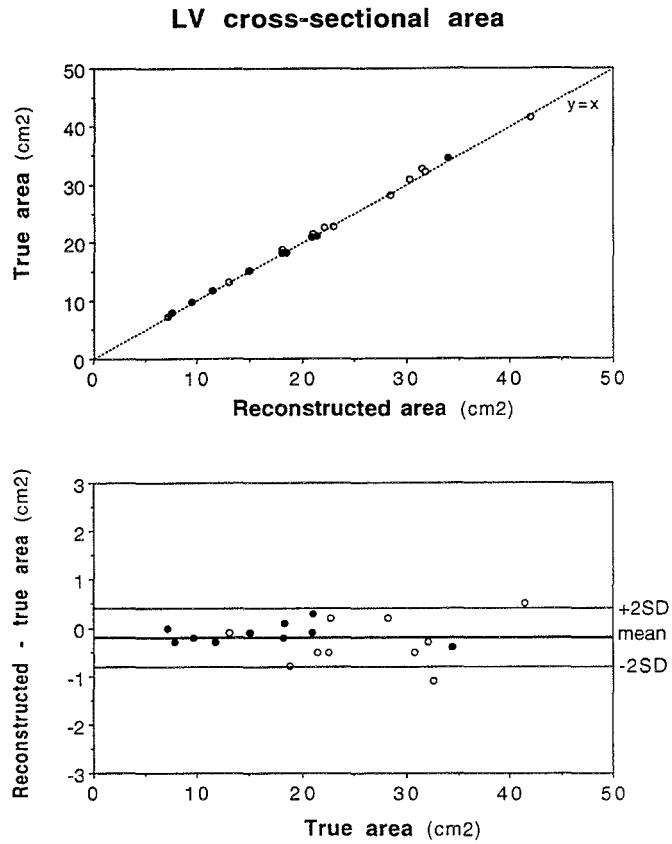

Figure 5 Validity of left ventricular *(LV)* reconstructed cross-sectional area. In vivo comparison (six subjects with and four without regional myocardial disease) of area within midventricular endocardial border (true area) as judged from parasternal short axis ultrasound image in end-diastole *(open circles)* and end-systole *(closed circles)*, and that reconstructed by cubic spline interpolation on six points on endocardial border corresponding to three apical imaging planes (0, 62, and 101 degrees). See also Figure 3. *Upper panel,* reconstructed areas, at abscissa, plotted against true areas, at ordinate. Line of identity (y = x) hides linear regression line ($R^2 = 0.999$, residual standard deviation 0.4 cm^2, $p < 0.001$). *Lower panel,* plot of difference between reconstructed and true areas, at ordinate, against true areas, at abscissa. Mean ± 2 SD indicated by continuous lines.

our experience it is less hampered by rib interference than with the parasternal position. Moreover, in most patients an image of the entire left ventricle can be obtained from this position by rotation of the probe. Whereas previous studies have used the rotational axis of the transducer as reference for 3D echocardiography,[10,17] the present method uses the major axis of the left ventricle. This allows adjustment of each imaging plane without changing the rotational angles, and image quality can be optimized. Furthermore the reconstruction is not significantly influenced by movement of the heart and patient, and accessory mechanical devices are obviated.

The present study shows that the volumes of objects with a wide range of shapes and sizes can be accurately reproduced by 3D echocardiography based on three or four imaging planes. A volume estimate based on three or four imaging planes in an asymmetric object would be within 11 or 7 cm^3 less than and 4 cm^3 greater than the true volume (95% confidentiality), respectively. This is similar to results obtained with a more complex system for 3D echo-

cardiography.[8] Hence we regard three apical imaging planes to be sufficient for volume estimates of symmetric and asymmetric objects. This is important, because recording of four imaging planes requires a new procedure for echocardiographic imaging of left ventricle, whereas the four-chamber, long-axis (two-chamber), and long-axis imaging planes are part of the routine clinical echocardiographic examination. When volumes of the asymmetrical objects were estimated from only two (biplane method) or one imaging plane(s) (single plane method), the bias and variability were greater and repeatability was lower. This is in agreement with results of previous studies of latex balloons[8] and excised hearts,[16] and is most likely due to the representation of object surface shape by 3D echocardiography than by the other methods. Moreover, in the present algorithm we have implemented automatic elongation of the major axes so that all equal the longest, and this feature may further improve the accuracy of volume estimation when the imaging planes occasionally are foreshortened. However, at least one imaging plane must make up the correct major axis for adequate surface reconstruction and volume estimation.

The present algorithm produces a bicubic spline representation of cavity surface from the input long axis traces and their measured or assumed spatial position. The cubic spline curve maintains both direction and curvature through the interpolation points. Of all the curves fulfilling this requirement, the cubic spline curve has minimum curvature variation and strain energy.[23] The present study shows that this curve is well suited for reconstruction of the endocardial border and produces areas within −1.9% and 4.3% (95% confidentiality) of true cross-sectional area of the endocardial border trace in left ventricles with and without regional disease when generated from six points (i.e., three apical imaging planes). Furthermore the disk area estimate is robust for deviations from the assumed image plane positions, and errors in disk area resulting from any 15 degrees deviation in the imaging planes would be within −6.0% to 6.9% with 95% confidentiality. The volume estimate is calculated by disk summation and is therefore equally robust for angular deviations.

We have tested the algorithm with different levels of axial resolution and have found that when the numbers of reconstructed cross-sections exceed 16, the volume estimate converges to be within 1% of that obtained when this number approaches infinity, as also indicated by Figure 6. Thus to obtain volume estimates with high accuracy and a fast surface reconstruction, we have chosen an axial resolution of 32. Higher resolution (i.e., 64 disks), adds computation time without increasing accuracy of volume determination.

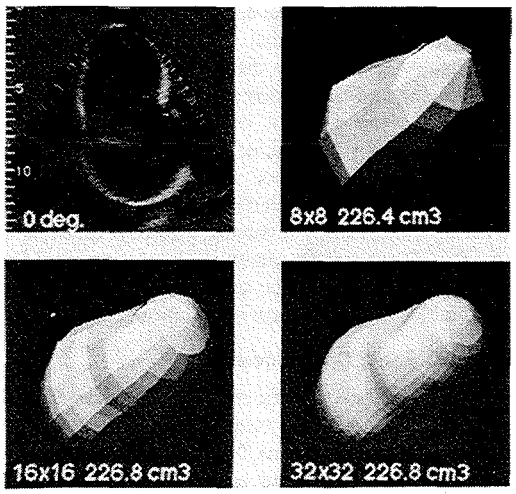

Figure 6 Examples of three-dimensional surface reconstructions with increasing axial resolution. Upper left panel shows two-dimensional long-axis ultrasound image (0 degree) of deformed latex phantom with true volume 230 cm^3. Subsequent panels show cavity surface reconstructions based on 0, 45, 90, and 135 degree images (latter three not shown) with increasing axial resolution (8, 16, and 32 points) and corresponding volume estimates. With increasing axial resolution, number of points displayed in circumferential direction is concordantly increased, and presented object surface approaches reconstructed smooth bicubic spline surface.

The present study assessed repeatability of volumes in patients who were not specifically selected for their image quality, and the results should therefore be relevant for everyday clinical practice. In contrast to most other reports on repeatability of 3D echocardiography,[7-8,14,16,24] the present study discriminates between the variability caused by recording and that caused by analysis of the ultrasound images. The interobserver repeatability was better for analysis than for recording and was generally best for end-diastolic volume and lowest for stroke volume, which is in agreement with results from 2D echocardiographic studies.[25] The lower repeatability for image recording than for analysis indicates how two investigators tend to image the left ventricle slightly differently. In serial studies this problem can be eliminated by allowing only one investigator to obtain the images. Repeatability for analysis of left ventricular volumes was approximately equal between (interobserver vari-

ability) and within (intraobserver variability) the investigators, indicating that the endocardial borders are defined similarly by different investigators and that tracing can be performed by more than one investigator when they are equally experienced. The repeatability for analysis of end-diastolic and end-systolic volumes was good with coefficients of variation at or below 4% and 6%, which is in agreement with a previous study involving a more complex system for 3D echocardiography.[24] The repeatability for analysis of stroke volume and ejection fraction was acceptable with coefficients of variation less than 9%.

Methodologic Considerations

We have assumed that the mitral annulus can be approximated by a planar curve, although it has been found to be saddle-shaped.[26] However, with the present algorithm the mitral annulus is reconstructed from the six or eight points on the true annulus identified on the three or four apical imaging planes, respectively, and represents in terms of volume an average of the spatial position of true annulus. Thus the reconstructed mitral annulus is not likely to produce significant errors in the estimate of left ventricular cavity volume.

Endocardial border definition is important for accurate 3D reconstruction and varies with image quality and heart rate. In our experience the precision of endocardial border tracing (on freeze frame) is markedly improved by use of the digital cineloop technology. Because the acquired images are transferred as digital scanline data directly to the computer, image quality and the high frame rate are preserved from recording to analysis with no need for video recording. We think that this is important for the good repeatability of analysis in this study of nonselected patients. Adequate reconstruction of left ventricular cavity requires regular cardiac rhythm, because data are sampled from different cardiac cycles. In this study all patients were in sinus rhythm.

We assessed clinical repeatability by sequential and blinded investigation of left ventricular volumes in patients during rest. Although the second assessment of each patient was performed immediately after the first and the total time for investigation of each subject was less than 1 hour, we cannot exclude small variations in true cardiac volumes between the assessments. The randomized sequence of the investigators should, however, ensure that this physiologic variation contributed equally to the results of the two investigators and did not influence repeatability results.

Conclusion

The present algorithm for 3D reconstruction of cavity surface is accurate over a wide range of shapes and volumes when both three or four image planes are used. Furthermore, volume estimates based on 3D reconstruction have less bias and are more repeatable than those of conventional biplane and single-plane methods. The algorithm performs well with standard ultrasound equipment without accessory devices and facilitates a feasible, repeatable, and relatively fast assessment of left ventricular volume in the clinical setting.

REFERENCES

1. Schiller NB, Acquatella H, Ports TA, et al. Left ventricular volume from paired biplane two-dimensional echocardiography. Circulation 1979;60:547-55.
2. Pearlman AS. Measurement of left ventricular volume by three-dimensional echocardiography—present promise and potential problems. J Am Coll Cardiol 1993;22:1538-40.
3. Nixon JV, Saffer SI, Lipscomb K, Blomqvist CG. Three-dimensional echoventriculography. Am Heart J 1983;106: 435-43.
4. Sawada H, Fujii J, Kato K, Onoe M, Kuno Y. Three dimensional reconstruction of the left ventricle from multiple cross sectional echocardiograms: value for measuring left ventricular volume. Br Heart J 1983;50:438-42.
5. Ariet M, Geiser EA, Lupkiewicz SM, Conetta DA, Conti CR. Evaluation of a three-dimensional reconstruction to compute left ventricular volume and mass. Am J Cardiol 1984;54:415-20.
6. Raichlen JS, Trivedi SS, Herman GT, St. John Sutton MG, Reichek N. Dynamic three-dimensional reconstruction of the left ventricle from two-dimensional echocardiograms. J Am Coll Cardiol 1986;8:364-70.
7. Zoghbi WA, Buckey JC, Massey MA, Blomqvist CG. Determination of left ventricular volumes with use of a new nongeometric echocardiographic method: clinical validation and potential application. J Am Coll Cardiol 1990;15: 610-7.
8. Schroeder KD, Sapin PM, King DL, Smith MD, DeMaria AN. Three-dimensional echocardiographic volume computation: in vitro comparison to standard two-dimensional echocardiography. J Am Soc Echocardiogr 1993;6:467-75.
9. Matsumoto M, Inoue M, Tamura S, Tanaka K, Abe H. Three-dimensional echocardiography for spatial visualization and volume calculation of cardiac structures. Journal of Clinical Ultrasound 1981;9:157-65.
10. Ghosh A, Nanda NC, Maurer G. Three-dimensional reconstruction of echocardiographic images using the rotation method. Ultrasound Med Biol 1982;8:655-61.
11. Fazzalari NL, Davidson JA, Mazumdar J, Mahar LJ, DeNardi E. Three dimensional reconstruction of the left ventricle from four anatomically defined apical two-dimensional echocardiographic views. Acta Cardiol 1984;39:409-36.
12. Geiser EA, Ariet M, Conetta DA, Lupkiewics SM, Christie LG, Conti CR. Dynamic three-dimensional echocardio-

graphic reconstruction of the intact human left ventricle: technique and initial observations in patients. Am Heart J 1982;103:1056-65.
13. Moritz WE, Pearlman AS, McCabe DH, Medema DK, Ainsworth ME, Boles MS. An ultrasonic technique for imaging the ventricle in three dimensions and calculating its volume. IEEE Trans Biomed Eng 1983;BME-30:482-91.
14. King DL, Harrison MR, King DL Jr, Gopal AS, Martin RP, DeMaria AN. Improved reproducibility of left atrial and left ventricular measurements by guided three-dimensional echocardiography. J Am Coll Cardiol 1992;20:1238-45.
15. Gopal AS, King DL, Katz J, Boxt LM, King DL Jr., Shao MY. Three-dimensional echocardiographic volume computation by polyhedral surface reconstruction: in vitro validation and comparison to magnetic resonance imaging. J Am Soc Echocardiogr 1992;5:115-24.
16. Sapin PM, Schroeder KD, Smith MD, DeMaria AN, King DL. Three-dimensional echocardiographic measurement of left ventricular volume in vitro: comparison with two-dimensional echocardiography and cineventriculography. J Am Coll Cardiol 1993;22:1530-7.
17. McCann HA, Sharp JC, Kinter TM, McEwan CN, Barillot C, Greenleaf JF. Multidimensional ultrasonic imaging for cardiology. Proceedings of the Institute of Electrical and Electronic Engineers 1988;76:1063-73.
18. Mæhle J, Bjørnstad K, Aakhus S, Torp HG, Angelsen BAJ. Three-dimensional echocardiography for quantitative left ventricular wall motion analysis: a method for reconstruction of endocardial surface and evaluation of regional dysfunction. Echocardiography 1994;11:397-408.
19. Henry WL, DeMaria A, Gramiak R, et al. Report of the American Society of Echocardiography Committee on nomenclature and standards in two-dimensional echocardiography. Circulation 1980;62:212-7.
20. Henry WL, DeMaria A, Feigenbaum H, et al. Report of The American Society of Echocardiography Committee on Nomenclature and Standards: identification of myocardial wall segments. 1982.
21. Altman DG. Practical statistics for medical research. London: Chapman & Hall, 1991.
22. Bland JM, Altman DG. Statistical methods for assessing agreement between two methods of clinical measurement. Lancet 1986;ii:307-10.
23. Farin G. Curves and surfaces for computer aided geometric design. Boston: Academic Press, Inc., 1988.
24. Handschumacher MD, Lethor JP, Siu SC, et al. A new integrated system for three-dimensional echocardiographic reconstruction: development and validation for ventricular volume with application in human subjects. J Am Coll Cardiol 1993;21:743-53.
25. Wallerson DC, Devereux RB. Reproducibility of quantitative echocardiography: factors affecting variability of imaging and Doppler measurements. Echocardiography 1986;3:219-35.
26. Levine RA, Handschumacher MD, Sanfilippo AJ, et al. Three-dimensional echocardiographic reconstruction of the mitral valve, with implications for the diagnosis of mitral valve prolapse. Circulation 1989;80:589-98.

Reconstruction and Analysis of Left Ventricular Surfaces by Three-Dimensional Echocardiography. I. Quantitation of the Endocardial Surface Area

Abstract

Objectives. The aim of this study was to test the accuracy of a new algorithm for three-dimensional reconstruction with respect to left ventricular (LV) surface area, and to study validity of endocardial surface areas (ESA) obtained from 3 standard LV long-axis apical ultrasound views.

Background. Three-dimensional reconstruction of LV cavity can be performed from endocardial tracings of apical images using bicubic spline interpolation. Previous studies have shown high accuracy for in vitro volume calculations and good reproducibility for in vivo determination of LV volumes, whereas the validity of the algorithm for calculations of ESA has not been established.

Methods. Surface area calculations of 9 predefined objects with rotational symmetry was obtained with the present algorithm. Validity of ESA derived from 3 apical views was studied by comparison of circumferences in manually drawn endocardial borders with those obtained by cubic spline interpolation on 6 sampled points. This was performed in 10 subjects (with and without wall motion abnormalities) at midventricular short-axis edges. The impact of error in assumed angles of the apical scan-planes was also tested in all views and all edges.

Results. Error in reconstructed surface areas of rotational symmetric models compared to the analytically calculated values were - 0.5 ± 0.8 %. The difference between circumference in interpolated and original edges was - 2.1 ± 0.9 %, and the error in circumference from error of ± 15 degrees in plane angles was 0.0 ± 1.6 %.

Conclusions. The present 3D algorithm calculates surface area accurately in models. LV circumferences, the major determinant for ESA, are reproduced with high precision by the cubic spline method on 6 points, defined by 3 apical planes, and with higher precision than for volumes validated in similar studies.

Key words: Echocardiography, Three-Dimensional Reconstruction, Endocardial Surface Area, Left Ventricular Function

Introduction

We have previously presented an algorithm for three-dimensional (3D) reconstruction of the left ventricular (LV) endocardial surface based on a limited number of two-dimensional (2D) echocardiographic images obtained from an apical transducer position [1]. The method has been validated for volume calculations [2-4] and for assessment of LV function from visual judgment of 3D geometry [5-7]. The method uses cubic spline interpolation, and gives a detailed description of the reconstructed endocardial surfaces. In addition to LV volumes several quantitative indices with clinical potential can be derived from such an endocardial surface description.

Quantitation of the total endocardial surface area (ESA) and the size of regional wall motion abnormalities by coronary artery disease has prognostic implications, and can be followed with serial studies [8]. One method for determination of ESA using multiple 2D echo-cardiographic scans has been proposed and validated [9-11], whereas such measurements have more recently been reported from 3D echocardiography [12,13]. The surface description obtained from our 3D reconstruction method allows surface area calculations, and further analysis of regional LV function as wall motion calculations for assessment of ischemic diseases [1,14].

The reproducibility of surface area calculation is crucial for the clinical value of the ESA as an index for serial studies, e.g. in ventricular remodelling after myocardial infarction [8]. Thus, we have tested the method in 2 ways; - 1) the precision in determination of surface area in rotational symmetric models, - and 2) by a study of reproducibility of endocardial borders in short-axis, the accuracy of surface area generated from only 3 apical imaging planes.

Methods

Computer program for 3D reconstruction of endocardial surfaces and analysis of LV function.

Reconstruction and representation of the endocardial surface. The reconstruction procedure is based on 3D data obtained by rotation of the imaging plane with the ultrasound transducer at the apical position [15-17]. The method has been described in details previously [1,2]. The input data for surface reconstruction are the LV endocardial borders from

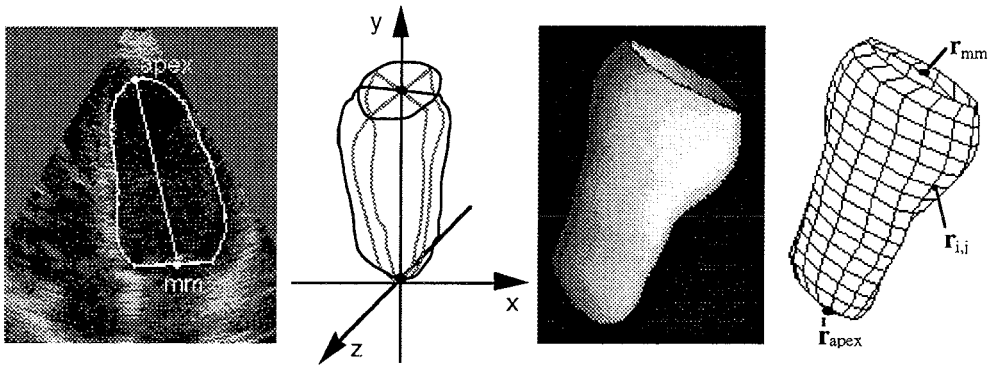

Figure 1. Procedure for reconstruction of the endocardial surface: - **a)** edge defining endocardial border in 2D ultrasound image obtained from apical transducer position, including left ventricular landmarks apex and mitral midpoint (see text). - **b)** Reassembling of edges in an 3D coordinate system. - **c)** Bicubic spline representation of the reconstructed endocardial surface (i. e. high resolution shadow display). - **d)** Wire-frame display of the same surface (low resolution) illustrating data format used for further analysis based on the reconstructed surface; the apex and the mitral midpoint, $\mathbf{r}_{apex}$ and $\mathbf{r}_{mm}$, and the points $\{ \mathbf{r}_{i,j} \}$ at the mesh corners.

2D images, and their spatial position given by the rotation angles of the imaging planes. The algorithm produces equidistant parallel short-axis contours by cubic spline curves interpolating the apical borders, which are aligned in the 3D space according to rotation angles of the imaging planes and by a common position of the ventricular apex and mitral plane midpoint (Fig. 1a,b). With this procedure the endocardium will be reconstructed as a smooth bicubic spline surface (Fig. 1c), including the mitral valve annulus and the ventricular apex. The algorithm compensates for foreshortened imaging by edge elongation so that the length of all the ventricular major axis (apex to mitral plane midpoint distance) equals the longest one. To reduce sensitivity of apex position to inaccuracy in edge drawing, the algorithm adjusts the apex position so that the major axis passes through the area center of the apical part of the ventricle.

For display and further calculation the algorithm provides geometric data comprising a matrix of 3D points $\{ \mathbf{r}_{i,j} \}$ on the reconstructed surface and the points $\mathbf{r}_{apex}$ and $\mathbf{r}_{mm}$ at the positions of the apex and the mitral plane midpoint respectively (Fig. 1d). The ventricular major axis is defined as the straight line connecting these latter points. Each point is given in Cartesian coordinates $\mathbf{r}_{i,j} = (x_{i,j} , y_{i,j} , z_{i,j})$ positioned in space with the center of mass of the LV cavity fixed at origo, and with a common direction of the major axis and the y-axis. The range of indexes, i and j, are optional according to axial and circumferential resolution denoting the

number of ventricular cross-sections to be reconstructed and the number of points to be stored on each reconstructed cross-section.

Volume calculations. Cavity volume (in ml) and the position of the center of mass is determined within the algorithm by successive calculations from the cubic spline representation of parallel cross-sections in the reconstructed surface. The volume is thereby determined from a disc summation method, where the number of discs equals the selected axial resolution. Because the spline format is used in these calculations, the volume estimates are not influenced by the circumferential resolution.

Surface rendering. The reconstructed 3D endocardial surface can be displayed by shadowing or wire-frame (Fig. 1), or by drawing of the reconstructed cross-sectional borders. By computerized rotations of the 3D object, the left ventricle can be viewed in 6 selectable anatomical projections according to anterior, posterior, superior, inferior, dexter, or sinister position of the observer.

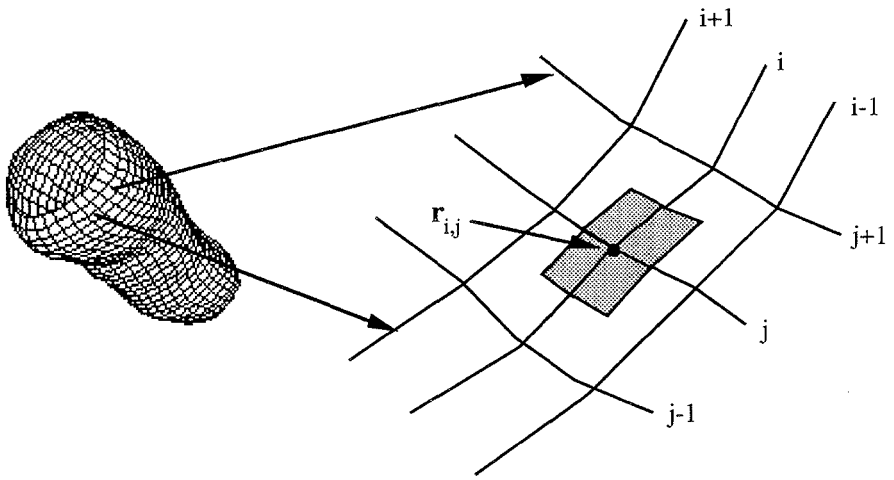

Figure 2. Geometric representation of area $a_{i,j}$ associated with point $\mathbf{r}_{i,j}$. A part of the wire-frame image is magnified, and the area at the point is composed of 4 parallelograms defined from of straight lines from the point halfway to its neighbours.

Surface area calculations. The reconstructed endocardial surface is subdivided into small areas $a_{i,j}$ surrounding each point $\mathbf{r}_{i,j}$ of the surface. Each little area $a_{i,j}$ includes the 4 parallelograms defined by the lines starting at the point $\mathbf{r}_{i,j}$ traversing half the distance to the

neighbour points (Fig. 2 and Appendix A). The results are stored in an matrix $\{ a_{i,j} \}$ for further calculations of ESA and regional indices of LV function. The endocardial surface area (in cm^2) is calculated as the sum of the matrix elements

$$ESA = \sum_{i,j} a_{i,j}$$

The mitral valve orifice is not included, whereas the aortic valve orifice is included in the ESA. The estimate converges to the surface area of reconstructed endocardial surface as the resolution increases.

Instrumentation

An ultrasound scanner (Vingmed 750, Vingmed Sound, Horten, Norway) with a 3.25 MHz annular array transducer was used for imaging. The ultrasound images were transferred as digital scan-line data to a computer (Macintosh series II, Apple Computers, Cupertino, California) for storage and further analysis. Computerized analysis was performed using commercially available software (EchoDisp version 3.0, Vingmed Sound). The algorithms for 3D reconstruction and analysis were implemented in so-called ECARs (EchoDisp Custom Analysis Routines, Vingmed Sound), a system allowing development of user specified routines to work inside the EchoDisp program.

Validity of surface area calculations from 3D echocardiographic reconstruction.

Accuracy of surface area in objects with rotational symmetry. Reproducibility of surface area calculations (and volumes) was tested by drawing of borders defining objects with axial symmetry in an arbitrary 2D ultrasound image on the computer, which were used to produce 3D objects with rotational axial symmetry (Fig. 3). This was obtained by using the same border with 3 different angles (0, 62, and 101 degrees [18]) within the 3D reconstruction method. We selected 3 objects in which volumes and surface areas could be calculated analytically from an one dimensional variable: 1) a sphere - 2) a "bullet" composed of a cylinder and a cone where the radius equals the height of both the cylinder and the cone -and 3) half of an ellipsoid where the minor axis length was 50 % of the major axis. Different dimensions of the

objects were used to obtain volumes ranging from 14 to 515 ml. The surface areas and volumes were determined from 3D reconstruction at the resolution of 32x32 and 64x64, and the results were compared to the corresponding analytical calculations.

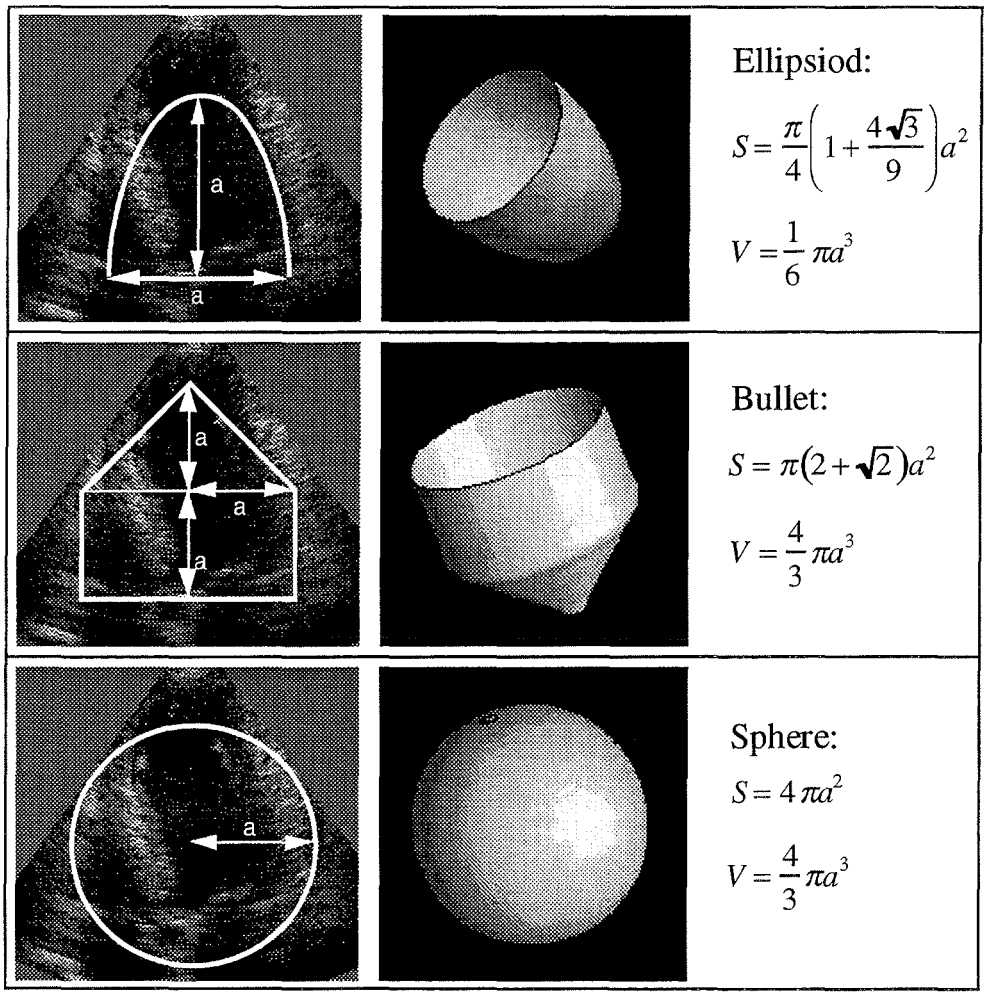

Figure 3. Models for validation of surface area calculations. Left panel shows 2D object of axial symmetry drawn in an arbitrary ultrasound image, middle panel the results from 3D surface reconstruction, and right panel the formulas used for exact calculations of volume and surface area.

Clinical echocardiographic study of reproducibility of short-axis endocardial borders from 3D reconstruction by apical rotation method and cubic spline interpolation.

Accuracy in circumference reconstructed from 3 apical views. In the non-symmetrical ventricles the reproducibility of circumferences in short-axis borders is the major factor determining the accuracy in the estimation of ESA. We have therefore tested 2 aspects of the reconstruction of short-axis circumferences from 3 apical imaging planes obtained by rotation. First, how well is circumferences reconstructed from 6 sampled points at the border according to the 3 imaging planes at 0, 62 and 101 degrees, and second, how are the estimates of circumference influenced by angular deviation (± 15 degrees) of the imaging planes from their assumed position? The actual values of these angles were decided from the assumed position of the 3 standard apical long axis views; 4-chamber, 2-chamber, and long-axis [18,19], and in accordance to previous studies for LV volumes [2-4].

The accuracy of short-axis circumference was tested in 10 patients (8 men and 2 women), aged 24 to 66 years, with (n=6) or without (n=4) LV regional wall motion abnormalities at rest due to previous myocardial infarction. All were in sinus rhythm. Cineloops of the midventricular short axis were recorded by imaging from parasternal position and transferred to the computer. The endocardial borders were traced by an experienced clinician in end-diastole and end-systole, ignoring the papillary muscles. At each border a closed cubic spline curve was generated by interpolation through 6 points defined from the intersection of the 3 apical imaging planes and the traced border (Fig. 4 a). The circumference of the spline curve was compared with that of the original traced border and the percent difference was recorded.

Impact of error in angular position of imaging planes. The 3 apical imaging planes (4-chamber, 2-chamber, and long axis) used for 3D reconstruction may deviate up to 15 degrees from their assumed spatial position [18]. In order to investigate how this deviation influenced the estimated cross-sectional circumference, and thereby estimated ventricular surface area, we successively rotated the lines representing the imaging planes + 15 and - 15 degrees, from their predefined positions, around the center of area within the traced border. Sampled points for border interpolation were found at the intersection of the traced border and these lines, and the points' position were defined by the rotation angle of the plane and the radial distance to

the center of rotation. The border reconstruction was performed by cubic spline interpolation assuming that these points (the radial distance) were found in imaging planes at the predefined angles 0, 62 and 101 degrees (Fig. 4 b). This process was repeated in all combinations (27) of angular deviations in both end-systole and end-diastole frames in all 10 subjects, and the difference in circumference between the reconstructed border with angular deviation and that with no angular deviation was calculated in percent of the latter.

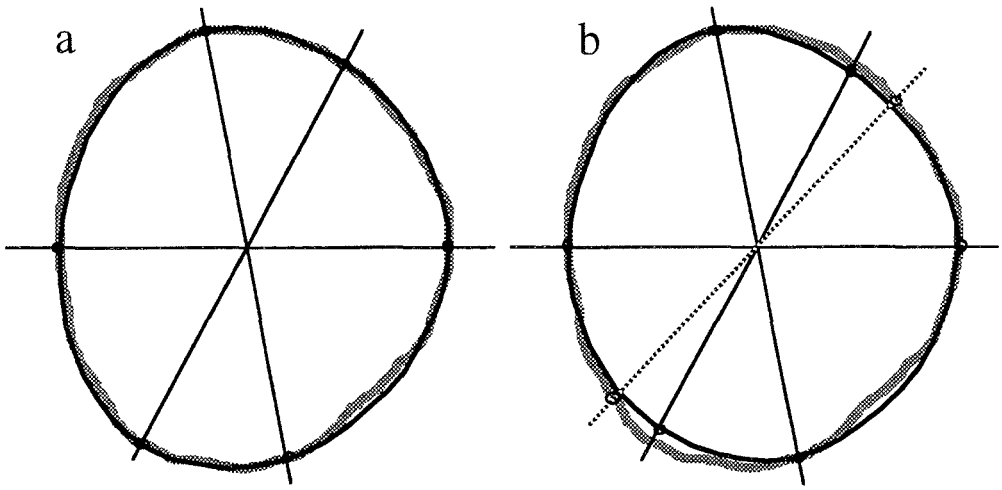

Figure 4. Reconstruction of LV short axis borders by cubic spline interpolation. - **a)** display of original short axis border (dotted) and the cubic spline curve (solid) defined from 6 points at the original border. The points are found at the intersection between the original border and lines corresponding to apical imaging plane at angles 0, 62, and 101 degrees. The circumference of the reconstructed border is 0.6 % less than the original. - **b)** illustration of result if one imaging plane deviates 15 degree from assumed angular position. Points are found along the dashed line, but the reconstruction is performed as if the points (i.e. their radial distance to the center) were found at the solid line with assumed angular position. The circumference of this reconstructed border is 1.4 % less than the circumference of the spline curve obtained with no angular deviation (a).

Statistical analysis

Values, differences between value from reconstruction method and original value in percent of the latter, are presented as mean ± standard deviation. Confidence limits are calculated by standard method. Surface area of rotational symmetric shape by 3D reconstruction and circumferences of reconstructed cross-sections by cubic spline interpolation are compared with respective true values by simple linear regression, and agreement was assessed with the correlation coefficient (r) and by standard error of estimate (SEE).

Results

Validity of surface area calculations from 3D echocardiographic reconstruction

Accuracy of surface area in objects with rotational symmetry. Both surface area and volumes determined from the 3D reconstruction agreed well with the corresponding values analytically calculated from exact formulas (Tab. 1, and Fig. 5). The difference in surface area from reconstruction and from formulas in percent of the latter was found to be - 0.46 ± 0. 84 % and - 0.14 ± 0.87 % (9 objects), respectively, for the selected resolution of 32x32 and 64x64. For volumes, the same difference was found to be - 0.25 ± 1.5 %, for selected resolution of 32x32 and 64x64. The estimated surface areas increased with increasing resolution, but the increase was less than 0.5 % when the resolution is changed from 32x32 to 64x64. Volumes estimates were not affected by the same increase in resolution.

Table 1. Computer study of models with rotational symmetry. Comparison of surface areas and volumes obtained from 3D reconstrution and values calculated by formul

	Surface area calculatio			Volume calculation		
		reconstruction - true			reconstruction - true	
shape (cm)	true (cm2)	32x32 (%)	64x64 (%)	true (cm3)	32x32 (%)	64x64 (%)
ellipsoid (3.0)	24.5	1.24	1.65	14.1	2.84	2.84
ellipsoid (6.0)	95.6	-1.14	-0.83	113.1	-1.68	-1.68
ellipsoid (8.0)	171.8	0.00	0.23	268.1	0.41	0.41
sphere (2.5)	78.5	0.00	0.38	65.5	0.46	0.46
sphere (4.0)	199.9	-0.60	-0.25	268.1	-0.07	-0.07
sphere (5.0)	311.2	-0.95	-0.57	523.6	-0.57	-0.55
bullet (2.0)	42.2	-1.63	-1.40	33.5	-2.39	-2.39
bullet (3.5)	131.1	-0.23	0.08	179.6	-0.17	-0.17
bullet (4.5)	215.3	-0.87	-0.55	381.7	-1.07	-1.10

Values denoted true are calculated from formulas given in Fig. 7. Values obtained from reco: struction at selected resolutions, 32x32 and 64x64, are given in percent deviation from corresponding true value: 100 * (value from reconstruction - true) / true

Using the drawing tools supplied in the EchoDisp program, the 2D axial symmetric shapes can be drawn with an accuracy of the characteristic dimensions (see Fig.3) at ± 1 %. Due to this accuracy the estimates of surface area and volumes can deviate respectively ± 2 and ± 3 % from the expected values (Appendix B), regardless of inaccuracy due to computer algorithms. In our material all the determined surface areas and volumes were within these limits, indicating that both surface area and volume of a reconstructed ventricle (i.e. the bicubic spline surface) can be determined at sufficient precision at selected resolution of 32x32. Thus, errors from numerical calculation of volumes and surface areas are negligible, and less important than potential inaccuracies due to imaging and edge drawing.

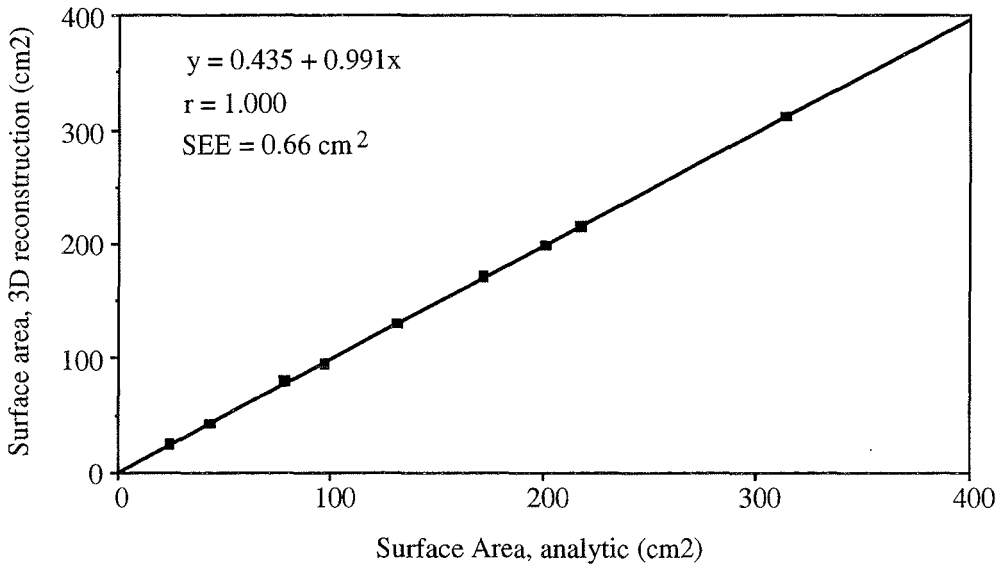

Figure 5. Plot of surface area of rotational symmetric models obtained from the 3D reconstruction algorithm against corresponding (true) values calculated by exact formulas (Fig. 3).

Clinical echocardiographic study of reproducibility of short-axis endocardial borders from 3D reconstruction by apical rotation method and cubic spline interpolation.

Accuracy in circumference reconstructed from 3 apical views. The circumferences of the traced endocardial short-axis borders analyzed in this study were in the

range of 9.8 to 23.4 cm. The average difference between circumference of the closed spline curve generated through 6 border points (i.e. at apical imaging planes at 0, 62, 101 degree of rotation) and that of the original short-axis endocardial border in percent of the latter was - 2.0 ± 0.9 % (20 edges), with 95 % limits of agreement: - 0.2 to - 3.9 %. The results were similar for end-systolic and end-diastolic circumferences (Fig. 6).

Impact of error in angular position of imaging planes. The average difference between the reconstructed circumference generated from the 6 points found at lines corresponding to successive deviation of ±15 degrees of the imaging planes from their assumed position and that of the curve generated from points found at the assumed position of the planes, was 0.0 ± 1.6 % (20 edges x 26 combinations), with 95 % limits of agreement: - 3.0 to 3.1 %. These results were also similar for end-systolic and end-diastolic circumferences (Fig.7).

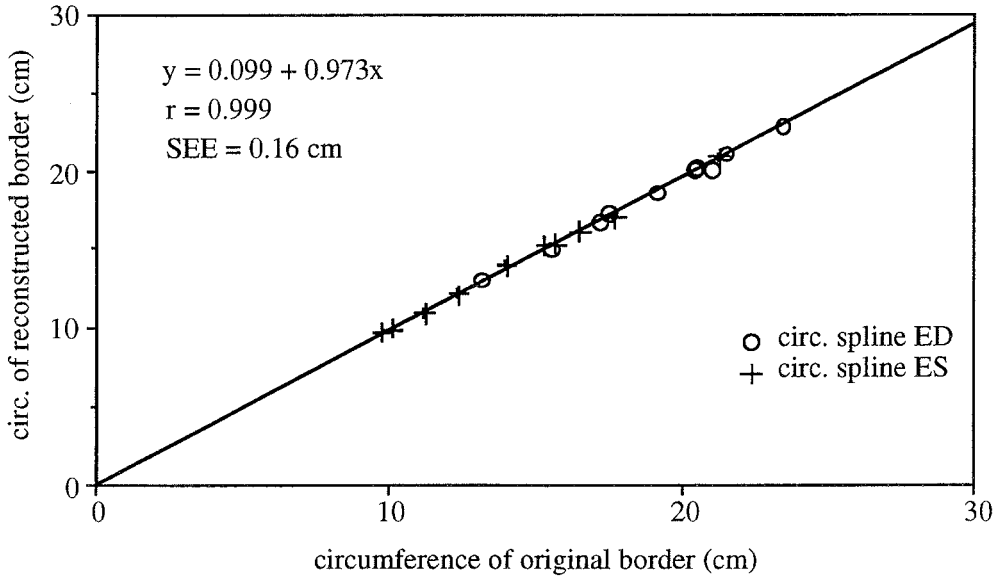

Figure 6. Plot of circumferences of curves obtained by cubic spline interpolation through 6 points at original (manually drawn) LV cross-sectional borders against circumferences of original borders. The interpolation points are found at the intersection between lines corresponding to apical planes at 0, 62, and 101 degrees and the original border (see Fig. 4a). End-systole borders are indicated with crosses, and end-diastole borders with circles. Simple regression is performed on the basis of all plotted values.

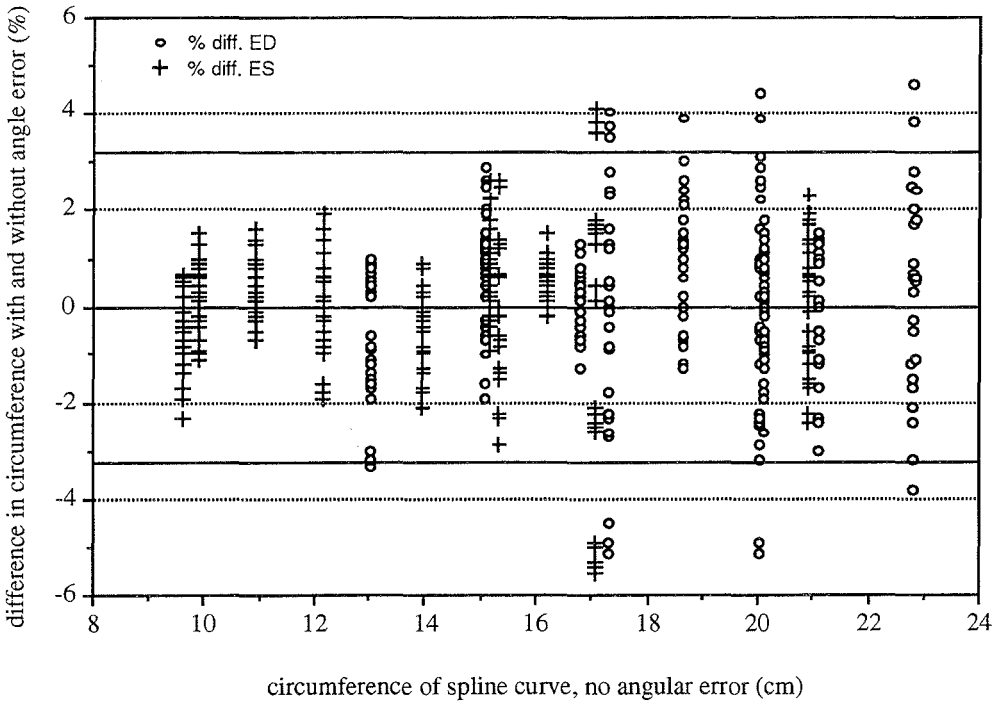

Figure 7. Plot of differences in circumference against circumference of the original spline curve. The differences are calculated as circumference of spline curves reconstructed from points found at lines with deviation from assumed angular position minus that of the original spline curve from point found at correct angular position, and the results are given in percent of the original circumference. At each original border the three lines (corresponding to apical planes at 0, 62 and 101 degrees) were deviated ± 15 degrees at the 26 possible combinations (see Fig. 4b). End-systole borders are indicated with crosses, and end-diastole borders with circles. Mean ± 2SD is represented with solid lines.

Discussion

In this work we have used a new simple echocardiographic method for reconstruction of endocardial surfaces. The reconstruction algorithm produces a mathematical description of the surface suitable for calculations of the ESA, and area of regions with abnormal LV function as presented in accompanying article [20]. The results in this study indicate that the ESA could be calculated with high precision using 2D data from routine echocardiographic investigations.

Echocardiographic surface reconstruction. The activity in 3D echocardiography during 2 decades has been motivated from volume calculation avoiding assumptions of idealized geometry, and for display of 3D and 4D (3D + time) cardiac structures [15-17,21-29]. Several methods of data collection for reconstruction of 3D geometry have been reported, and are based on different techniques for spatial registration and reassembly of ultrasound 2D scans. The apical rotation method has the advantage of being simple since no or little extra instrumentation is needed for registration or control of spatial position of the imaging plane. All the imaging views are obtained from one transducer position, and the apical window is generally recommended for 2D ultrasound imaging in patients with coronary artery diseases [30].

The present algorithm for surface reconstruction is flexible as it can handle input data from a variable number (3-12) of imaging planes. In clinical practice it is of great importance to keep the time and complexity of data acquisition at a minimum. Therefore the clinical potential of surfaces generated from only 3 imaging planes collected in routine echocardiographic examinations is of great interest. Previous works have shown that 3D echo in general gives more accurate volume estimates than standard 2D echocardiographic methods [31-34], and in particular that volumes calculated from 3 apical planes are more accurate than the 2D methods [2-4,35]. Surface areas of objects are in general more difficult to determine than volumes, and for irregular shapes like the LV endocardium the variation in curvature in both axial and circumferential direction have to be taken into account, while the accuracy of cavity volumes from disk summation only depends on accuracy in areas inside planar circumferential contours. Calculations of ESA should therefore be based on adequate 3D description of the endocardium obtained from 3D reconstruction.

The application of cubic spline interpolation produces optimal curves in respect to smoothness; of all possible curves preserving smoothness and direction (i.e. continuous first and second derivatives) through the interpolation points, the cubic spline curve has minimum variation in curvature. The minimum variation in curvature coincides with the minimum strain energy [36], thus providing a highly probable guess for the position of the surface in intervals between sampled geometry. By interpolation, the endocardium is generated as a smooth continuous bicubic spline surface, which for further display and quantitative analysis is described by a selectable number of data points at the smooth reconstructed surface.

Endocardial surface area calculation. The algorithm calculated exactly the surface area of rotational symmetric objects, and at sufficient precision using 32x32 surface points.

Due to the method of triangle summation this result can be extrapolated also to yield for asymmetric objects, whereas the sum converges to the true area of the computer generated smooth surface representing the endocardium [appendix A]. The triangle summation is also used by King et. al. [12], while the area mapping method, used in several works [8,10,11,37,38], came out with a systematic error of 7 % applied to spherical models [9]. Our results (Tab. 1) show less error (lower SD) in surface areas than for volumes due to inaccuracy in edge definition, as expected because a lower exponent of power in area calculations than in volume calculations [appendix B]. Therefore, ESA may be suggested for comparative and serial studies as being less sensitive for errors due to edge detection in ultrasound images than volumes.

With our reconstruction algorithm the reproducibility of circumferences in cross-sectional contours will correspond closely to the reproducibility of the surface area of the endocardium, similarly to how cross-sectional disk areas correspond to volumes [2]. Reproducibility of circumferences with spline interpolation - 2.0 ± 0.9 %, is comparable with that for cross-section areas - 1.2 ± 1.6%, and less sensitive to angular deviation (0.0 ± 1.6 % vs. 0.3 ± 3.2 %), using 3 apical imaging planes at 3 assumed angular positions. These results are consistent with those from the rotational symmetric shapes, favouring ESA compared LV volumes with respect to reproducibility in estimates and low sensitivity to errors in rotation angles of the imaging planes. We observe an increased bias represented by underestimation in circumferences compared to cross-section areas. This underestimation in circumference is partly caused by high frequency noise in manually drawn edges that is removed by interpolation. Nevertheless, the study of surface areas by circumference reconstruction has limitations, while curvature in axial direction not affect LV volume estimation it does for ESA. The influence of this curvature cannot be ignored, however, for the LV the curvature in circumferential direction will be the dominant factor in calculation of the ESA.

Compared to method of Guyer et. al. using 5 standard views (2 apical, and 3 short-axis) [9], and the method of King et. al. [12] which requires additional hardware for registration of scan-plane position, the present method provides estimates of ESA at sufficient accuracy from 3 standard apical view and predefined angles in spline interpolation for surface generation.

Limitations and future work. Although this study give a strong indication of increased repeatability in estimation of ESA as compared to LV volumes, and that volumes are accurately estimated by the present algorithm, we have not validated the method for ESA in

asymmetric ventricular shapes. Further studies should be performed evaluating 3D determination of surface area in phantoms and in vitro ventricles, and for assessment of interobserver repeatability of ESA calculations in vivo.

The quantitation of area of abnormal wall motion (AWM) is the natural next step; the two quantities, ESA and AWM, form a strong basis for prognostic and serial studies of LV remodelling. The clinical importance and potential of ESA and AWM for prognostic evaluation of myocardial infarction is discussed in works from Picard et. al. [8,37,38], and for serial follow-up studies it is of great importance that thansthoracic echocardiographic techniques are both noninvasive and time effective. The surface representation from our algorithm is prepared for calculations of AWM, and method for estimation and display of AWM are proposed in accompanying article [20].

The reconstructed endocardium will represent a smoothed version of the real endocardium without the papillary muscles and high frequency surface irregularities by the trabecular web. These structures would increase the ESA, however, they are not relevant for the ventricular dimension expressed in ESA. In fact, the papillary muscles are a source of error for volume estimation, but not for ESA calculated by the present method.

The shape of the LV outflow tract will be poorly reconstructed due to low spatial sampling. To improve the reconstruction of this region a higher number of scan-planes for the algorithm is needed, and it would be of general interest to study how the number of imaging planes influence accuracy of ESA and volumes [39]. Adding more scan-planes for surface reconstruction would require extra devices for measurement of rotation angles or for controlled rotation of the imaging plane [1]. With 3 standard apical plane used for surface reconstruction, we have seen that both volumes and ESA in minor degree are influenced by deviation from the assumed rotation angles of the imaging planes. However, angle measurements should ideally be applied in this situation, and it remains to determine optimal values of the predefined angles to be used for LV reconstruction from the 3 standard apical planes.

The use of 3 apical planes is very appealing because they are usually collected by standard echocardiographic examinations, and the time needed for 3D estimates of volumes and ESA should be within an acceptable range. Manual drawing of edges (at end-diastole and end-systole frames) normally requires less than 10 min., and the computer processing is completed within a few seconds. Edge detection in ultrasound images of suboptimal quality remains the crucial source of error and time consumption for extraction of quantitative indices from 2D

echocardiography. The ongoing development in image enhancement and computerized edge detection will most probably increase the effectivity and outcome of 3D quantitative echocardiographic analysis.

Clinical applications and conclusions. Left ventricular volumes and ejection fraction are desired quantities for assessment of LV function. Compared to recommended methods for echocardiographic volume estimation from 2 apical planes [40, 41], the presented method with only one imaging plane extra increases the accuracy in volume estimation, display the reconstructed 3D shape of the endocardium, provides accurate estimates of ESA, and finally enables calculation of areas with abnormal wall motion. The present method is optimal in respect to simplicity, thus enables ESA calculation at sufficient precision in clinical practice.

Appendix

Appendix A. Vector algebra applied in computer implementations for calculations of surface areas

Algebra of 3-dimensional vectors. A point **r** in 3D Cartesian coordinate system is represented as a vector (Fig. A1):

$\mathbf{r} = (x, y, z)$ where the real number x, y, z are the coordinates of the point

The length (norm) of the vector, is denoted $|\mathbf{r}|$ and equals the distance between the point and origo, is calculated by

$$|\mathbf{r}| = \sqrt{x^2 + y^2 + z^2} \qquad \text{(A.1)}$$

Addition, subtraction (Fig. A1) and multiplication with a scalar is defined by

$\mathbf{r}_1 + \mathbf{r}_2 = (x_1 + x_2, y_1 + y_2, z_1 + z_2)$

$\mathbf{r}_1 - \mathbf{r}_2 = (x_1 - x_2, y_1 - y_2, z_1 - z_2)$

$a\mathbf{r} = (ax, ay, az)$, a is an arbitrary real number

The expression $|\mathbf{r}_1 - \mathbf{r}_2|$ will calculate the distance between the points $\mathbf{r}_1$ and $\mathbf{r}_2$.

The cross-product of 2 vectors $\mathbf{r}_1$ and $\mathbf{r}_2$ produces a new vector by

$$\mathbf{r}_1 \times \mathbf{r}_2 = (y_1z_2 - y_2z_1, x_2z_1 - x_1z_2, x_1y_2 - x_2y_1) \qquad \text{(A.2)}$$

with $\mathbf{r}_3 = \mathbf{r}_1 \times \mathbf{r}_2$, the vector $\mathbf{r}_3$ is perpendicular to both $\mathbf{r}_1$ and $\mathbf{r}_2$, and the magnitude $|\mathbf{r}_3|$ equals the area of a parallelogram defined from the vectors $\mathbf{r}_1$ and $\mathbf{r}_2$ (Fig. A1).

Application to surface area calculations. The part of endocardial surface $a_{i,j}$ associated to each point $\mathbf{r}_{i,j}$ (see Fig. 2) in the ventricle is calculated by

$$a_{i,j} = \frac{1}{4}\left|\left(\mathbf{r}_{i-1,j} - \mathbf{r}_{i,j}\right) \times \left(\mathbf{r}_{i,j-1} - \mathbf{r}_{i,j}\right)\right| + \frac{1}{4}\left|\left(\mathbf{r}_{i-1,j} - \mathbf{r}_{i,j}\right) \times \left(\mathbf{r}_{i,j+1} - \mathbf{r}_{i,j}\right)\right|$$
$$+ \frac{1}{4}\left|\left(\mathbf{r}_{i+1,j} - \mathbf{r}_{i,j}\right) \times \left(\mathbf{r}_{i,j-1} - \mathbf{r}_{i,j}\right)\right| + \frac{1}{4}\left|\left(\mathbf{r}_{i+1,j} - \mathbf{r}_{i,j}\right) \times \left(\mathbf{r}_{i,j+1} - \mathbf{r}_{i,j}\right)\right| \qquad \text{(A.3)}$$

and at points $\mathbf{r}_{n,j}$ in the mitral valve annulus by

$$a_{n,j} = \frac{1}{4}\left|\left(\mathbf{r}_{n-1,j} - \mathbf{r}_{n,j}\right) \times \left(\mathbf{r}_{n,j-1} - \mathbf{r}_{n,j}\right)\right| + \frac{1}{4}\left|\left(\mathbf{r}_{n-1,j} - \mathbf{r}_{n,j}\right) \times \left(\mathbf{r}_{n,j+1} - \mathbf{r}_{n,j}\right)\right| \qquad \text{(A.4)}$$

n is the axial resolution and refers to the cross-section at the mitral valve annulus and at points $\mathbf{r}_{1,j}$ connected to the apex by

$$a_{1,j} = \frac{1}{4}\left|\left(\mathbf{r}_{apex} - \mathbf{r}_{1,j}\right)\times\left(\mathbf{r}_{1,j-1} - \mathbf{r}_{1,j}\right)\right| + \frac{1}{4}\left|\left(\mathbf{r}_{apex} - \mathbf{r}_{1,j}\right)\times\left(\mathbf{r}_{1,j+1} - \mathbf{r}_{1,j}\right)\right| \tag{A.5}$$

i = 1 refers to a cross-section nearest to the ventricular apex.

The surface area of the mitral valve orifice is calculated by

$$S_{mp} = \frac{1}{2}\sum_{i}\left|\left(\mathbf{r}_{n,i} - \mathbf{r}_{mm}\right)\times\left(\mathbf{r}_{n,i+1} - \mathbf{r}_{mm}\right)\right| \tag{A.6}$$

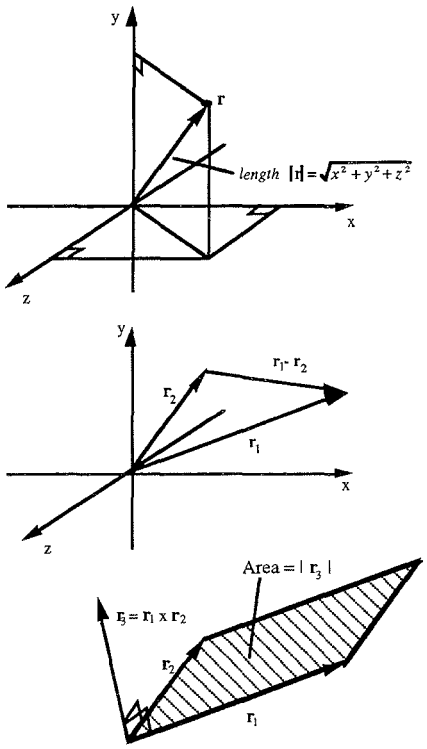

Figure A1. Vectors and vector operations in three dimensions. Top: vector representation of point and the length of a vector. Middle: difference between two vectors. Bottom: cross-product of two vectors.

Estimation of surface area of a patch defined from 4 point in space: surface area are usually calculated numerically by summation of areas in planar triangular patches by use of formula (A.2). The part of a surface area within 4 points can be estimated by 2 different sub-divisions in triangular planar patches as illustrated in Fig. A2. Both subdivisions will give the

correct areas only if the 4 points were situated on a planar surface. By application of formula (A.3) the (endocardial) surface area in a patch defined by 4 point will be calculated as the average of the areas from the 2 possible subdivision in triangular patches.

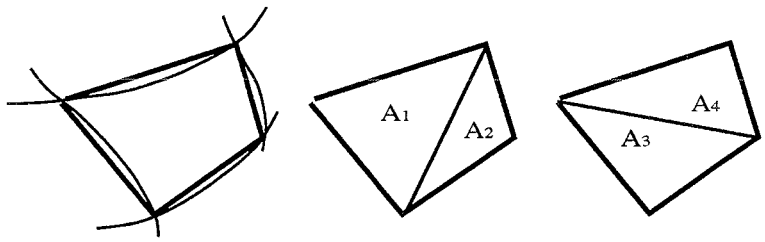

Figure A2. Two choices for estimation of surface area inside a patch defined from 4 points by subdivision in triangular patches (middle and right panel). The left panel illustrates the 4 points connected with solid lines, whereas the curved lines resides on the smooth surface. The calculation by formula (A.3) represents the estimate determined from an average: $A = 0.5\,(A_1 + A_2) + 0.5\,(A_3 + A_4)$.

Appendix B. Accuracy in determination of surface area and volume of an object due to inaccuracy in estimation of characteristic length of the object.

Given a characteristic length, a (e. g. radius, height, major axis), of an 3D object with defined geometry, surface area and volume can be calculated by formulas

$$S = k_S a^2 \qquad and \qquad V = k_V a^3 \tag{B.1}$$

where the constants are specific for the geometry of the object (see Fig. 3).

By differentiation we obtain the relation between error in surface area dS and error in the characteristic length as

$$\frac{dS}{da} = 2k_S a \qquad \Leftrightarrow \qquad dS = 2k_S a da \tag{B.2}$$

Division by $S = k_S a^2$ gives the relation between relative error in surface area and length as

$$\frac{dS}{S} = 2\frac{da}{a} \tag{B.3}$$

Similarly we find the relation between relative error in volume and length as

$$\frac{dV}{V} = 3\frac{da}{a} \tag{B.4}$$

We conclude that a relative error in estimation of length will be doubled and tripled in derived estimates of surface area and volume respectively.

Acknowledgement

Svend Aakhus, MD, at Section of Cardiology, University of Trondheim, has provided echocardiographic data for this study.

References

1. Mæhle J, Bjoernstad K, Aakhus S, Torp H G, Angelsen BAJ. Three-dimensional echocardiography for quantitative left ventricular wall motion analysis. A method for reconstruction of endocardial surface and evaluation of regional dysfunction. Echocardiography 1994;11:397-408.

2. Aakhus S, Mæhle J, Bjoernstad K. A new method for echocardiographic computerized three-dimensional reconstruction of left ventricular endocardial surface: In vitro accuracy and clinical repeatability of volumes. J Am Soc Echocardiogr 1994;7:571-81.

3. Mele D, Mæhle J, Pratola C, Pedini I, Alboni P, Levine RA. Application in patient of a new simplified system for 3D-echo reconstruction of the left ventricle. J Am Soc Echocardiogr 1995;8:343 (abstract).

4. Mele D, Pratola C, Pedini I, Alboni P, Levine RA. Validation and application in patients of a new system for three-dimensional echocardiographic reconstruction of the left ventricle. Circulation 1994;90:I-337 (abstract).

5. Fehske W, Mæhle J, Olstad B, Rabahieh R, Smekal A, Seelos K, Köhler U, Lüderitz B. Frame-by frame threedimensional echocardiographic reconstruction of the left ventricle. J Am Coll Cardiol 1993;19 (abstract supplement):4A.

6. Tardif JC, Cao QL, Pandian NG, Azevedo J, Schwartz S, Rastegar H. Dynamic three-dimensional echocardiographic evaluation of the impact of ventricular endoaneurysmorrhaphy on regional and global left ventricular size, shape and function in patients with left ventricular aneurysm. J Am Soc Echocardiogr 1994;7:S33(abstract).

7. Vannan M, Cao QL, Freire M, Azevedo J, Pandian NG. Utility of serial three-dimensional echocardiography in the study of ventricular remodeling and function in patients after first anterior myocardial infarction. J Am Soc Echocardiogr 1994;7:S34 (abstract).

8. Picard MH, Wilkins GT, Ray PA, Weyman AE. Natural history of left ventricular size and function after acute myocardial infarction - assessment and prediction by echocardiographic endocardial surface mapping. Circulation 1990;82;484-494.

9. Guyer DE, Gibson TC, Gillam LD, King ME, Wilkins GT, Guerrero JL, Weyman AE. A new echocardiographic model for quantifying three-dimensional endocardial surface area. J Am Coll Cardiol 1986;8:819-29.

10. Guyer DE, Foale RA, Gillam LD, Wilkins GT, Guerrero JL, Weyman AE. An echocardiographic technique for quantifying and displaying the extent of regional left ventricular dyssynergy. J Am Coll Cardiol 1986;8:830-834.

11. Wilkins GT, Southern JF, Choong CY, Thomas JD, Fallon JT, Guyer DE, Weyman AE. Correlation between echocardiographic endocardial surface mapping of abnormal wall motion and pathologic infarct size in autopsied hearts. Circulation 1988;77:978-87.

12. King DL, Gopal AS, King Jr. DL, Shao MY. Three-dimensional echocardiography: In vitro validiation of quantitative measurement of total and"infarct" surface area. J Am Soc

Echocardiogr 1993;6:69-76.

13. Picard MH, Siu SC, Lethor JP, Handschumacher MD. Three-dimensional echocardiographic reconstruction and quantitation of the left ventricular endocardial surface. Circulation 1991;84 (abstract Suppl.2):685.

14. Bjoernstad K, Maehle J, Aakhus S. Quantitative computerized analysis of left ventricular wall motion. In Domenicucci S, Roelandt J, Pezzano A. (Eds.), Computerized Echocardiography, Centro Scientifico Editore, Torino,1993;41-55.

15. Ghosh A, Nanda NC, Maurer G. Three dimensional reconstruction of echocardiographic images using the rotation method. Ultrasound Med Biol 1982;8:655-661.

16. Fazzalari NL, Davidson JA, Mazumdar J, Mahar LJ, DeNardi E. Three dimensional reconstruction of the left ventricle from four anatomically defined apical two-dimensional echocardiographic views. Acta Cardiologica 1984;XXXIX(6):409-436.

17. McCann HA, McEwan CN, Sharp JC, Kinter TM, Greenleaf JF, Barillot C. Multidimensional ultrasonic imaging for cardiology. Proc IEEE 1988;76;1063-1073.

18. Henry WL, DeMaria A, Feigenbaum H, Kerber R, Kisslo J, Weyman AE, Nanda N, Popp RL, Sahn D, Schiller NB, Tajik AJ. Identification of Myocardial Wall Segments: The American Society of Echocardiography Committee on Nomenaclature and Standards 1982.

19. Henry WL, DeMAria A, Gramiak R, King DL, Kisslo JA, Popp RL, Sahn DJ, Schiller NB, Tajik A, Teichholz LE, Weyman AE. Report of the American society of echocardiography commitee on nomenclature and standard in two-dimensional echocardiography. Circulation 1980;62:212-217.

20. Mæhle J. Reconstruction and analysis of left ventricular surfaces by three-dimensional echocardiography. II. New indices for global and regional systolic function in patients with myocardial infarction. 1996 - art. D in thesis.

21. Dekker DL, Piziali RL, Dong E. A system for ultrasonically imaging the human heart in three dimensions. Computers and Biomedical Research 1974;7:544-553.

22. Fine DG, Sapoznikov D, Mosseri M, Gotsman MS. Three-dimensional echocardiographic reconstruction: qualitative and quantitative evaluation of ventricular function. Computer Methods and Programs in Biomedicine 1988;26:33-44.

23. Levine RA, Handschumacher MD, Sanfilippo AJ, Hagege AA, Harrigan P, Marshall JE, Weyman AE. Three-dimensional echocardiographic reconstruction of the mitral valve, with implications for the diagnosis of mitral valve prolaps. Circulation 1989;80:589-598.

24. Gopal AS, King DL, Katz J, Boxt L, King Jr. DL, Shao MY. Three-dimensional echocardiographic volume computation by polyhedral surface reconstruction: In vitro validiation and comparison to magnetic resonance imaging. J Am Soc Echocardiogr 1992;5:115-124.

25. King DL, Harrison MR, King Jr. DL, Gopal AS, Martin RP, DeMaria AN. Improved reproducibility of left atrial and left ventricular measurements by guided three-dimensional echocardiography. J Am Coll Cardiol 1992;20:1238-1245.

26. Handschumacher MD, Lethor JP, Siu SC, Mele D, Rivera JM, Picard MH, Weyman AE, Levine R. A new intergratet system for three-dimensional echocardiographic reconstruction: Development and validiation for ventricular volume with application in human subjects. J Am Coll Cardiol 1993;21:743-753.

27. Nikravesh PE, Skorton DJ, Chandran KB, Atterwala YM, Pandian N, Kerber RE. Computerized Three-Dimensional Finite Element Reconstruction of the Left Ventricle from Cross-Sectional Echocardiograms. Ultrasonic Imaging 1984;6:48-59.

28. Linker DT, Moritz WE, Pearlman A. A new three-dimensional echocardiographic method of right ventricular volume measurement: in vitro validation. J Am Coll Cardiol 1986;8:101-106.

29. Pandian NG, Roelandt J, Nanda N, Sugeng L, Cao Q, Azevedo J, et. al. Dynamic three-dimensional echocardiography: methods and clinical potential. Echocardiography 1994;11:237-59.

30. Feigenbaum H. Echocardiography 5th. ed. ch. 8. Philadelphia, Lea & Febiger, 1994.

31. Fazzalari NL, Goldblatt E, Adams APS. A composite three-dimensional echocardiographic technique for left ventricular volume estimation in children: comparison with angiography and established echographic methods . J Clinical Ultrasound 1986;14:663-674.

32. Zoghbi WA, Buckey JC, Massey MA, Blomqvist CG. Determination of Left Ventricular Volumes With Use of a New Nongeometric Echocardiographic Method: Clinical Validation and Potential Application. J Am Coll Cardiol 1990;15:610-17.

33. Sapin PM, Schroeeder KD, Smith MD, DeMaria AN, King DL. Three-dimensional echocardiographic measurement of left ventricular volume in vitro: Comparison with two-dimensional echocardiography and cineventriculography. J Am Coll Cardiol 1993;22:1530-37.

34. Schröder KM, Sapin PM, King DL, Smith MD, DeMaria AN.. Three-dimensional echocardiographic volume computation: In vitro comparisom to standard two-dimensional echocardiography. J Am Soc Echocardiogr 1993;6:467-75.

35. Mæhle J, Aakhus S, Bjørnstad K, Torp HG. How many apical imaging planes should be used for determination of left ventricular volumes by three-dimensional echocardiography. In Abstracts of the11th Symposium in Echocardiology, Rotterdam, 1995:193.

36. Farin G. Curves and surfaces for computer aided geometric design - A practical guide. 3. ed., Academic press Inc., Boston, 1993.

37. Picard MH, Wilkins GT, Gillam LD, Thomas JD, Weyman AE. Immediate regional endocardial surface expansion following coronary occlusion in the canine left ventricle: disproportionate effects of anterior versus inferior ischemia. Am Heart J 1991;121:753-762.

38. Picard MH, Wilkins GT, Ray PA, Weyman AE. Progressive changes in ventricular structure and function during the year after acute myocardial infarction. American Heart J 1992;124:24-31.

39. Mæhle J. Left ventricular dimensions and shape by three-dimensional echocardiography: how many apical imaging views should be used for reconstruction of endocardial short axis borders by cubic spline interpolation? 1996 - art. F in thesis.

40. Schiller NB, Shah PM, Crawford M, DeMaria A, Devereux R, Feigenbaum H, Gurgesell H, Reichek N, Sahn D, Schnittger I, Silvermann NH, Tajik AJ. Recommendations for quantitation of the left ventricle by two-dimensional echocardiography. J Am Soc Echocardiogr 1989;2:358-67.

41. Schiller NB. Two-Dimensional Echocardiographic Determination of Left Ventricular Volume, Systolic Function, and Mass. Summary and Discussion of the 1989 Recommandation of the American Society of Echocardiography. Circulation 1991;84(Supplement I):280-87.

Reconstruction and Analysis of Left Ventricular Surfaces by Three-Dimensional Echocardiography. II. New Indices for Global and Regional Systolic Function in Patients with Myocardial Infarction

Abstract

Objectives. The aim of this work was to develop new indices of systolic left ventricular (LV) function based on a quantitative description of the endocardial surfaces obtained from three-dimensional (3D) echocardiography, and to test their usefulness for identification of global and regional dysfunction after myocardial infarction (MI). **Background.** A method for 3D reconstruction of LV has previously been presented and validated for estimation of volumes and endocardial surface areas based on a limited number of apical imaging planes. The reconstruction algorithm generates a detailed description of endocardial surfaces, from which several quantitative indices with potential use for diagnosis of ischemic heart disease can be derived. **Methods.** A shape index (3DSI) was calculated from LV volume and endocardial surface area. Global systolic contraction was calculated from change in endocardial surface area (FCESA). Regional wall motion was derived from end-diastolic and end-systolic surfaces, and combined with area in statistical parameters characterizing systolic contraction, and a bull's eye map was used for display of location and extent of dysfunction. The area representing abnormal wall motion (AWM) was estimated after selecting a threshold value for normal wall motion. The indices were studied in 15 subjects (10 with recent MI, and 5 healthy subjects) based on 3D reconstruction from 3 apical imaging planes, and compared to 2D echocardiographic analysis by wall motion score index (WMSI). **Results.** Location of regional dysfunction from 3D analysis agreed well with WMSI. The indices FCESA and AWM distinguished between normals and MI ($p<0.0001$), and correlated well to WMSI ($r = 0.93$, $r = 0.87$). **Conclusions.** Analysis of endocardial surfaces, generated from clinical ultrasound images, provides quantitative indices and visual tools illustrating global and local left ventricular function by MI.

Key words: Echocardiography, Three-Dimensional Reconstruction, Left Ventricular Function, Wall Motion Analysis, Myocardial Infarction

Introduction

We have previously presented an algorithm for three-dimensional (3D) reconstruction of the left ventricular (LV) endocardial surface from a limited number of two-dimensional (2D) echocardiographic images obtained from an apical transducer position [1]. The method is accurate in terms of volume calculations [2-4], and assessment of LV contraction from visual judgment of displayed dynamic 3D geometry [5-7]. The reconstruction uses cubic spline interpolation, and gives a detailed mathematical description of the reconstructed endocardial surface . In addition to estimation of endocardial surface areas (ESA) described in accompanying article [8], quantitative indices of LV function which may be important in clinical decision making, can be derived from this surface description.

Assessment of LV regional function by 2D echocardiography is accepted as a noninvasive and reliable methodology in routine clinical practice. The interpretation of 2D echocardiography depends, however, on the skill and subjective judgment of the investigator, and more objective indices of LV dysfunction are therefore desired. A semiquantitative approach to wall motion analysis is the wall motion score index (WMSI) using a 16 segment division of LV for assessment of regional wall motion for obtaining a global index of LV function [9,10]. Several singleplane methods have been used for quantitative assessment of regional wall motion by comparison of borders defining the endocardium in end-diastolic and end-systolic 2D ultrasound images [11-21]. These methods are limited as they rely on reference systems for alignment of edges due to translation and rotation of the heart. Furthermore, they cannot quantify the extent of dysfunction in terms of endocardial area or LV mass. Determination of both the total endocardial surface area and the area and location of regional dysfunction induced by ischemic heart disease are needed for prognostic and serial studies [22-24]. A method using multiple 2D echocardiographic scans has been proposed and validated [25-27]. The surface description produced by our 3D reconstruction method enables assessment of regional dysfunction by surface area calculations combined with wall motion calculations. In addition, the 3D reconstruction method provides compensation for off-axis imaging, and new references for wall motion analysis based on 3D geometry [1,28]. Regional wall motion analysis based on 3D endocardial surfaces should therefore, compared with the singleplane methods, have potential for improved accuracy in localization and quantitation of areas with abnormal function.

The most common index characterizing global LV systolic function is ejection fraction of

volume (EF) [29]. From the present 3D reconstruction both volumes, and subsequently EF, and ESA can be determined accurately. The ESA combined with volume may also give a basis for new indices of global ventricular shape and contraction. Synergy of systolic contraction will be reflected in the distribution of local wall motion, thus the 3D analysis may be used for extraction of global indices expressing synergy in LV systolic contraction.

In this work new indices were studied in patients with recent myocardial infarction, based on reconstructed endocardial surfaces at end-diastole and end-systole. The algorithm for surface reconstruction is flexible as it can handle input data from a variable number (3-12) of imaging planes. In clinical practice it is of great importance to keep the time and complexity of data acquisition at a minimum, so another intention was to illustrate possible clinical applicability of the presented methodology by analysis of surfaces generated using data from only 3 imaging planes collected in routine echocardiographic examinations.

Methods

Computer progam for 3D reconstruction of endocardial surfaces and analysis of LV function.

Surface reconstruction and description. The reconstruction procedure has previously been described in [1,2,8].

Calculation of LV indices was based on the geometric data representing the endocardial surface comprising a matrix of 3D points $\{ \mathbf{r}_{i,j} \}$ on the reconstructed surface and the points $\mathbf{r}_{apex}$ and $\mathbf{r}_{mm}$ at positions of the apex and the mitral plane midpoint respectively (Fig. 1). The ventricular major axis is defined as the straight line connecting these latter points. Each point is given in Cartesian coordinates $\mathbf{r}_{i,j} = (x_{i,j} , y_{i,j} , z_{i,j})$ positioned in space with the center of mass of the ventricle fixed at origo, and with a common direction of the major axis and the y-axis. The range of indexes, i and j, are selectable according to axial and circumferential resolution respectively denoting the number of ventricular cross-sections to be reconstructed, and the number of points to be stored on each reconstructed cross-section. A resolution of 32 both in axial and circumferential direction was chosen for this work, producing a matrix of 1024 points (in total 3072 + 6 coordinates including apex and mitral midpoint).

Cavity volume (in ml) and the position of center of mass is determined by the algorithm

by successive calculations from the cubic spline representation of parallel cross-sections in the reconstructed surface. For further calculation of surface areas the reconstructed endocardial surface was subdivided into small areas $a_{i,j}$ surrounding each point $\mathbf{r}_{i,j}$ of the surface as described in accompanying article [8]. The results are stored in an matrix $\{ a_{i,j} \}$, and the total endocardial surface area (ESA) was calculated (in cm^2) by summation of the matrix elements.

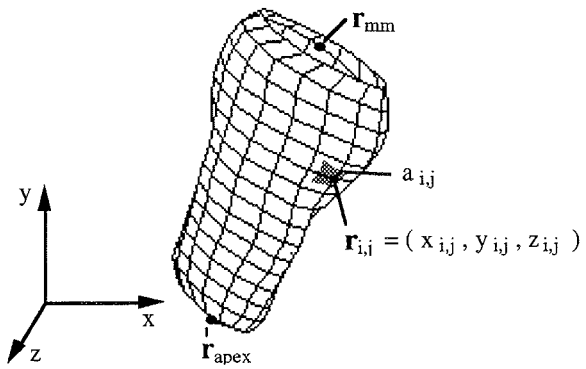

Figure 1. Wire-frame display (low resolution) illustrating data format used for analysis of the reconstructed endocardial surface. $\mathbf{r}_{apex}$ and $\mathbf{r}_{mm}$ are coordinates of the apex and the mitral midpoint, respectively; $\{ \mathbf{r}_{i,j} \}$ are coordinates of the the points at the mesh corners; $a_{i,j}$ refer to the portion of the subdivided endocardial surface area in conjunction to the marked point.

Three-Dimensional Shape Index. The 3D shape Index (3DSI) expresses the ratio between object volume and the volume of a sphere having the same surface area as the closed object:

$$3DSI = \frac{V}{\frac{4}{3}\pi\sqrt{\frac{S_{tot}}{4\pi}}} \qquad \left(S_{tot} = ESA + S_{mp}\right)$$

S_{tot} in the formula comprises the total inner area of the ventricle, the endocardial surface area plus the mitral valve orifice S_{mp} (see appendix A in [8]).

A sphere will produce the maximum shape index equal one, while a less ideal shape will give a smaller index. This index extends the Gibson shape index [30] from 2 to 3 dimensions, since the Gibson index express the ratio between the area inside the endocardial contour, and the area of a circle with a circumference which equals the length of the endocardial border.

Fractional change in endocardial surface area (FCESA). From the left ventricular surface area at both end-diastole and end-systole the index Fractional Change of Endocardial Surface Area (FCESA) is calculated by

$$FCESA = \frac{ESA_{end-diastole} - ESA_{end-systole}}{ESA_{end-diastole}}$$

The index FCESA calculates the relative change in the size of the LV endocardial surface area in systole. This index expresses global systolic contraction similar to EF, but in terms of area instead of volume. Alternatively, an index derived from areas could be calculated to express contraction in terms of length, fiber shortening or by volume ejection (see appendix B).

Three dimensional wall motion analysis. Regional wall motion is calculated from comparison using points at the geometric description of end-diastolic and end-systolic endocardial surfaces (Fig. 2). The two surfaces are aligned in a common reference systems defined from ventricular landmarks in order to compensate for translation of the ventricle, and for rotation due to change in direction of the ventricular major axis. Local wall motion at each point is calculated and stored in a matrix $\{ c_{i,j} \}$. The value of on $c_{i,j}$ express fractional shortening to a reference or absolute displacement of the wall at position i,j from end-diastole to end-systole (Fig. 3).

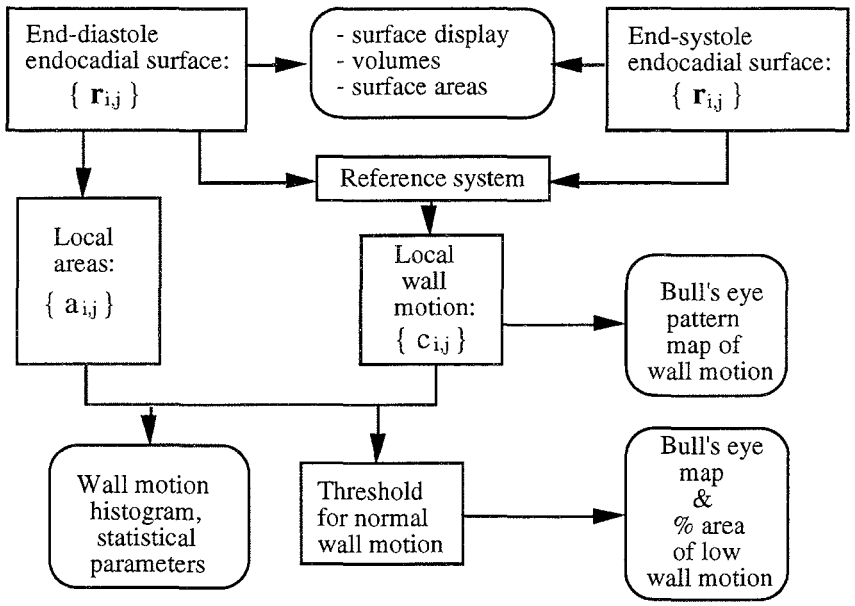

Figure 2. Flow-chart illustrating the analysis of LV function based on a mathematical description of the endocardial surface at end-diastole and end-systole.

Six methods are implemented according to different reference systems and different methods for calculation of local wall motion. In 3 methods the local motion during systole is calculated as fractional change in distance to a reference point (see appendix A):

a) center of mass in the cavity enclosed by the endocardial surface

b) major axis, i.e. fractional change in distances perpendicular to the ventricular major axis

c) center of major axis

The last 3 method measures local wall motion as the distance from the end-diastolic surface to the end-systolic surface (in mm). The surfaces are then aligned by a common direction of the major axis and by a common position of:

d) center of mass

e) midpoint of the mitral valve plane ($\mathbf{r}_{mm}$)

f) center of major axis

The contents of the wall motion matrix { $c_{i,j}$ } is visualized in 2 dimensions in a bull's eye map (Fig. 4) using different pattern to indicate the extent of wall motion. Spatial correspondence between the endocardial surface and the bull's eye map is achieved as axial and circumferential position in the left ventricle respectively coincides to radial and angular position in the bull's eye map [1]. This map will show the location of and qualitatively the size of areas with abnormal wall motion.

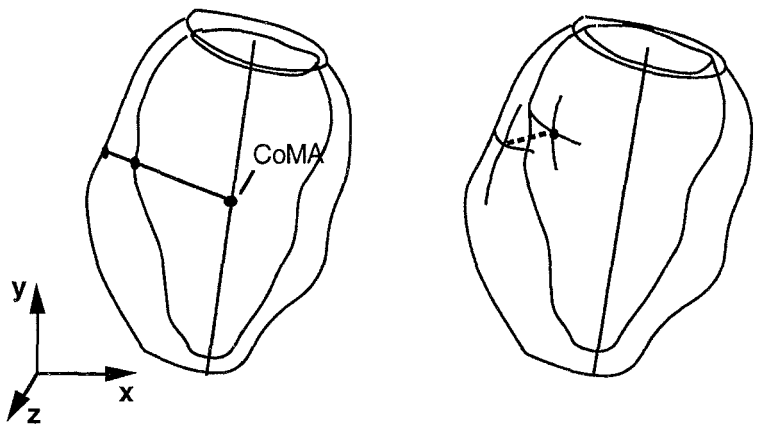

Figure 3. Reference systems for calculation of local wall motion. - Left: calculation of local wall motion as fractional change in distance to the center of the LV ventricular major axis. - Right: calculation of local wall motion as distance between endocardial surfaces after alignment to a common midpoint of the mitral plane and a common LV major axis.

The calculations of wall motion and end-diastolic endocardial area, { $c_{i,j}$ } and { $a_{i,j}$ }, are combined in a histogram (Fig. 4) which display the percent of the ventricle, in terms of end-diastolic endocardial surface area, at different levels of wall motion. Global LV systolic function is characterized from the mean value (^c), the variance (σ^2), and the coefficient of variation (CoV) of wall motion calculated by

$$\hat{c} = \frac{1}{ESA}\sum_{i,j} c_{i,j} a_{i,j} \qquad \sigma^2 = \frac{1}{ESA}\sum_{i,j}\left(c_{i,j} - \hat{c}\right)^2 a_{i,j} \qquad CoV = \frac{\sigma}{\hat{c}} \qquad \left(ESA = \sum_{i,j} a_{i,j}\right)$$

The mean value will indicate global pump function and will be close to the volume ejection fraction, whereas variance will be related to the extent of dysfunction. The CoV will increase both from reduced ejection fraction and from the extent of abnormal motion, in correspondence to a histogram shifted towards zero and/or broadened.

The size of areas with abnormal wall motion (AMW) is estimated from a manually chosen constant threshold level, t , by

$$AWM = \sum_{c_{i,j} < w_i t} a_{i,j} \qquad (w_1 \ldots\ldots w_{28} = 1, w_{29} = 0.8, w_{30} = 0.5, w_{31} = 0.2, w_{32} = 0)$$

The estimated area with reduced wall motion is expressed in percent of the end-diastole endocardial surface area (% AMW), and its location is displayed in a bull's eye map (Fig. 4). The weight factors w_i are introduced to compensate for relative normal low wall motion in the basal region (numbers refers to the actual axial resolution of 32).

The combination of two wall motion methods is also implemented by union and intersection. In union, an area $a_{i,j}$ is classified as abnormal when wall motion is lower than the threshold level in both methods. In intersection, an area is classified abnormal if one or both methods results in reduced wall motion (Fig. 5). Manual interaction is available by drawing of regions that will be ignored in the threshold calculation (Fig. 6).

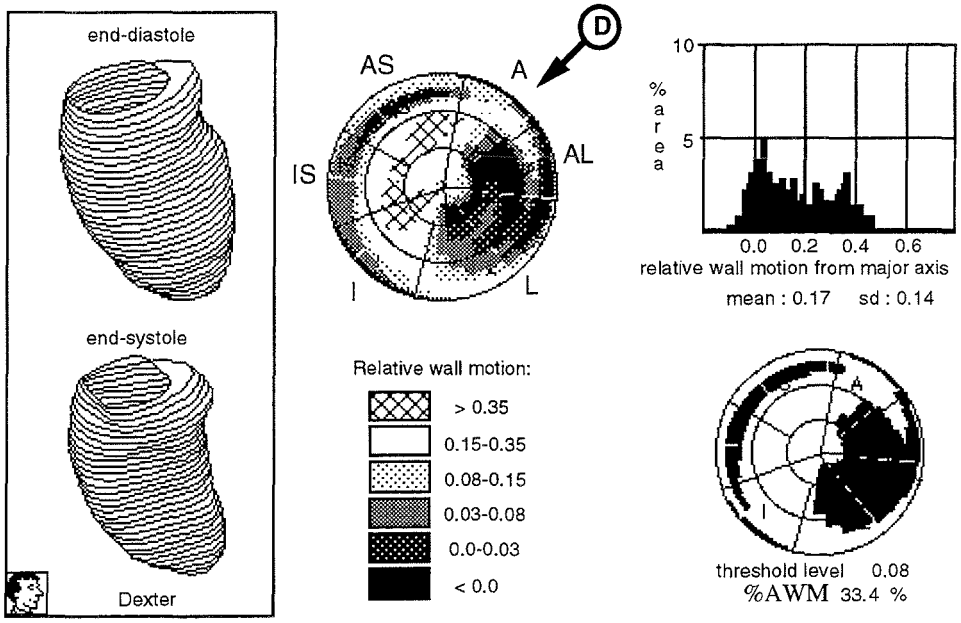

Figure 4. Example showing results from 3D wall motion analysis. Local wall motion is measured relative (perpendicular) to the major axis (reference system b). - Left panel: the reconstructed endocardium is displayed at end-diastole and end-systole in the projection corresponding to the viewer position at the dexter side of the patient. - Middle panel: regional wall motion displayed in a bull's eye map using the pattern code below. The map reveals ventricular dysfunction (reduced wall motion) in the lateral wall, which also appears by little or no change in shape from end-diastole to end-systole in the corresponding part of displayed surfaces (left panel). Position relative to the bull's eye is indicated: A-anterior, L-lateral, I-inferior, S-septal, D indicates the observer's position for the displayed surface. - Right panel: histogram displaying the percent of the end-diastole endocardial surface area at different levels of wall motion. Application of a threshold value equal 50 % of the mean value of wall motion determines a region of low wall motion displayed in the bull's eye map. The extent of this surface area is 33.4 % of the end-diastolic endocardial surface area (not necessarily of the bull's eye area).

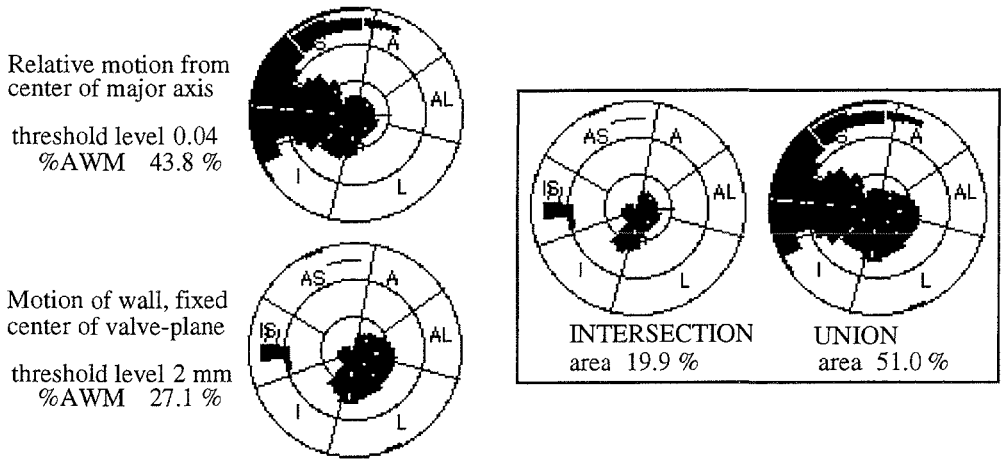

Figure 5. Combination of two 3D wall motion reference systems by intersection and union (see text).

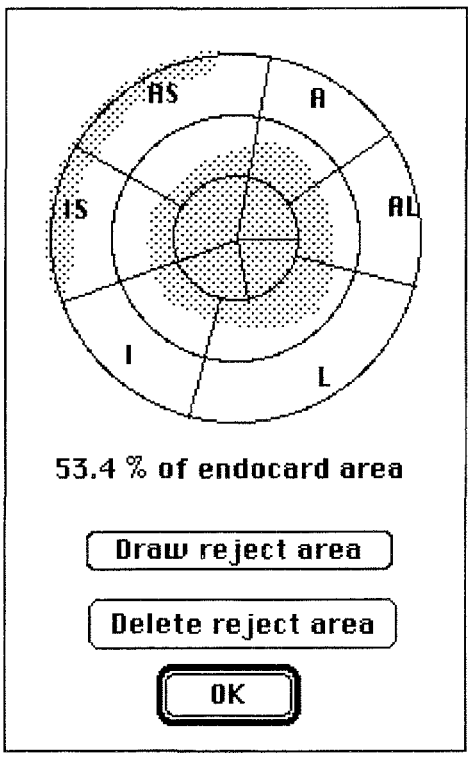

Figure 6. Dialog box for drawing of area (dotted region) to be excluded from wall motion analysis by thresholding. The displayed area (53.4 %) is calculated from the corresponding part of the actual end-diastolic surface area.

Clinical study

Fifteen subjects were studied, 10 with recent (≤ 10 days) myocardial infarction, and 5 healthy control subjects without clinical evidence of coronary artery disease. In the patients myocardial infarction was documented by at least 2 of the 3 following criteria: 1) typical chest pain lasting more than 30 minutes; 2) typical serial electrocardiographic changes; and 3) arise in serum cardiac enzymes to at least twice normal values. Eight patients had anterior wall infarction by electrocardiographic criteria, 1 had inferior wall infarction, and 1 had lateral wall infarction.

Instrumentation. An ultrasound scanner (Vingmed 750, Vingmed Sound, Horten, Norway) with a 3.25 MHz annular array transducer was used for all imaging. The ultrasound images were transferred as digital scan-line data to a computer (Macintosh series II, Apple Computers, Cupertino, California) and computerized analysis was performed using commercially available software (Echo-Loops/EchoDisp version 3.0, Vingmed Sound). The algorithms for 3D reconstruction and analysis are implemented in so-called ECARs (EchoDisp Custom Analysis Routines, Vingmed Sound).

Data acquisition. Ultrasound 2D images were obtained using apical access to the 4-chamber, long axis (2-chamber), and long axis imaging planes, which were identified by anatomical landmarks [31,32]. Cineloops consisting of the systolic part of the cardiac cycle were sampled during held end-expiration and transferred to the computer. A one vector electrocardiogram was recorded with the ultrasound data.

Two-dimensional echocardiographic analysis of wall motion - WMSI. Semiquantitative wall motion analysis was based on visual evaluation during continuous replay of the 2D cineloops. From the three apical 2D views all the segments in an 16-segments model of the LV are visualized [9,10]. All segments are given a score due to performance as normal wall motion are assigned a score of 1, hypokinesia = 2, akinesia = 3, dyskinesia = 4, and aneurysmal segments = 5. The segmental scores are displayed in a bull's eye map, and the wall motion score index (WMSI) is calculated as the ratio of the sum of all segmental scores and the number of visualized segments. The bull's eye map illustrates the location and extent of the wall motion abnormality, while the WMSI characterizes the total systolic function of the ventricle.

Reconstruction of endocardial surfaces. The endocardial borders in all the 2D ultrasound images were manually traced at end-diastolic and end-systolic frames using a mouse driven cursor on the computer screen. The papillary muscles were excluded, and in the apical

long axis view, the LV outflow tract was traced to aortic valve. The mitral valve plane was defined by a straight line between the mitral annulus points, and in the reconstruction algorithm the mitral plane midpoint (see Fig. 1) is recognized as the midpoint of this line. The border tracing was optimized by adequate contrast setting, and by repeated evaluation of traces against the moving endocardium and mitral annulus by use of the cineloop replay function. In each subject the endocardial surfaces at end-diastole and end-systole were generated from borders at 3 spatial position. The borders were assigned angles corresponding to counter-clockwise rotation of the transducer, starting at zero for the apical 4-chamber view, while apical 2-chamber and long-axis views are assigned 62 and 101 degrees, respectively [33].

Display of endocardial shape and derived calculations. Endocardial surfaces were generated at end-systole and end-diastole, and the shapes were displayed at three different projections, together with the calculated values for cavity volume, surface area, and length of the ventricular major axis. Stroke volume was calculated as the difference between the end-diastolic and end-systolic volumes, and ejection fraction (EF) was calculated as the ratio between stroke volume and end-diastolic volume. The indices 3DSI and FCESA were calculated from the formulas given above.

Regional 3D wall motion analysis was performed using fractional change in distance to the center of major axis (reference system c) and, wall motion calculations of mean, variance, and CoV were recorded together with the wall motion histogram and bull's eye maps. The % AMW was estimated from a threshold level chosen at 50 % of the mean wall motion, and the location and extent of AMW was displayed in a bull's eye map.

Comparison of 3D indices with WMSI, and statistical analysis. Global LV indices obtained from 3D reconstruction were compared with WMSI by simple linear regression and the correlation coefficient (r) was recorded. The unpaired t test was used for comparison of mean values in normals and MI patients, whereas probability less than 0.05 was considered statistically significant. The ability of the 3D method for localization of regional wall motion abnormalities was assessed by visual comparison of the pattern bull's eyes with those from WMSI.

Results

Physiological indices and left ventricular dimensions extracted from the mathematical description of end-diastole and end-systole endocardial surfaces are collected together with electrocardiographic location of MI and WMSI for all subjects in Table 1.

Global indices derived from volume and ESA. Both EF and FCESA correlates well with WMSI (Fig. 7a,b), whereas FCESA shows the highest ability to distinguish between MI patients and controls ($p = 0.00002$ compared to $p = 0.0002$ for EF). The shape index, 3DSI, can be regarded as an index of globularity (max. 1 for a sphere), and calculated values agree well with the globularity visually assessed in the respective displayed LV shapes (see Fig.8, and Tab. 1). However, the shape index did not work as an index for identification of MI. Neither end-diastolic nor end-systolic index 3DSI, nor the difference between them correlated to WMSI ($r = 0.16$ / 0.13 / 0.37 respectively), and no significant difference in values for MI patients and controls was found.

Localization of AMW. The location of regions with reduced wall motion showed by pattern bull's eye (Fig. 8) and from thresholding (Fig.9) agrees well with electrographic location of infarction (Tab. 1) and with the WMSI bull's eyes (Fig.10). Location of AMW were also visualized by surface rendering as the reconstructed endocardial surfaces were displayed at 3 different projections (Fig. 8). The 3D geometry of the endocardial surface is well illustrated, and shape and contraction abnormalities can be observed (Fig. 8). In subject II the display reveals apical dilation and reduced contraction in the anterior apical/mid-ventricular region.

Quantification of AMW. An estimate for the size of the wall motion abnormality is obtained by the percent of the endocardial surface area with relative wall motion below 50 % of the mean value of wall motion (Fig. 9). The % AMW estimates correlates well to WMSI (Fig. 7c), and in the controls only very small parts of the endocardial surface areas were classified as abnormal.

Statistical indices from 3D wall motion analysis. Compared to the histogram of normal contraction (subject III, Fig. 8) the histograms associated with ischemic heart disease displays different types of change in the left ventricular contraction. We observe a shift in histogram toward zero (subject I. Fig. 8) indicating an overall reduced contraction and ejection fraction. In the second case (subject II, Fig. 8) a broadening of the histogram and an additional peak indicates compensatory hyperkinesis in unaffected regions. In both cases, the difference from the normal histogram are reflected in an increase in the index CoV (Tab. 1) due to a low mean value and a high standard deviation of wall motion respectively. The index CoV also correlates to WMSI (Fig. 7d), and was significantly increased in MI patients compared with controls ($p = 0.0006$). Histograms with calculated mean and standard deviation of wall motion in all subjects are shown in Fig. 10.

Table 1. Individual results in subjects from reconstruction and analysis of endocardial surfaces

			volume (ml)	axis (cm)	surface area (cm2)	3DSI			3D wall motion	
no.	MI-localization	WMSI	ed / es	ed / es	ed / es	ed / es	EF	FCESA	CoV	% AMW
1	anterior	2.00	132 / 89	8.9 / 8.9	127 / 105	0.82 / 0.75	0.32	0.17	1.44	45.9
2 (I)	inferior	1.75	132 / 89	8.1 / 7.5	123 / 98	0.88 / 0.84	0.33	0.20	0.67	14.3
3	anterior	1.81	100 / 67	8.2 / 8.2	107 / 88	0.83 / 0.77	0.33	0.18	0.78	27.0
4	anterior	2.00	118 / 73	9.9 / 9.7	129 / 105	0.77 / 0.66	0.38	0.19	1.27	39.7
5	lateral	1.25	107 / 67	7.5 / 6.9	108 / 84	0.89 / 0.81	0.37	0.22	0.85	24.7
6	anterior	1.56	84 / 44	8.0 / 8.0	100 / 71	0.79 / 0.70	0.48	0.29	0.92	33.9
7	anterior	1.25	110 / 47	9.0 / 8.7	117 / 76	0.82 / 0.65	0.57	0.35	0.75	28.3
8	anterior	1.31	122 / 57	8.0 / 7.5	124 / 82	0.82 / 0.72	0.53	0.34	0.65	21.4
9	anterior	1.94	107 / 85	9.1 / 9.0	118 / 105	0.79 / 0.74	0.21	0.11	1.83	40.8
10 (II)	anterior	1.62	114 / 68	9.0 / 8.6	124 / 96	0.80 / 0.72	0.40	0.23	0.85	34.6
11	-	1.00	132 / 58	9.6 / 8.7	135 / 83	0.80 / 0.72	0.56	0.39	0.45	5.1
12	-	1.00	114 / 48	8.5 / 7.2	119 / 70	0.84 / 0.76	0.58	0.41	0.41	0.0
13	-	1.00	86 / 32	7.5 / 6.4	99 / 55	0.83 / 0.77	0.63	0.44	0.35	1.9
14	-	1.00	81 / 32	8.3 / 6.6	97 / 58	0.80 / 0.69	0.60	0.40	0.41	4.3
15 (III)	-	1.00	97 / 41	8.5 / 7.4	109 / 66	0.80 / 0.67	0.58	0.39	0.26	0.3

MI-localization = electrocardiographic localization of myocardial, WMSI = wall motion score index, es = end-systole, ed = end-diastole, 3DSI = 3D shape index (see text), EF = volume ejection fraction, FCESA = fractional change in endocardial surface area (see text), CoV = ratio of standard deviation and mean wall motion (see text), % AWM = percent of endocard area displaying local wall motion below 50 % of mean value (see text). Roman number in parentheses corresponds to subjects analyzed in Fig. 8 & 9.

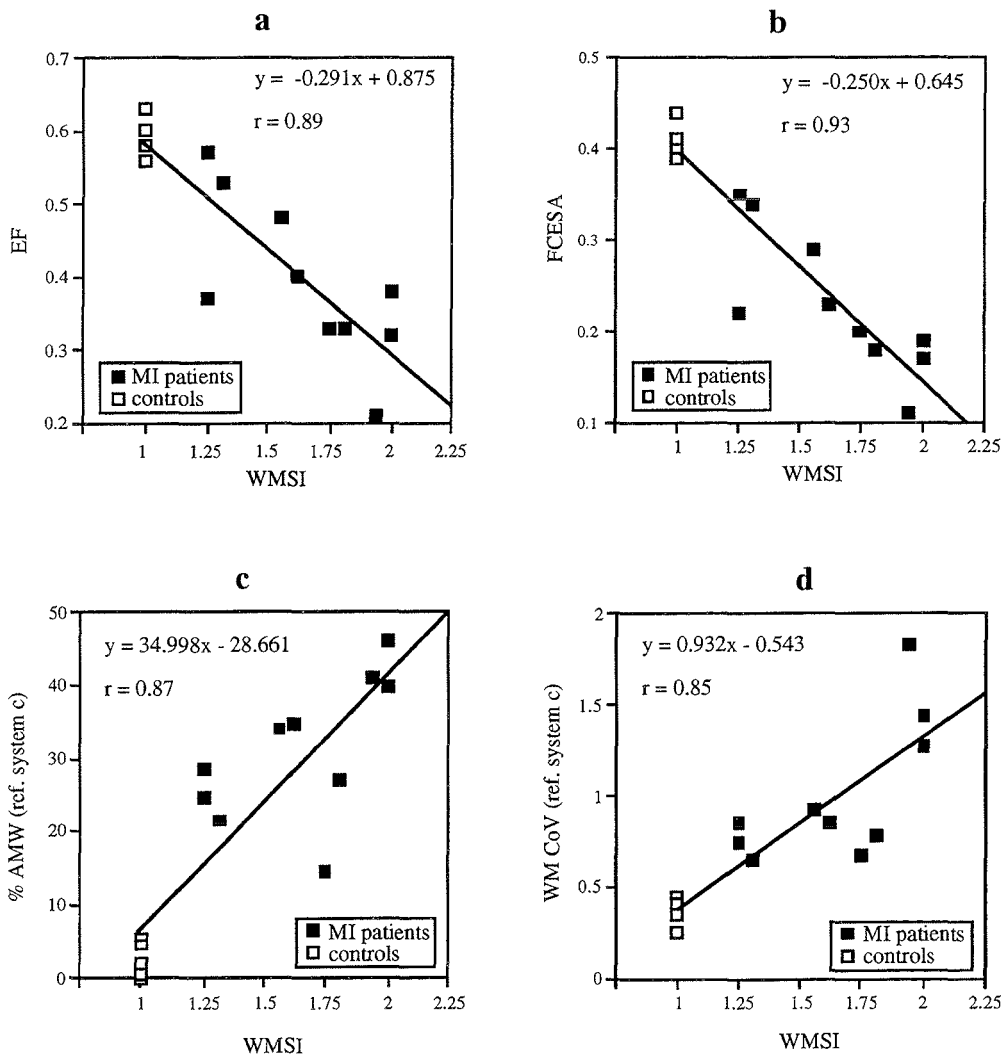

Figure 7. Indices of LV function correlated to the wall motion score index (WMSI): - a) left ventricular volume ejection fraction (EF) - b) fractional change in endocardial surface area (FCESA) - c) percent area with abnormal wall motion (% AWM) determined from thresholding - d) wall motion coefficient of variation (CoV).

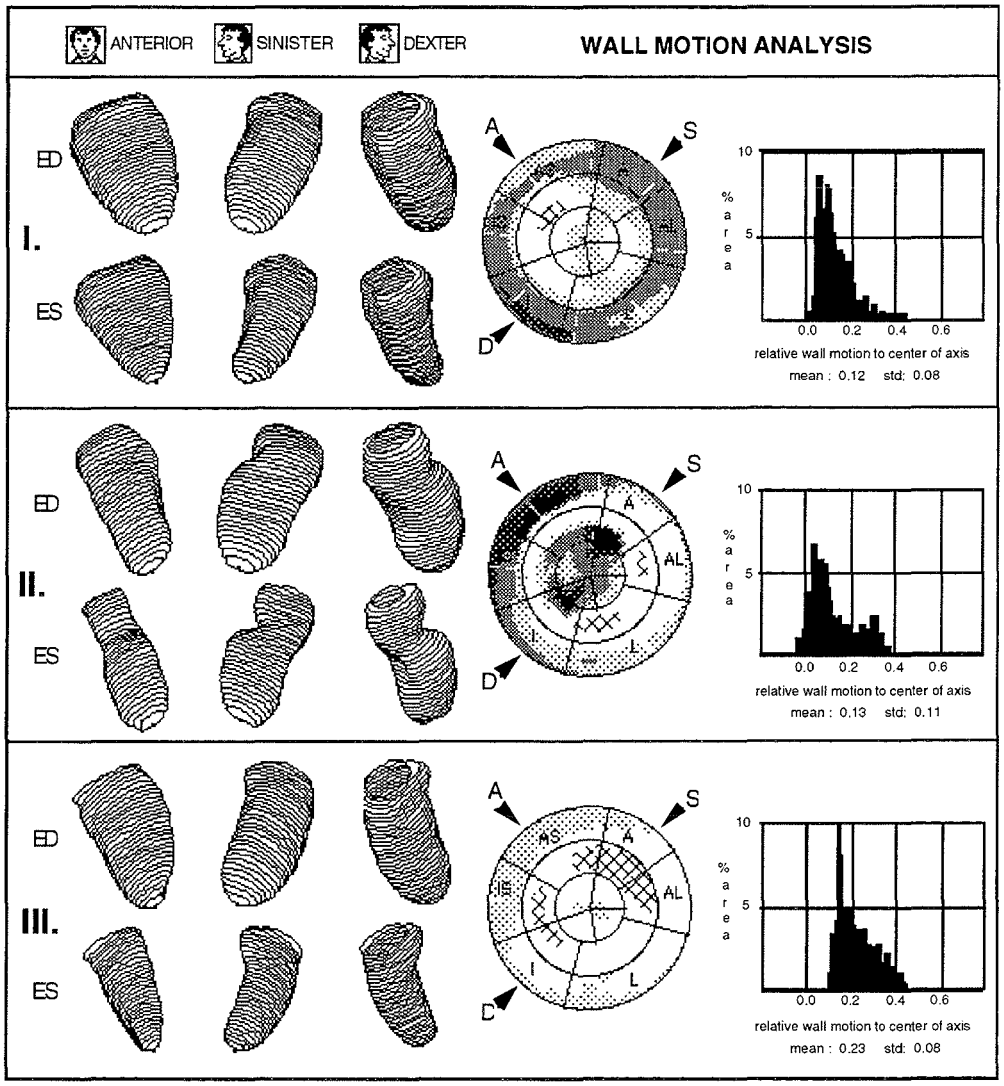

Figure 8. Results of wall motion analysis in 3 subjects (marked I, II and III in Tab. 1). For each subject the endocardial surfaces are reconstructed in end-diastole and end-systole and displayed from 3 viewpoints: Anterior, Sinister, and Dexter - directions are indicated with arrows in the pattern bull's eye. The pattern code is given in Fig. 4, and wall motion histogram is explained in text.

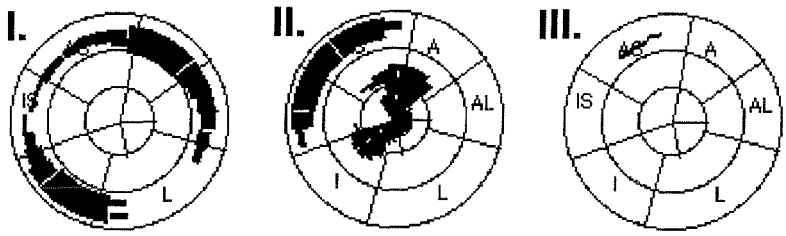

threshold level 0.06 %AWM 14.3 %

threshold level 0.06 %AWM 30.1 %

threshold level 0.11 %AWM 0.3 %

Figure 9. Bull's eyes displaying extent and location of regional wall motion below selected threshold level (50 % of mean wall motion) in subjects presented in Fig. 8.

Discussion

In this work we have presented new indices for quantification of global and regional LV function derived from the mathematical description of end-diastolic and end-systolic endocardial surfaces. These indices facilitated identification of reduced systolic regional wall motion in MI patients, and the extent and location of regional dysfunction was determined in agreement with findings from conventional 2D echocardiography. The presented indices can be obtained from other methods of imaging and surface reconstruction (Fig. 2), however, the main goal in this study has been to provide quantitative indices for diagnosis in ischemic diseases from noninvasive echocardiographic measurements. The present study was performed with 2D ultrasound data, 3 apical planes normally acquired during routine echocardiography, with no extra instrumentation for measuring or controlling the position of the imaging planes. Time for computer postprocessing, including edge drawing and computer calculations, was approx. 10 min. for each subject.

Echocardiographic surface reconstruction. The clinical value of indices depends on the accuracy of the reconstructed endocardial surface. For clinical use the efforts involved with 3D analysis should be minimized. The present algorithm calculates LV volume and ESA accurately from only 3 standard ultrasound imaging planes [2-4], while the accuracy of wall motion calculations have not been tested previously. In the present algorithm short-axis cross-sectional borders are generated by cubic spline interpolation through points located on long-axis

endocardial borders, and accuracy in reconstructed surface depends on: 1) accuracy of edge detection in the apical 2D images, 2) the accuracy in temporal and spatial alignment of 2D edges in a 3D coordinate system, 3) simplifications of LV shape in the reconstruction algorithm, 4) accuracy in reconstructed cross-sectional LV shape from a small number of sampled points.

1) Edge detection: accurate edge detection is crucial for quantitative analysis from ultrasound images, and high image quality and experience are required. Automatic border detection algorithms are available and may supplement manual drawing [34]. Furthermore, ongoing technical development in ultrasound imaging may improve the potential of edge detection both in respect to accuracy and effectivity.

2) Alignment of endocardial edges: the reconstruction algorithm aligns the input edges in the 3D space by the rotation angles of the imaging planes and by geometrically defined landmarks. For estimation of volumes and surface areas, errors in these positions have minor influence results [2,3,8], however, the local estimates of wall motion will presumably be more sensitive to errors in alignment of 2D edges. This problem is expected to be most pronounced in the apical region due to the ability of the algorithm to define a common point, or apex, for alignment of 2D edges. The optimum criteria for automatic detection of a common reference, not necessarily the LV apex, remains to be determined. Previously, automatic apex recognition has received little attention, but has been studied in angiography [35]. Off-axis imaging, and translation and/or rotation of the heart in the cardiac cycle, will also induce errors since the imaging plane then do not coincide with the LV major axis [36]. The present algorithm compensates for off-axis imaging by assuming that the edge with the longest major axis is the best estimate of the true long axis. The other edges are stretched so that all major axis have equal length. This compensation enlarges the edge only in axial direction, and should work adequately when the imaging planes are positioned in the middle of the mitral valve. This stretching works in contradiction to the fact that the mitral valve annulus is saddle shaped [37], but the off-axis imaging is assumed to be a more important factor.

The reconstruction algorithm uses endocardial borders from multiple heart beats, and temporal alignment by use the electrocardiographic trace. The method is therefore not applicable during arrhythmia, and beat to beat variation due to patient motion and expiration should be avoided. One advantage of the present reconstruction method is the use of anatomically defined landmarks for reconstruction, making this method less sensitive to motion of the patient relative to a 3D coordinate system defined by the position of the ultrasound imaging plane.

3) Simplifications in the reconstruction algorithm: the mitral valve annulus is by the

algorithm approximated to reside in a plane, and LV shape discontinuities at the aorta valve level are smoothed and becomes a part of the continuous reconstructed endocardial surface. These simplification introduces inaccuracy in local wall motion in this region, whereas calculations of volumes and surface area are less affected.

4) How many apical planes that are necessary to obtain an adequate reconstruction of the endocardium. Previous works have shown that volumes and ESA are calculated accurately by 3 imaging planes [2-4, 8], and that the precision for volumes was not significantly increased by use of more than 4 planes [38]. For wall motion studies, 3 planes are insufficient because the optimal smooth shape generated from cubic spline interpolation deviates from the real LV shape, whereas a higher number of imaging planes are required for quantifying small wall motion abnormalities [39]. However, the use of 3 standard plane as in the present study represents a simple and applicable approach for quantitation of wall motion in terms of area, for calculation of the present LV indices, and for display of LV shape and location of abnormal wall motion.

Indices of global LV function derived from volumes and surface areas. The endocardial surface reconstruction provides calculation of volumes and surface areas, e.g. for serial studies of LV dimensions, and global systolic function can be expressed by the fractional changes EF and FCESA. In the present study material FCESA was a more sensitive index for identification of MI than EF, and distinguished excellently between MI patients and controls (Fig. 7 a, b). The index FCESA will indicate reduced wall motion concordant to changes in EF, but in addition reveal abnormalities where shape change contributes to volume ejection (e.g. like squeezing a plastic bottle).

Shape indices are appealing because of simple calculation and interpretation, and in several works cardiac disease have been investigated with shape indices extracted from 2D images [30, 40-44]. However, the index 3DSI, expressing globularity, did not differentiate between patients with MI and controls, but may have potential in serial studies or for evaluation of dilated ventricles after surgical intervention in specific types of cardiac diseases.

Indices derived from 3D wall motion analysis. One main goal of 3D wall motion is to determine the location and size of regions with abnormal function due to coronary artery diseases. Electrocardiography has been the standard procedure, however, visual assessment by 2D real-time echocardiography, has become a highly reliable and reproducible method for localization of ischemic regions [9,10]. In the study material the localization of abnormal wall motion by the 3D method corresponded well to the visual evaluation (Fig. 10), and % AWM correlates to WMSI. However, the area AWM found by thresholding must be

regarded as a crude estimate, and it has so far not been compared with accurate measurements of ischemic LV areas or masses. Wall motion analysis based on 3D geometry can be considered as extensions of commonly used 2D single-plane methods [12-21]. One important advantage of 3D analysis compared with 2D is that surface areas can be included in the analysis (Fig. 2), enabling the area of regions with abnormal function to be determined.

Translatory and rotational motion of the ventricle are sources of inaccuracy in single-plane methods as not exactly the same part of the LV will be found in end-systole frame compared to the end-diastole frame [36]. By 3D wall motion this problem will be diminished, because the surface reconstruction algorithm includes compensation for off-axis imaging, and because wall motion is calculated locally using points at end-diastole and and end-systole surfaces located due to 3D LV geometry. Still, how to choose a reference system for measurement of local wall motion, remains an essential question in 3D as it is for single-plane analysis. Six different reference systems (a-f) were implemented and preliminary investigated [28]. An optimum reference could not be unambiguously decided, and none can be considered to be ideal from geometrical considerations. The methods using the center of mass (a,d) as reference point were least recommendable, as alignment of end-diastolic and end-systolic surfaces by center of mass will average the wall motion around the surface and thereby mask both reduced wall motion and potential hyperkinesia. The center of valve plane plane or the center of major axis (c, e, f, and Fig 10) are better choices from geometrical considerations, and similar alignment are recommended from studies of single-plane methods [12,17,18]. However, these methods can introduce erratic localization of dysfunction by reduced contraction in the axial direction; axial contraction will be equally distributed to basal and apical region by method c and f, and apical dysfunction will be masked due to axial contraction in method e. This problem is avoided by wall motion measurements normal to the major axis (method b), however, in this method the information of axial contraction is lost (see Appendix A). Therefore, from a geometrical viewpoint, it can be argued for a combination of methods, e.g. method b combined with c, e, or f, by union and intersection as illustrated in Fig. 5.

The bull's eye map is commonly used for displaying distribution of regional LV properties on a flat medium [10, 45], and a one to one correspondence between the circular map and the reconstructed endocardial surface is achieved [1]. By this map a continuous 2D representation where the regional function is easily located relative to the position in heart and to coronary arteries. For illustration of dimensions one must be aware of that relation between area of regions are distorted, e.g. an area in the basal region will be much larger in the bull's eye than

the same area in the apical region. Low motion in basal region can therefore be overrepresented, visually by the bull's eye, and by simplifications in LV shape reconstruction in this region. An leaflet map used by Guyer et. al. [25, 26], could be an actual supplement illustrating size and shape, but on the cost of continuity and compactness of the bull's eye map.

New indices of LV systolic function are obtained from calculation of wall motion statistics, whereas synergy is illustrated in the wall motion histogram. It's shape will express different types of reduced systolic function compared to those of controls (Fig. 10); e.g. reduced but uniform contraction by a shift towards zero, asynergy by a broad histogram, dyskinesia by the portion of the histogram below zero, and compensatory hyperkinesis will be displayed by an additional peak in the histogram. Furthermore, the standard deviation and CoV of wall motion provides quantitative indices of dyssynergy. The CoV correlates to WMSI (Fig. 7), and may to some extent compensate for load variations as both mean and standard deviation of wall motion can be affected in similar direction by change of loading condition. Compared with the indices derived from volume and ESA, some simplicity is lost for the latter indices because of their dependence of reference system of wall motion. The indices AWM and % AWM additionally depend on the selected threshold level. By the the use of a threshold level equal 50 % of the calculated mean value of wall motion, % AWM can be interpreted as index of dyskinesia or an estimate of the area of abnormal wall motion. Accurate determination of endocard surface area, ESA, and the infarction area, AWM, are desired for serial and prognostic studies [22-24]. An optimal procedure for the determination of AWM remains to be developed. One possible direction is to use a distributed threshold level from a normal population [12,17,18,20], or in stress echo by comparison of bull's eyes obtained at rest and at stress. Manual delineation of abnormal function in 2D echocardiography could additionally be applied in combination with 3D reconstruction and analysis.

Limitations and future work. In this study LV function by MI has been quantified on the basis of a mathematical description of the endocardial surfaces at end-diastole and end-systole. To increase the outcome of the analysis future work should aim at improved accuracy in reconstructed surface, and to include more temporal and spatial data for analysis. Accuracy can be improved by adding more imaging planes for reconstruction, as shape irregularities by papillary muscle and in the basal region requires higher density of samples to be reconstructed adequately. The addition of short-axis planes in the reconstruction algorithm could be advantageous, although performed at the cost of method simplicity.

At the present time much interest is paid to full 3D echocardiographic imaging, by the

use of a high density of 2D imaging planes building a data structure of voxels describing cardiac geometry in a volume segment [46,47]. So far most the main interest has been the visualization of details in cardiac structures, however, extraction of quantitative indices from the 3D voxel data is an important motivation. Detection of endocardial surface from 3D voxel data including the LV should be possible, enabling calculation of LV indices presented in this work .

Abnormal systolic contraction or diastolic relaxation with coronary artery disease is not always revealed in analysis of end-diastolic and end-systolic frames only [48]. Quantitative wall motion analysis should therefore increase its potential if edges from the whole cardiac cycle or at least the entire systole were included. Correlation analysis of systolic wall motion as described of Gillam and co-workers was more sensitive than methods using only two frames [19], while 3D phase analysis can be applied with the present method if edges from the whole cycle are available [1]. Tracing of the necessary number of edges for these analysis is tedious and time-consuming if not facilitated by reliable automatic border detection.

Wall thickening analysis is considered to be a more sensitive method for detection of local dysfunction with coronary artery disease than wall motion analysis [14, 48]. By visual assessment contraction abnormalities in 2D images wall thickening is an important part of the analysis, while quantitative measurements are difficult because of normally poor definition of epicardial edges in ultrasound images. One major advantage of wall thickening analysis is that no reference system is needed as translation and rotation do not influence the measurements. With epicardial and endocardial edges available the present 3D methodology can be extended to use for LV mass calculation, and for quantitative assessment of regional function by 3D wall thickening analysis. With a mathematical representation of endocardial surfaces, and additional epicardial LV surfaces, more or less sophisticated analysis methods can be applied for evaluation of regional or global LV function by estimation of curvature and wall stress, e. g. analysis of regional function by the finite element method [49].

Clinical applications and conclusions. Quantitative indices for LV function can easily be obtained from a limited number of apical ultrasound views. The method can supplement bedside echocardiography for assessment of MI; by quantifying LV dimensions and function, and by visualisation of reconstructed surfaces for appreciation of dynamic 3D LV geometry. Indices expressing surface area and systolic function presented in this work are available from noninvasive transthoracic ultrasound, and may be useful in serial studies following LV remodelling.

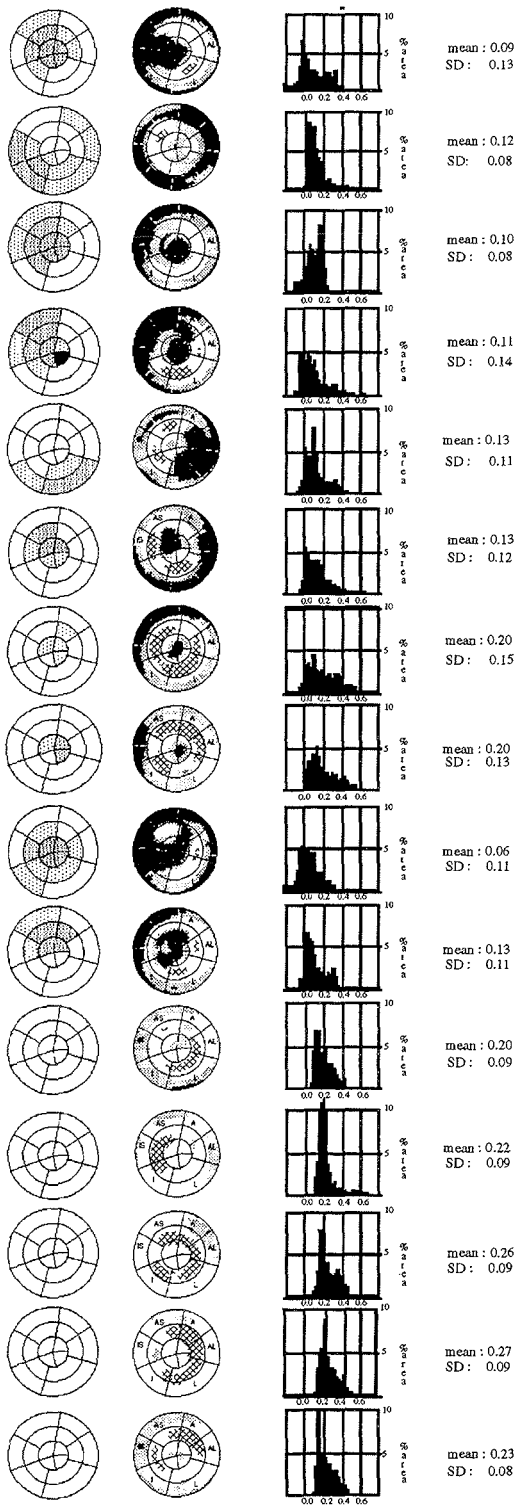

Figure 10. Comparison of bull's eyes and wall motion histograms illustrating extent and location of abnormal wall motion. The descending order of bull's eyes and histograms corresponds to the descending order of subjects in Table 1. - Left panel: WMSI bull's eyes with low density of dots showing regions assessed as hypokinetic; medium density akinetic regions; and high density dyskinetic regions. Middle panel: pattern bull's eyes from 3D wall motion analysis (pattern code is given in Fig. 4) - Right panel: wall motion histograms (see text).

Appendix

Appendix A. Vector algebra applied in computer implementations for calculations of regional wall motion.

Algebra of 3-dimensional vectors. A point **r** in 3D Cartesian coordinate system is represented as a vector:

$\mathbf{r} = (x, y, z)$ where the real number x, y, z are the coordinates of the point

The length (norm) of the vector, is denoted $|\mathbf{r}|$ and equals the distance between the point and origo, is calculated from:

$$|\mathbf{r}| = \sqrt{x^2 + y^2 + z^2}$$

Addition, subtraction and multiplication with a scalar is defined from:

$\mathbf{r}_1 + \mathbf{r}_2 = (x_1 + x_2, y_1 + y_2, z_1 + z_2)$
$\mathbf{r}_1 - \mathbf{r}_2 = (x_1 - x_2, y_1 - y_2, z_1 - z_2)$
$a\mathbf{r} = (ax, ay, az)$, a is an arbitrary real number

The expression $|\mathbf{r}_1 - \mathbf{r}_2|$ will calculate the distance between the points $\mathbf{r}_1$ and $\mathbf{r}_2$.

Application to local wall motion calculations. The fractional change in distance at position $\mathbf{r}_{i,j}$ relative to a reference $\mathbf{r}_{ref}$ is calculated by

$$c_{i,j} = \frac{\left|\mathbf{r}_{i,j} - \mathbf{r}_{ref}\right|_{diastole} - \left|\mathbf{r}_{i,j} - \mathbf{r}_{ref}\right|_{systole}}{\left|\mathbf{r}_{i,j} - \mathbf{r}_{ref}\right|_{diastole}}$$

Selectable references are:

a) center of mass in the cavity enclosed by the endocardial surface: $\mathbf{r}_{ref} = (0, 0, 0)$, as the 3D reconstruction algorithm produces ventricles with the center of mass in origo

b) major axis, fractional change in distances perpendicular to the ventricular major axis: this is realized with $\mathbf{r}_{ref.} = \mathbf{r}_{mm}$ and by setting the y-coordinates in all vectors to zero, as the major axis is parallel with the y-axis (by setting all y-coordinates to zero "one dimension is lost": the axial contraction is not taken into account)

c) center of major axis: $\mathbf{r}_{ref.} = 0.5 \times (\mathbf{r}_{mm} + \mathbf{r}_{apex})$

In the methods measuring local wall motion as the distance between the end-diastolic and end-systolic surfaces the surfaces are aligned by a common direction of the major axis, and by translation so that one of the following selectable points coincides for both surfaces:

d) center of mass: $\mathbf{r}_{ref} = (0, 0, 0)$

e) midpoint of the mitral plane: $\mathbf{r}_{mm}$

f) center of major axis: $\mathbf{r}_{ref.} = 0.5 \times (\mathbf{r}_{mm} + \mathbf{r}_{apex})$

The local wall motion at position $\mathbf{r}_{i,j}$ is then calculated by

$$c_{i,j} = c_{i,j}' \cdot sign\left(\left|\mathbf{r}_{i,j,dia} - \mathbf{r}_{ref}\right| - \left|\mathbf{r}_{i,j,sys} - \mathbf{r}_{ref}\right|\right) \quad c_{i,j}' = \min_{k,l}\left(\left|\mathbf{r}_{i,j,dia} - \mathbf{r}_{k,l,sys}\right|\right)$$

Appendix B. *Indices of global systolic contraction derived from calculations of endocardial surface areas*

The fractional change in endocardial surface area (FCESA) is suggested as an index of global left venticular systolic function and can calculated by

$$FCESA = 1 - \frac{ESA_{end-systole}}{ESA_{end-diastole}}$$

This index express contraction in terms of surface area reduction from end-diastole to end-systole. Alternatively the formula could be modified to express contraction related to geometrical or physiological magnitudes by

$$FCESA_q = 1 - \left(\frac{ESA_{end-systole}}{ESA_{end-diastole}}\right)^q$$

The interpretation of this expression depends on the exponent q:

q = 1 : relative change in surface area (the original index)

q = 0.5: relative change in surface area expressed in the dimension of length, e. g radius of a sphere, or the average shortening in length of curves on the surface

q = 1.5: relative change in surface area expressed in the dimension of volume; with uniform contraction the index would have the same value as the volume ejection fraction (EF), while a value lower than the conjugate EF indicates that shape change have contributed to volume ejection (as by squeezing a plastic bottle)

q = 2 : relative average shortening of endocardial muscle fibers; assuming that the muscle fibers are incompressible and maintains circular cross-sectional shape by contraction

Acknowledgements

Knut Bjørnstad, MD, and Svend Aakhus, MD, at Section of Cardiology, University of Trondheim, have provided echocardiographic data for this study. Edge drawing and 2D wall motion analysis (WMSI) has been performed by Knut Bjørnstad.

References

1. Mæhle J, Bjoernstad K, Aakhus S, Torp HG, Angelsen BAJ. Three-dimensional echocardiography for quantitative left ventricular wall motion analysis. A method for reconstruction of endocardial surface and evaluation of regional dysfunction. Echocardiography 1994;11:397-408.

2. Aakhus S, Mæhle J, Bjoernstad K. A new method for echocardiographic computerized three-dimensional reconstruction of left ventricular endocardial surface: In vitro accuracy and clinical repeatability of volumes. J Am Soc Echocardiogr 1994;7:571-81.

3. Mele D, Mæhle J, Pratola C, Pedini I, Alboni P, Levine RA. Application in patient of a new simplified system for 3D-echo reconstruction of the left ventricle. J Am Soc Echocardiogr 1995;8:343 (abstract).

4. Mele D, Pratola C, Pedini I, Alboni P, Levine RA. Validation and application in patients of a new system for three-dimensional echocardiographic reconstruction of the left ventricle. Circulation 1994;90:I-337 (abstract).

5. Fehske W, Mæhle J, Olstad B, Rabahieh R, Smekal A, Seelos K, Köhler U, Lüderitz B. Frame-by frame threedimensional echocardiographic reconstruction of the left ventricle. J Am Coll Cardiol 1993;19 (abstract supplement):4A

6. Tardif JC, Cao QL, Pandian NG, Azevedo J, Schwartz S, Rastegar H. Dynamic three-dimensional echocardiographic evaluation of the impact of ventricular endoaneurysmorrhaphy on regional and global left ventricular size, shape and function in patients with left ventricular aneurysm. J Am Soc Echocardiogr 1994;7:S33 (abstract).

7. Vannan M, Cao QL, Freire M, Azevedo J, Pandian NG. Utility of serial three-dimensional echocardiography in the study of ventricular remodeling and function in patients after first anterior myocardial infarction. J Am Soc Echocardiogr 1994;7:S34 (abstract).

8. Mæhle J. Reconstruction and analysis of left ventricular surfaces by three-dimensional echocardiography. I. Quantitation of the endocardial surface area. 1996 - art. C in thesis

9. Schiller NB, Shah PM, Crawford M, DeMaria A, Devereux R, Feigenbaum H, Gurgesell H, Reichek N, Sahn D, Schnittger I, Silvermann NH, Tajik AJ. Recommendations for quantitation of the left ventricle by two-dimensional echocardiography. J Am Soc Echocardiogr 1989;2:358-67.

10. Bjoernstad K, Aakhus S, Lundbom J, Bolz KD, Rokseth R, Skjaerpe T, Hatle L. Digital dipyridamole stress echocardiography in silent ischemia after coronary artery bypass grafting and/or after healing of acute myocardial infarction. Am J Cardiol 1993;72:640-46.

11. Bjoernstad K, Maehle J, Aakhus S. Quantitative computerized analysis of left ventricular wall motion. In Domenicucci S, Roelandt J, Pezzano A. (Eds.), Computerized Echocardiography, Centro Scientifico Editore, Torino,1993;41-55

12. Ginzton LE, Conant R, Brizendine M, Thigpen T, Laks M. Quantitative analysis of segmental wall motion during maximal upright dynamic exercise: Variability in normal adults. Circulation 1986;73:268-75.

13. Zoghbi WA, Charlat ML, Bolli R, Zhu W, Hartley CJ, Quinones MA. Quantitative assessment of left ventricular wall motion by two-dimensional echocardiography: Validation during reversible ischemia in the conscious dog. J Am Coll Cardiol 1988;11:851-60.

14. McGillem MJ, Mancini GBJ, DeBoe SF, Buda AJ. Modification of the centerline method for assessment of echocardiographic wall thickening and motion: A comparison with area of risk. J Am Coll Cardiol 1988;11:861-66.

15. Moynihan PF, Parisi AF, Feldman CL. Quantitative detection of regional left ventricular contraction abnormalities by two-dimensional echocardiography. I. Analysis of methods. Circulation 1981;63:752-60.

16. Parisi AF, Moynihan PF, Folland ED, Feldman CL. Quantitative detection of regional left ventricular contraction abnormalities by two-dimensional echocardiography. II. Accuracy in coronary artery disease. Circulation 1981;63:761-67.

17. Schnittger I, Fitzgerald PJ, Gordon EP, Alderman EP, Popp RL. Computerized quantitative analysis of left ventricular wall motion by two-dimensional echocardiography. Circulation 1984;70:242-54.

18. Force T, Bloomfield P, O'Boyle JE, Khuri S, Josa M, Parisi A. Quantitative two-dimensional echocardiographic analysis of regional wall motion in patients with perioperative myocardial infarction. Circulation 1984;70:233-241.

19. Gillam LD, Hogan RD, Foale RA, Franklin TD, Newell JB, Guyer DE, Weyman AE. A comparison of quantitative echocardiographic methods for delineating infarct-induced abnormal wall motion. Circulation 1984;70;113-22.

20. Assmann PE, Slager CJ, van der Borden S, Sutherland GR, Roelandt JR. Reference system in echocardiographic quantitative wall motion analysis with registration of respiration. J Am Soc Echocardiogr 1991; 4:224-34.

21. Assmann PE, Slager CJ, van der Borden SG, Tijssen JGP, Oomen JA, Roelandt JR. Comparison of models for quantitative left ventricular wall motion analysis from two-dimensional echocardiograms during acute moycardial infarction. Am J Cardiol 1993;71:1262-69.

22. Picard MH, Wilkins GT, Ray PA, Weyman AE. Natural history of left ventricular size and function after acute myocardial infarction - assessment and prediction by echocardiographic endocardial surface mapping. Circulation 1990;82:484-94.

23. Picard MH, Wilkins GT, Ray PA, Weyman AE. Progressive changes in ventricular structure and function during the year after acute myocardial infarction. Am Heart J 1992;124:24-31.

24. Weyman AE. Principles and Practice of Echocardiography 2. ed. ch. 22,. Lea & Febiger, Philadelphia, 1994.

25. Guyer DE, Foale RA, Gillam LD, Wilkins GT, Guerrero JL, Weyman AE. An echocardiographic technique for quantifying and displaying the extent of regional left ventricular dyssynergy. J Am Coll Cardiol 1986;8:830-834.

26. Guyer DE, Gibson TC, Gillam LD, King ME, Wilkins GT, Guerrero JL, Weyman AE. A new echocardiographic model for quantifying three-dimensional endocardial surface area. J Am Coll Cardiol 1986;8:819-29.

27. Wilkins GT, Southern JF, Choong CY, Thomas JD, Fallon JT, Guyer DE, Weyman AE. Correlation between echocardiographic endocardial surface mapping of abnormal wall motion and pathologic infarct size in autopsied hearts. Circulation 1988;77:978-87.

28. Bjørnstad K, Mæhle J, Aakhus S, Torp H. Evaluation of reference systems for describing regional left ventricular wall motion abnormalities by using 3-dimensional endocardial surface reconstruction. Eur Heart J 1995;16 (abstract suppl.):205.

29. Shapiro SM, Ginzton LE. Quantitative stress echocardiography. Echocardiography 1992;9:85-96.

30. Gibson DG, Brown DJ. Continuous assessment of left ventricular shape in man. Br. Heart J 1975;37:904-10.

31. Henry WL, DeMAria A, Gramiak R, King DL, Kisslo JA, Popp RL, Sahn DJ, Schiller NB, Tajik A, Teichholz LE, Weyman AE. Report of the American society of echocardiography commitee on nomenclature and standard in two-dimensional echocardiography. Circulation 1980;62:212-217.

32. Schiller NB, Acquatella H, Ports TA, Drew D, Goerke J, Ringertz H, Silverman NH, Brundage B, Botvinick EH, Boswell R, Carlsoson E, Parmley WW. Left ventricular volume from paired biplane two-dimensional echocardiography. Circulation 1979;60:547-55.

33. Henry WL, DeMaria A, Feigenbaum H, Kerber R, Kisslo J, Weyman AE, Nanda N, Popp RL, Sahn D, Schiller NB, Tajik AJ. Identification of Myocardial Wall Segments: The American Society of Echocardiography Committee on Nomenaclature and Standards 1982.

34. Olstad B. Automatic wall motion detection in the left ventricle using ultrasound images. Proc of SPIE/SPSE 1991;1450:243-254.

35. Brower RW. Evaluation of pattern recognition rules for the apex of the heart. Catheterization and Cardiovascular Diagnosis 1980;6:145-57.

36. Mann DL, Gillam LD, Weyman AE. Cross-sectional echocardiographic assessment of regional left ventricular performance and myocardial perfusion. Progress in Cardiovascular Diseases 1986;XXIX:1-52.

37. Levine RA, Handschumacher MD, Sanfilippo AJ, Hagege AA, Harrigan P, Marshall JE, Weyman AE. Three-dimensional echocardiographic reconstruction of the mitral valve, with implications for the diagnosis of mitral valve prolaps. Circulation 1989;80:589-598.

38. Mæhle J, Aakhus S, Bjørnstad K, Torp HG. How many apical imaging planes should be used for determination of left ventricular volumes by three-dimensional echocardiography. In Abstracts of the11th Symposium in Echocardiology, Rotterdam, 1995:193.

39. Mæhle J. Left ventricular dimensions and shape by three-dimensional echocardiography: how many apical imaging views should be used for reconstruction of endocardial short axis borders by cubic spline interpolation ? 1996; art. F in thesis.

40. D'Cruz IA, Daly DP, Shroff SG. Left ventricular shape and size in dilated cardiomyopathy: quantitative echocardiographic assessment. Echocardiography 1991;8:187-93.

41. Mitchell GF, Lamas GA, Vaughan DE, Pfeffer MA. Left ventricular remodeling in the year after first anterior myocardial infarction: a quantitative analysis of contractile segment lengths and ventricular shape. J Am Coll Cardiol 1992;19:1136-44.

42. Ryan T, Petrovic O, Dillon JC, Feigenbaum H, Conley MJ, Armstrong WF. An echocardiographic index for separation of right ventricular volume and pressure overload. J Am Coll Cardiol 1985;5:918-24.

43. Vandenbossche JL, Massie BM, Schiller NB, Karliner JS. Relations of left ventricular shape to volume and mass in patients with minimally symptomatic chronic aortic regurgitation. Am Heart J 1988;116:1022-27.

44. Reisner SA, Azzam Z, Halman M, Rinkevich D, Sideman S, Markiewicz W, Beyar R. Septal/free wall curvature ratio: a noninvasive index of pulmonary arterial pressure. J Am Soc Echocardiogr 1994;7:27-35.

45. Stamm RB, Gibson RS, Bishop HL, Carabello BA, Beller GA, Martin RP. Echocardiographic detection of infarct-localized asynery and remote asynergy during acute myocardial infarction: correlation with the extent of angiographic coronary disease. Circulation 1983;67:233-44.

46. Pandian NG, Roelandt J, Nanda N, Sugeng L, Cao Q, Azevedo J et. al. Dynamic three-dimensional echocardiography: methods and clinical potential. Echocardiography 1994;11:237-59.

47. Salustri A, Roelandt J. Three dimensional reconstruction of the heart with rotational acquisition: methods and clinical applications. Br Heart J 1995;73 (Supplement 2);10-15.

48. Feigenbaum H. Echocardiography 5. ed., ch. 8. Lea & Febiger, Philadelphia, 1994.

49. McPherson DD, Skorton DJ, Kodiyalam S, Petree L, Noel MP, Kieso R, Kerber RE, Collins SM, Chandran KB. Finite element analysis of myocardial diastolic function using three-dimensional echocardiographic reconstructions: application of a new method for study of acute ischemia in dogs. Circulation Research 1987;60:674-82.

Evaluation of Reference Systems for Quantitative Wall Motion Analysis From Three-Dimensional Endocardial Surface Reconstruction.

An echocardiographic study in subjects with and without myocardial infarction.

Knut Bjørnstad, MD, Jørgen Mæhle*, MSc, Svend Aakhus, MD, Hans G. Torp*, Dr. Techn, Liv K. Hatle, MD, Bjørn A. J. Angelsen*, Dr. Techn.

Department of Medicine, Section of Cardiology, and

*Department of Physiology and Biomedical Engineering,

University Hospital of Trondheim

7006 Trondheim, Norway

Short title: *Quantitative wall motion analysis*

Correspondence:

Knut Bjørnstad, MD,

Department of Medicine, Section of Cardiology,

University Hospital of Trondheim,

N-7006 Trondheim, Norway

Fax no.: + 47 73997546

Telephone: + 47 73998514

ABSTRACT

Six relevant computer implemented reference systems for 3-dimensional quantitative assessment of left ventricular wall motion abnormalities were compared with visual wall motion analysis of 2-dimensional images. Endocardial borders were traced in 3 apical echocardiographic views at end-diastole and end-systole in 10 patients with myocardial infarction and 5 healthy subjects, and 3-dimensional reconstruction of endocardial surfaces was performed. End-diastolic and end-systolic surfaces were aligned in a common axis system depending on the reference system, and systolic wall motion was assessed at 1024 points on the endocardial surface. The localization of abnormal wall motion was displayed in bull´s-eye maps, and the area was determined as a percentage of total endocardial area. For each reference system, the segmental concordance between 3-dimensional computerized and visual assessment was determined. The best agreement between computerized and visual analysis was obtained with a reference system based on wall motion towards the major ventricular axis, whereas the poorest result was obtained using the center of left ventricular cavity as reference. Correlation between the estimated area of wall motion abnormality and visually determined wall motion score index was best using the aligned center of mitral valve plane as reference ($r = 0.92$).

Key words:

Echocardiography, left ventricular wall motion, myocardial infarction, three-dimensional reconstruction.

Two-dimensional echocardiography is commonly used for evaluation of left ventricular systolic function in patients with coronary artery disease. Chamber dimensions, volumes, ejection fraction, and the presence and location of regional wall motion abnormalities can be assessed [1-3]. The extent of myocardial damage has been shown to be a major prognostic determinator after myocardial infarction [4,5]. Clinical evidence of left ventricular failure may present when 20-25% of the myocardium is injured, and cardiogenic shock may result if more than 40% is affected [6,7]. Unfortunately, conventional echocardiographic methods for quantitative left ventricular wall motion analysis are not sufficiently accurate for serial assessment of regional function. Single plane methods have been described for comparison of end-diastolic and end-systolic endocardial borders [8-12], but have not been adapted for clinical use. Wall motion score index [13], although based on subjective interpretation, is at present the most commonly used method for describing the severity of left ventricular dysfunction.

Advances in computer processing of image data have facilitated the search for more accurate quantitative wall motion analysis. In former studies, visual analysis combined with computer processing have been used to obtain estimates of the extent of myocardial infarction [14-17]. In the present study, quantitative wall motion analysis was performed with 3-dimensional reconstruction of endocardial surfaces from apical 2-dimensional views [18]. The reconstruction algorithm has been presented previously and shown to reproduce volumes in vitro with high accuracy [19]. In this study, the algorithm was used to describe regional wall motion in subjects with and without myocardial infarction.

METHODS

Patient selection. Fifteen subjects were studied, 10 with recent myocardial infarction (< 2 weeks, group A), and 5 healthy subjects without evidence of coronary artery disease (group B). In group A, myocardial infarction was documented by at least 2 of the following criteria: 1) typical chest pain lasting at least 30 minutes; 2) typical serial electrocardiographic changes; and 3) rise in serum cardiac enzymes to more than twice the

normal values. Patients with unacceptable echocardiographic image quality, previous myocardial infarction, unstable angina pectoris, or atrial fibrillation were not included. Group A patients had 12-lead electrocardiography and cardiac enzymes taken at admission for the acute infarction and thereafter at 12 hour intervals for 48 hours. Individual data for group A and B subjects are presented in Table 1. All gave informed consent to participate in the study.

Echocardiographic data aquisition. The subjects were examined in the left lateral decubitus position, using an ultrasound scanner (Vingmed CFM 750, Vingmed Sound A/S, Horten, Norway) with a 3.25 MHz annular array transducer. All images were obtained at held end-expiration. Care was taken to position the transducer over the cardiac apex, as defined by minimal displacement of apex during systole and by alignment with the left ventricular major axis and the midpoint of the mitral valve plane. Input data to the computer consisted of cineloops of standard apical 4-chamber, 2-chamber and long-axis left ventricular views, obtained by apical rotation of the transducer with adjustment to maintain the imaging plane in the ventricular major axis. Images were transferred to a personal computer (MacIntosh II series, Apple Computers, Cupertino, CA, USA), and subsequent analysis was performed using specifically designed software operating under a general program for handling of digital ultrasound data (EchoDisp 3.0, Vingmed Sound). Cineloops were transferred as digital scanline data with a frame rate of 47 frames/s using a sector angle of 60° and depth of 16 cm. An electrocardiographic tracing was transferred simultaneously with the cineloop.

Endocardial surface reconstruction. End-diastole was defined as the frame corresponding to the peak of the R-wave of the electrocardiogram, and end-systole as the last frame before mitral valve opening. On these 2 frames, left ventricular endocardial border was traced in each of the apical views, using an automatic edge detection program (EdgeFinder, Vingmed Sound) [20] with manual correction of the detected edge as necessary. The endocardium was traced at the echogenic transition zone between left ventricular cavity and myocardial wall, excluding the papillary muscles, and including the left ventricular outflow tract up to the aortic valve level in apical long-axis

view (Fig. 1). The mitral valve plane was defined as the straight line between the mitral annulus echo boundaries, i.e. at the ventricular aspect of the insertion of the mitral valve leaflets. The endocardial traces were assigned an angle corresponding to the respective rotation of the transducer around its center axis, starting at zero degrees for the apical four-chamber view. Apical 2-chamber and apical long-axis views were assumed to be at 62 and 101 degrees counter-clockwise rotation, respectively [21]. The endocardium was automatically reconstructed as a smooth bicubic spline surface (Fig. 1). The reconstruction algorithm has previously been described in detail [18].

Quantitative wall motion analysis. The reconstructed end-diastolic and end-systolic endocardial surfaces were represented by 1024 numbered points [Appendix]. To determine regional wall motion, end-diastolic and end-systolic surfaces were aligned in common coordinate systems, and wall motion was calculated at each point. Six different reference systems were evaluated for quantitative wall motion analysis, differing in the way the 2 surfaces are aligned. In reference systems a), b), and c), systolic wall motion is determined as fractional change in distance to a selected point or axis (Fig. 2). This reference point or axis were: a) center of ventricular cavity; b) major ventricular axis, along lines perpendicular to the axis; and c) center of major axis. With reference systems d), e), and f), regional wall motion was determined as the shortest distance from the end-diastolic to the end-systolic surface in millimeters (Fig. 2). The surfaces were aligned by a common direction of the major axis and by a common position of the: d) center of ventricular cavity; e) midpoint of the mitral valve plane; and f) center of major axis.

Regional wall motion was displayed in bull´s-eye maps for visualization of the extension and location of wall motion abnormalities as determined by each reference method. A pattern code was applied to illustrate variation in regional wall motion (Fig. 3). Mean wall motion was calculated for each subject and each reference system [Appendix], and a threshold value of 50% of mean wall motion was used to distinguish between normal and abnormal motion. The endocardial area representing a wall motion

abnormality was determined as a percentage of total end-diastolic endocardial surface area, and the location was graphically displayed within the bull´s-eye maps.

Visual wall motion scoring. The 3 apical left ventricular cineloops used for endocardial tracing were also analysed visually on the computer monitor, using a specific software for wall motion display and analysis (EchoLoops version 3.0, Vingmed Sound). A 16-segment model of the left ventricle was used [13]. Each segment was assigned a score based on wall motion and myocardial thickening: normal = 1, hypokinetic = 2, akinetic = 3, dyskinetic = 4, or aneurysmal = 5. Wall motion score index (WMSI) was calculated as the sum of the segmental scores, divided by number of observed segments, and expressed a semi-quantitative index of the severity of wall motion abnormality. The location and extent of abnormal wall motion was displayed within the bull´s-eye maps (Fig. 4).

Analysis. The individual results of the 3-dimensional computerized wall motion analysis for each of the six reference systems were compared with visually determined wall motion on a segmental basis. Using bull´s-eye maps from the computerized analysis, each of the 16 segments was classified as normal or abnormal. Segments partially or completely affected by wall motion abnormality were defined as abnormal. By visual assessment of 2-dimensional images, segments scored as hypokinetic or worse were defined as abnormal. The number of the segments classified equally by computerized analysis and visual analysis as normal or abnormal was expressed as a percentage of the total 16 segments. For each of the reference systems, mean values ± SD are calculated. The percentage of the endocardial area representing abnormal wall motion by each reference system was compared to wall motion score index using correlation coefficient (r-value).

RESULTS

The agreement between computerized wall motion analysis by each of the reference systems and visual analysis is shown in Table 2, comprising segmental agreement as well as the correlation between % area of abnormal wall motion and wall

motion score index. Individual patient bull's-eye maps as determined by computerized wall motion analysis for the different reference systems, and visual wall motion scoring are shown in Fig. 5.

All reference systems differentiated well between healthy subjects and patients with myocardial infarctions. Minor differences were found between the reference systems based on major ventricular axis (system b), center of major axis (system c), fixed center of mitral valve plane (system e), and fixed center of major axis (system f), with segmental agreement varying from 76 ± 13% to 78% ± 17%. Poorest results were obtained with reference system a, based on the center of ventricular cavity as reference. Using reference system c, which showed the optimal specificity, none of the healthy subjects were found to have abnormal wall motion involving more than 5% of the endocardial surface (Fig. 5 and 6).

Regression plots for % area calculations and wall motion score index for each reference method are shown in Fig. 6. The % endocardial area of abnormal wall motion correlated best with wall motion score index when reference systems c, e, or f were applied, with r-values in the range of 0.87 to 0.92.

DISCUSSION

Single plane methods are traditionally classified as using a fixed or a floating reference. With a fixed reference system, no correction for translatory and rotational cardiac motion is applied, whereas a floating reference system is based on realignment of the edges by geometrically defined landmarks. The present study investigated 6 different floating reference systems for quantitative left ventricular wall motion analysis. Wall motion analysis based on 3-dimensional geometry can be considered as extensions of conventional 2-dimensional single plane methods, but has the important advantage that regions with abnormal wall motion as well as the total endocardial surface area can be quantitated [Appendix].

Regional wall motion analysis. Reference systems a, b, and c assume that the ventricular contraction approximates a single center or axis, whereas reference

systems d, e, and f measure the actual distance between the 2 surfaces. Each system has specific advantages and shortcomings, as illustrated by the results of this study:

Reference system a: This system is based on a common center of left ventricular cavity for wall motion analysis. In general, the center of cavity will be shifted towards an akinetic or dyskinetic region during systole and thus tends to average regional wall motion. Accordingly, both reduced wall motion and hyperkinesia may be masked. In the present study, the majority of patients had anterior or apical infarctions, however, the wall motion abnormality tended to be displayed in the basal left ventricular regions (Fig. 5). This reference system showed the poorest overall results of those evaluated.

Reference system b: The best results in our study were obtained with this reference system, based on calculation of wall motion along lines perpendicular to the major left ventricular axis. This is the only reference system analyzing basal and apical contraction separately, and the dominant wall motion abnormality was correctly identified in all patients. However, axial shortening is not taken into account with this reference system, and this may explain the suboptimal correlation between the % area calculation and wall motion score index.

Reference system c: This system is based on the center of major ventricular axis as reference. As illustrated by Fig. 5 and 6, this reference system showed the best ability to differentiate between healthy subjects and patients with myocardial infarction. However, axial contraction may be distributed both to the basal and the apical regions. Accordingly, a severe apical wall motion abnormality will be underestimated and partly projected to the basal portion of the left ventricle. As illustrated by the bull´s-eye maps in Fig. 5, analysis with this reference system tended to display wall motion abnormalities in both the apical and basal left ventricular regions in patients with apical infarctions.

Reference system d: This reference system has the same shortcomings as system a, and did not have a favourable outcome in our study patients.

Reference system e: This system aligns the reconstructed left ventricular surfaces by a common center of the mitral valve planes. Like reference system c, this system will be inaccurate in localizing abnormal contraction along the ventricular long

axis, and apical hypokinesia may be masked in patients with axial shortening (e.g. subjects no. 7 and 8, Fig. 5). However, more severe apical wall motion abnormalities will be identified, and the results obtained with this system were almost as good as with reference b.

Reference system f: Although quite similar to reference system c, this system did not differentiate quite as well between patients with myocardial infarction and healthy subjects.

Echocardiographic surface reconstruction. The results of wall motion analysis depend not only on the reference system, but also on the accuracy of the reconstructed endocardial surface. Important factors are correct endocardial visualization and tracing, correct spatial orientation of the edges from 2-dimensional images in the 3-dimensional coordinate system, as well as the validity of the assumptions and simplifications of the reconstruction algorithm. Correct endocardial tracing of the apical 2-dimensional views depends on adequate visualization of the endocardial border in the end-diastolic and end-systolic frames. According to the recommendations of the American Society of Echocardiography [13], endocardial tracing is not recommended if less than 80% of the endocardial border is visualized. The high frame rate of the scanconverted cineloops (47 frames/s) allows slow motion display for accurate edge detection. Advances in automatic edge detection may improve the reconstruction procedure by increasing the accuracy and reducing the time needed for edge tracing, as this is the most time-consuming part of the present technique.

The surface reconstruction is based on assumed angles between the different apical views. For volume estimates, deviations within 15 degrees from these angles have only minor impact on the results [19]. However, correct spatial orientation is likely to be more important for regional wall motion analysis. This problem can be solved by using a device for exact, predetermined steps of rotation, or by measuring the actual angle of imaging plane rotation.

The assumptions and simplifications of left ventricular geometry refer to the smoothing of the left ventricular outflow tract, which becomes a part of the reconstructed

endocardial surface. Also, the mitral valve annulus is assumed to be planar, in contrast to the findings in echocardiographic studies [22]. These factors may cause errors in regional wall motion in the basal portion of the ventricle, whereas volumes and endocardial surface area calculations are less affected.

Methodological considerations and limitations. Three-dimensional reconstruction based on apical echocardiographic images with transducer rotation around the major ventricular axis has previously been used to assess left ventricular geometry [23-25]. A major advantage with the apical approach as compared to other 3-dimensional techniques is the simplicity of obtaining images. In this study, no special instrumentation for measuring or controlling the position of the imaging planes was applied. The algorithm used for 3-dimensional reconstruction provides accurate assessment of volumes in vitro, and interobserver and intraobserver repeatability for analysis of ventricular volumes in the clinical setting are good with coefficients of variation ranging from 3.5% to 6.2% [19]. The time needed to trace 3 cineloops at end-systole and end-diastole is 5-10 minutes, and the processing and display of quantitative wall motion data can be performed within a few seconds.

As illustrated by Fig. 5, patients with myocardial infarctions commonly had several regions with abnormal wall motion, and the % area calculation summarized all areas. A threshold value served to make a crude distinction between normal and abnormal wall motion. Whereas pattern bull´s-eye maps serve best for illustration of regional wall motion (Fig. 3), a threshold value is necessary to quantitate the area extension of dysfunction. However, the threshold value does not take into account the variation in normal wall motion for different regions of the left ventricle with the exception of adjustments in the basal left ventricular region [Appendix].

In the bull´s-eye maps, the ratio between surface areas in different endocardial regions are distorted, e.g. an area in the basal region appears larger than the same area in the apical region. Impaired basal wall motion will thus be visually overrepresented by the bull´s-eye mapping technique.

Although 3 apical imaging views have been shown to give accurate volume determinations with the presently used algorithm [19], a higher number of views may be required in order to detect more subtle wall motion abnormalities.

Future directions. The shortcomings of the individual reference systems may be reduced by combining different reference systems. Although it was not investigated with the present study design, the software has been designed to allow this option. In order to detect more subtle wall motion abnormalities, the number of imaging planes can be increased, and the angle between imaging planes can be standardized by using a device for transducer rotation . Furthermore, more powerful computers and improvements in the automatic edge detection algorithm will reduce the time needed for image processing and analysis.

APPENDIX

Mathematical description of reconstructed endocardial surfaces. With the present computer algorithm, the endocardium will be reconstructed as a smooth bicubic spline surface. Calculation of left ventricular wall motion is based on geometric data representing the endocardial surface at a selected number of points on this reconstructed smooth surface. The data used comprised a matrix of points $\{ \mathbf{r}_{i,j} \}$ on the reconstructed surface, and the points $\mathbf{r}_{apex}$ and $\mathbf{r}_{mm}$ positioned at the apex and at the mitral plane midpoint, respectively (Fig. A, Upper panel). The ventricular major axis is defined as the straight line connecting $\mathbf{r}_{apex}$ and $\mathbf{r}_{mm}$. Each point is given in Cartesian coordinates $\mathbf{r}_{i,j} = (x_{i,j} , y_{i,j} , z_{i,j})$ positioned in space with the center of ventricular cavity fixed at origo, and with left ventricular major axis along the y-axis. The range of indexes, i and j, was selected to be 32 both in axial and circumferential direction, with a total of 1024 points representing the endocardial surface.

Calculation of surface areas. The reconstructed endocardial surface is divided into small areas $a_{i,j}$ surrounding each point $\mathbf{r}_{i,j}$ of the surface. Each area $a_{i,j}$ includes the 4 parallellograms defined by the lines starting at the point $\mathbf{r}_{i,j}$, and extending half the distance to the adjacent points. The results are stored in a matrix $\{ a_{i,j} \}$ for further calculations. The endocardial surface area (ESA, cm^2) was calculated as the sum of the matrix elements by

$$ESA = \sum_{i,j} a_{i,j}$$

This estimate converges to the surface area of the smooth reconstructed endocardial surface as the resolution increases.

Three-dimensional wall motion analysis. Regional wall motion is calculated at each point of the geometric description of the endocardial surface and stored in a matrix $\{ c_{i,j} \}$ (Fig. A, Middle panel). The value of one $c_{i,j}$ expresses fractional shortening to a reference (reference system a-c) or absolute displacement (reference system d-f) of the wall at position i,j from end-diastole to end-systole. The contents of

the wall motion matrix { $c_{i,j}$ } is displayed in two dimensions in a bull´s-eye map (Fig. 3).

The calculated values of regional wall motion and end-diastolic endocardial area, { $c_{i,j}$ } and { $a_{i,j}$ }, are combined for further calculations. A histogram displays the percent of the ventricle, in terms of end-diastolic endocardial surface area, at different levels of wall motion along the horizontal axis (Fig. A, Lower panel). The calculated mean value and its variance of wall motion are expressed by

$$\hat{c} = \frac{1}{ESA}\sum_{i,j} c_{i,j}a_{i,j} \qquad \sigma^2 = \frac{1}{ESA}\sum_{i,j}\left(c_{i,j} - \hat{c}\right)^2 a_{i,j} \qquad ESA = \sum_{i,j} a_{i,j}$$

The size of areas with abnormal wall motion (AMW) is estimated from the constant threshold level, t (50% of mean wall motion), by

$$AWM = \sum_{c_{i,j} < w_i t} a_{i,j} \qquad (w_1 \ldots\ldots w_{28} = 1, w_{29} = 0.8, w_{30} = 0.5, w_{31} = 0.2, w_{32} = 0)$$

The estimated area with reduced wall motion is expressed as a percentage of the end-diastolic endocardial surface area (% AMW), and its location is displayed in the bull´s-eye map. The weight factors w_i are introduced to avoid relative low wall motion in the basal region to be detected as abnormal (numbers refer to the axial resolution of 32). The choice of a threshold level equal to 50% of the mean wall motion was motivated from the shape of histograms; healthy controls have narrow (low variance) histograms centered around a high mean value, whereas regional systolic dysfunction was reflected in a shift in the histogram towards zero combined with a higher variance.

References:

1. Peels CH, Visser CA, Funke Kupper AJ, et al: Usefulness of two-dimensional echocardiography for immediate detection of myocardial ischemia in the emergency room. Am J Cardiol 65:687-691, 1990.

2. Heger JJ, Weyman AE, Wann LS, et al: Cross-sectional echocardiography in acute myocardial infarction: detection and localization of regional left ventricular asynergy. Circulation 60:531-538, 1979.

3. Buda A: The role of echocardiography in the evaluation of mechanical complications of acute myocardial infarction. Circulation 84:I-109-I-121, 1991 (suppl).

4. Horowitz RS, Morganroth J: Immediate detection of early high-risk patients with acute myocardial infarction using two-dimensional echocardiographic evaluation of left ventricular regional wall motion abnormalities. Am Heart J 103:814-822, 1982.

5. Nishimura RA, Reeder GS, Miller FA et al: Prognostic value of predischarge 2-dimensional echocardiogram after acute myocardial infarction. Am J Cardiol 53:429-432, 1984.

6. Miller RR, Olson HG, Vismara LA et al: Pump dysfunction after myocardial infarction: importance of location, extent and pattern of abnormal left ventricular segmental contraction. Am J Cardiol 37:340-345, 1976.

7. Page DL, Caulfield JB, Kastor JA et al: Myocardial changes associated with cardiogenic shock. N Engl J Med 285:133-137, 1971.

8. Ginzton LE, Conant R, Brizendine M, et al: Quantitative analysis of segmental wall motion during maximal upright dynamic exercise: Variability in normal adults. Circulation 73:268-275, 1986.

9. Force T, Bloomfield P, O'Boyle JE et al: Quantitative two-dimensional echocardiographic analysis of regional wall motion in patients with perioperative myocardial infarction. Circulation 70:233-241,1984.

10 Schnittger I, Fitzgerald PJ, Gordon EP et al: Computerized quantitative analysis of left ventricular wall motion by two-dimensional echocardiography. Circulation 70:242-254, 1984.

11. Assmann PE, Slager CJ, van der Borden S, et al: Reference systems in echocardiographic quantitative wall motion analysis with registration of respiration. J Am Soc Echocardiogr 4:224-234, 1991.

12. Assmann PE, Slager CJ, van der Borden SG, et al: Comparison of models for quantitative left ventricular wall motion analysis from two-dimensional echocardiograms during acute moycardial infarction. Am J Cardiol 71:1262-1269, 1993.

13. Schiller NB, Shah PM, Crawford M et al: American Society of Echocardiography committee on standards, subcommittee on quantitation of two-dimensional echocardiograms: Recommendations for quantitation of the left ventricle by two-dimensional echocardiography. J Am Soc Echocardiogr 2:358-367, 1989

14. Guyer DE, Foale RA, Gillam LD, et al: An echocardiographic technique for quantifying and displaying the extent of regional left ventricular dyssynergy. J Am Coll Cardiol 8:830-834, 1986.

15. Guyer DE, Gibson TC, Gillam LD et al: A new echocardiographic model for quantifying three-dimensional endocardial surface area. J Am Coll Cardiol 8:819-829, 1986.

16. Wilkins GT, Southern JF, Choong CY et al: Correlation between echocardiographic endocardial surface mapping of abnormal wall motion and pathologic infarct size in autopsied hearts. Circulation 77:978-987, 1988.

17. Picard MH, Wilkins GT, Ray PA, et al: Natural history of left ventricular size and function after acute myocardial infarction - assessment and prediction by echocardiographic endocardial surface mapping. Circulation 82:484-494, 1990.

18. Mæhle J, Bjoernstad K, Aakhus S, et al: Three-dimensional echocardiography for quantitative left ventricular wall motion analysis. A method for reconstruction of endocardial surface and evaluation of regional dysfunction. Echocardiography 11:397-408, 1994.

19. Aakhus S, Mæhle J, Bjoernstad K: A new method for echocardiographic computerized three-dimensional reconstruction of left ventricular endocardial surface: In

vitro accuracy and clinical repeatability of volumes. J Am Soc Echocardiogr 7:571-581, 1994.

20. Olstad B: Automatic wall motion detection in the left ventricle using ultrasonic images. Proc of SPIE 1450:243-254, 1991.

21. Henry WL, DeMaria A, Feigenbaum H et al: Identification of myocardial wall segments. Report of The American Society of Echocardiography committee on nomenclature and standards 1982.

22. Levine RA, Handschumacher MD, Sanfilippo AJ et al: Three-dimensional echocardiographic reconstruction of the mitral valve, with implications for the diagnosis of mitral valve prolapse. Circulation 80:589-598, 1989.

23. Ghosh A, Nanda NC, Maurer G: Three dimensional reconstruction of echocardiographic images using the rotation method. Ultrasound Med Biol 8:655-661, 1982.

24. McCann HA, McEwan CN, Sharp JC, et al: Multidimensional ultrasonic imaging for cardiology. Proc IEEE 76:1063-1073, 1988.

25. Fazzalari NL, Davidson JA, Mazumdar J, et al: Three dimensional reconstruction of the left ventricle from four anatomically defined apical two-dimensional echocardiographic views. Acta Cardiologica 39:409-436, 1984.

Table 1. Baseline patient characteristics.

Pat. no.	Age (years)	Sex	AMI	AMI region (ECG)	ASAT (mmol/l)	CK (μmol/l)	WMSI
1	66	M	+	Anterior	278	1786	1.81
2	68	M	+	Inferior	685	3607	1.75
3	73	M	+	Anterior	545	2201	1.81
4	70	M	+	Anterior	707	4884	2.00
5	65	M	+	Lateral	323	2350	1.25
6	68	M	+	Anterior	366	2079	1.56
7	58	M	+	Anterior	215	1558	1.06
8	53	M	+	Anterior	357	2142	1.50
9	66	M	+	Anterior	143	602	2.06
10	71	M	+	Anterior	485	1524	1.56
11	36	M	-	Normal	-	-	1.00
12	62	M	-	Normal	-	-	1.00
13	35	F	-	Normal	-	-	1.00
14	29	M	-	Normal	-	-	1.00
15	26	M	-	Normal	-	-	1.00

AMI = acute myocardial infarction; ECG = electrocardiography; WMSI = wall motion score index.

Table 2. Comparison between computerized and visual wall motion analysis.

Reference system:		Segmental agreement (%). Mean ± SD	Range	Corr. %area/WMSI r-value
a	Center of left ventricular cavity	58 ± 20	31 - 88	0.77
b	Major left ventricular axis	78 ± 13	56 - 94	0.79
c	Center of major left ventricular axis	76 ± 15	50 -100	0.87
d	Aligned center of cavity	69 ± 18	38 - 94	0.82
e	Aligned center of mitral valve plane	77 ± 13	56 - 94	0.92
f	Aligned center of major axis	77 ± 17	31 -100	0.87

Confer text for explanation of calculated segmental agreement and correlation of %area and wall motion score index (WMSI).

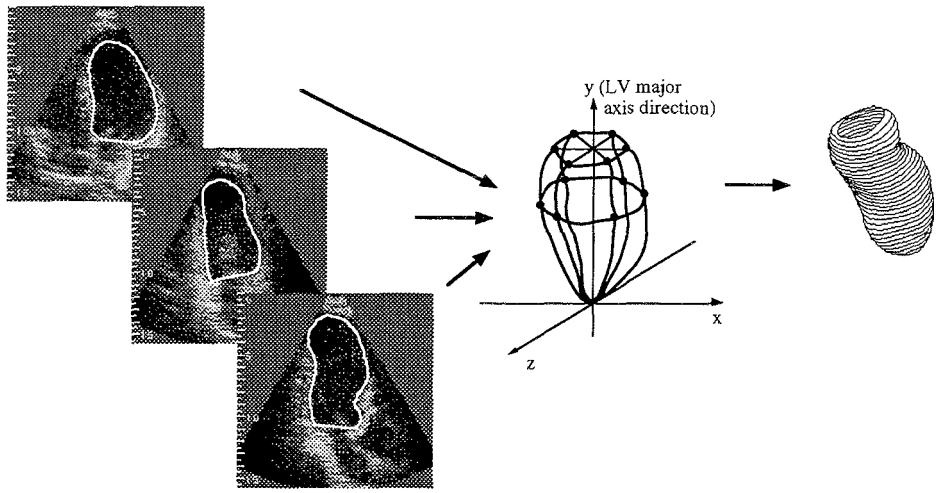

Figure 1. Three-dimensional reconstruction of endocardial surface from 3 apical views of the left ventricle. The endocardium is reconstructed as a smooth bicubic spline surface, the apical borders are described by cubic spline curves, and cross-sections are reconstructed by a closed cubic spline curve interpolating the apical borders.

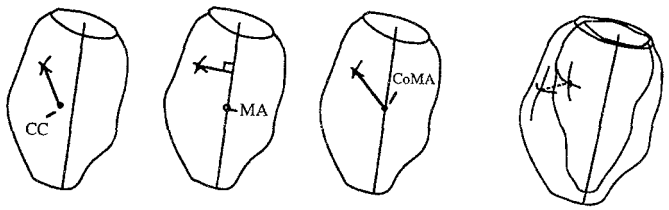

Figure 2. Reference systems for wall motion calculations from end-diastolic and end-systolic endocardial surfaces. From left to right, reference systems a, b, c, and e are illustrated. CC = center of left ventricular cavity; CoMA = center of major axis; MA = major axis.

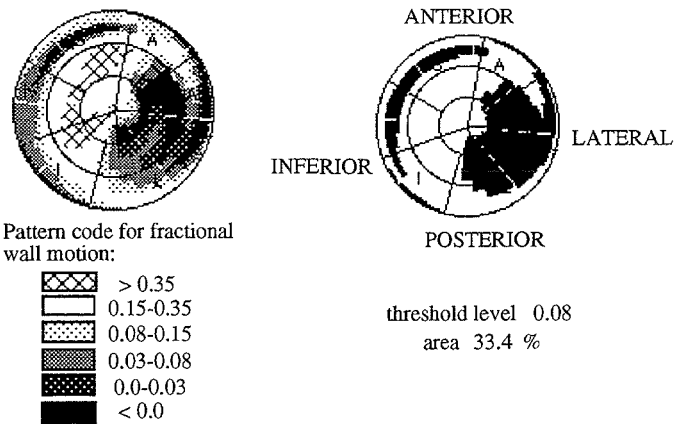

Figure 3. Example of computerized wall motion analysis (patient no. 5, analyzed with reference system b).

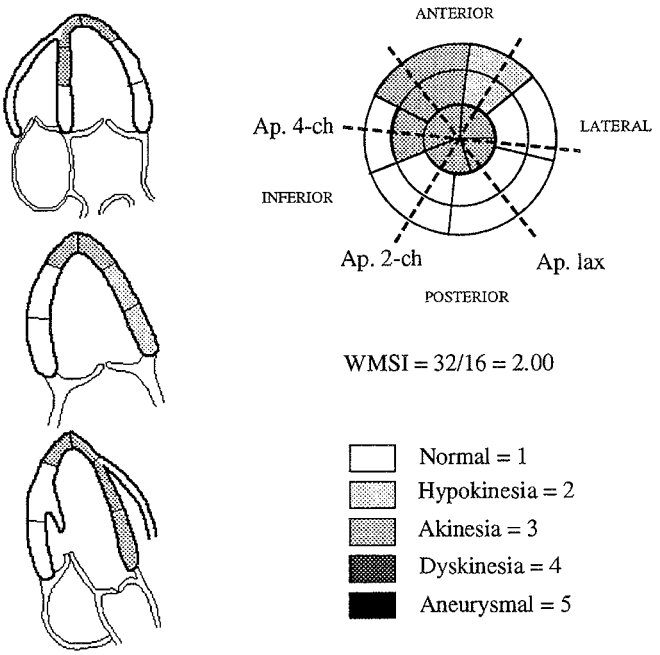

Figure 4. Example of visual wall motion analysis with wall motion score index calculation. See text for explanantion.

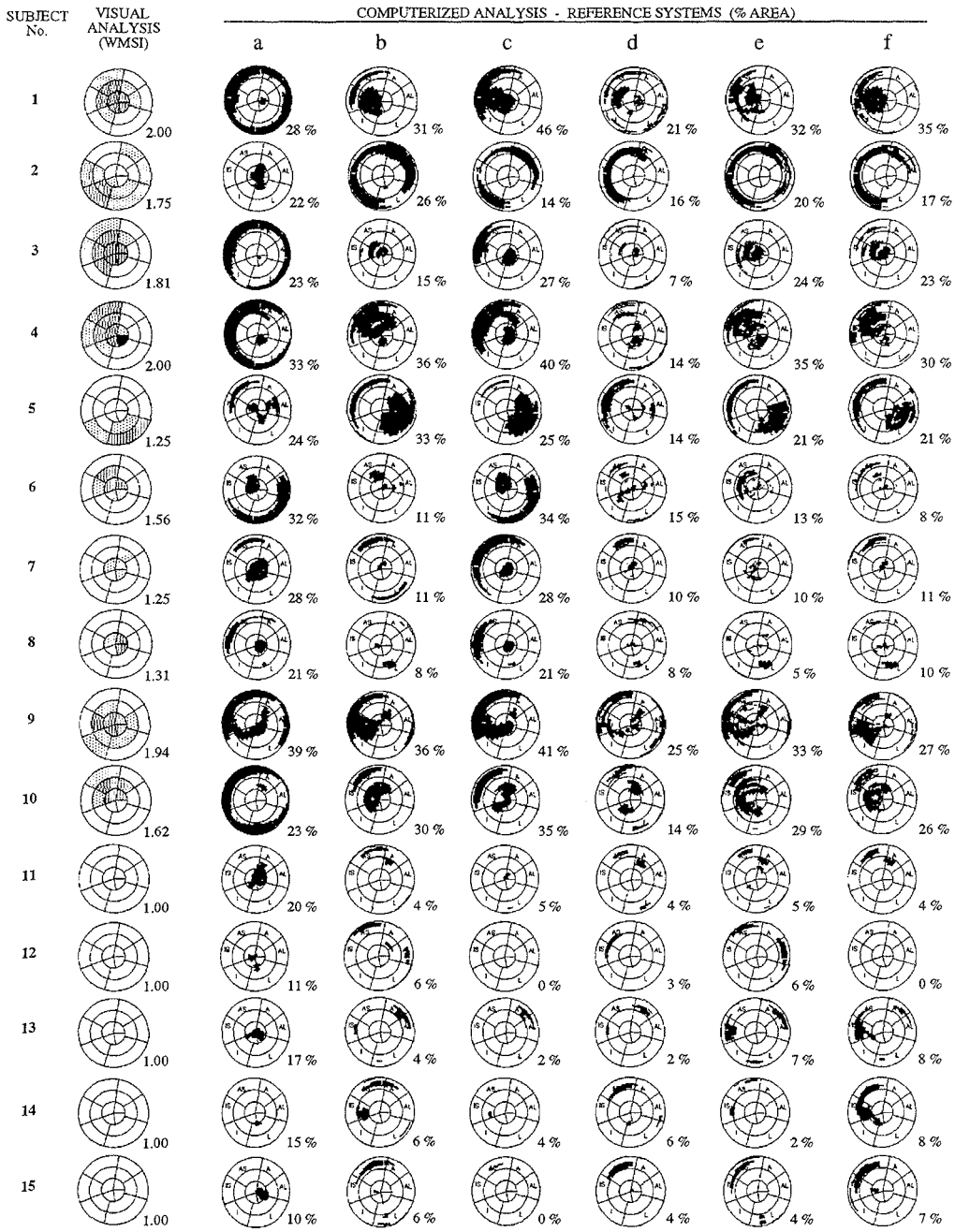

Figure 5. Bull´s-eye maps from individual patients, with visual wall motion analysis (left column) and computerized wall motion analysis with different reference systems.

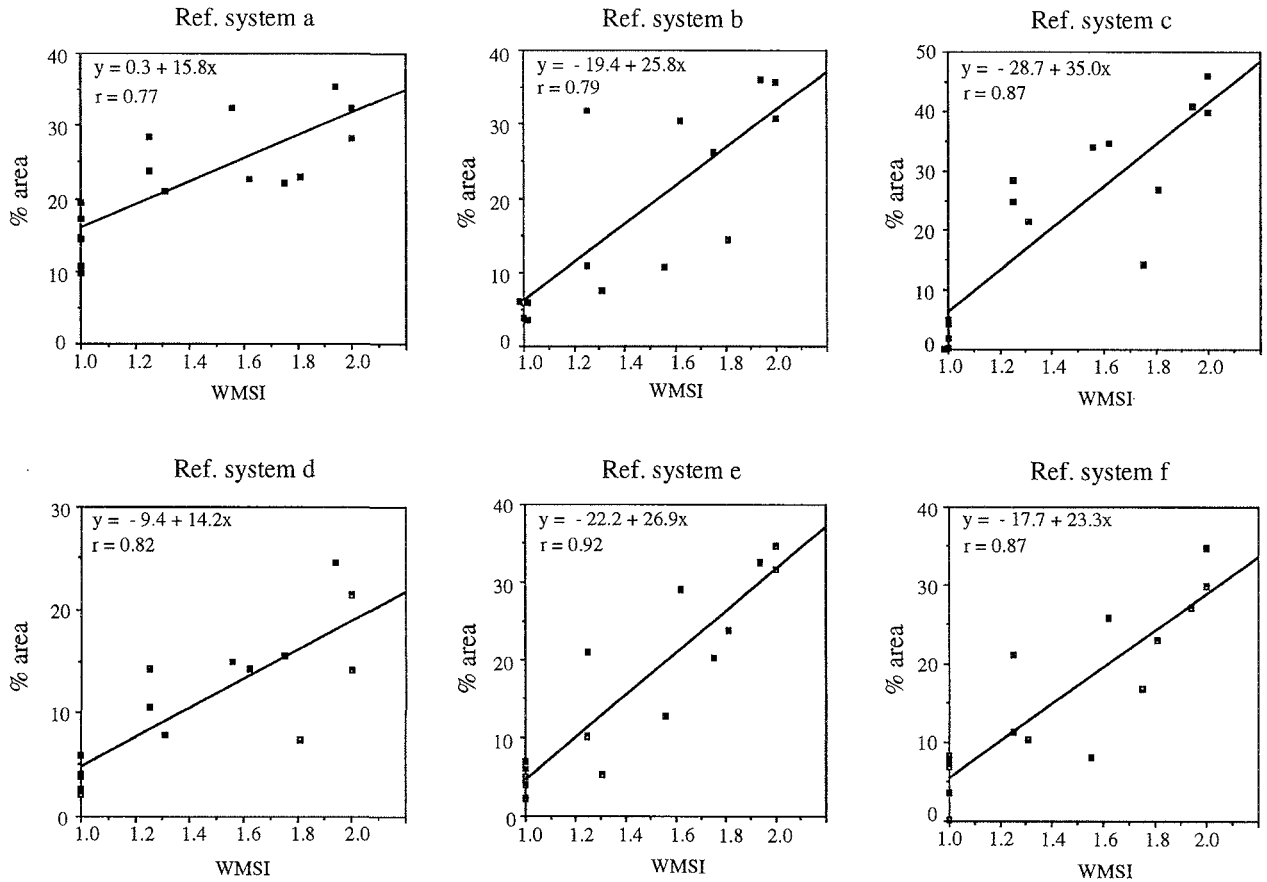

Figure 6. Regression plots for % area calculations and wall motion score index for the 6 different reference systems.

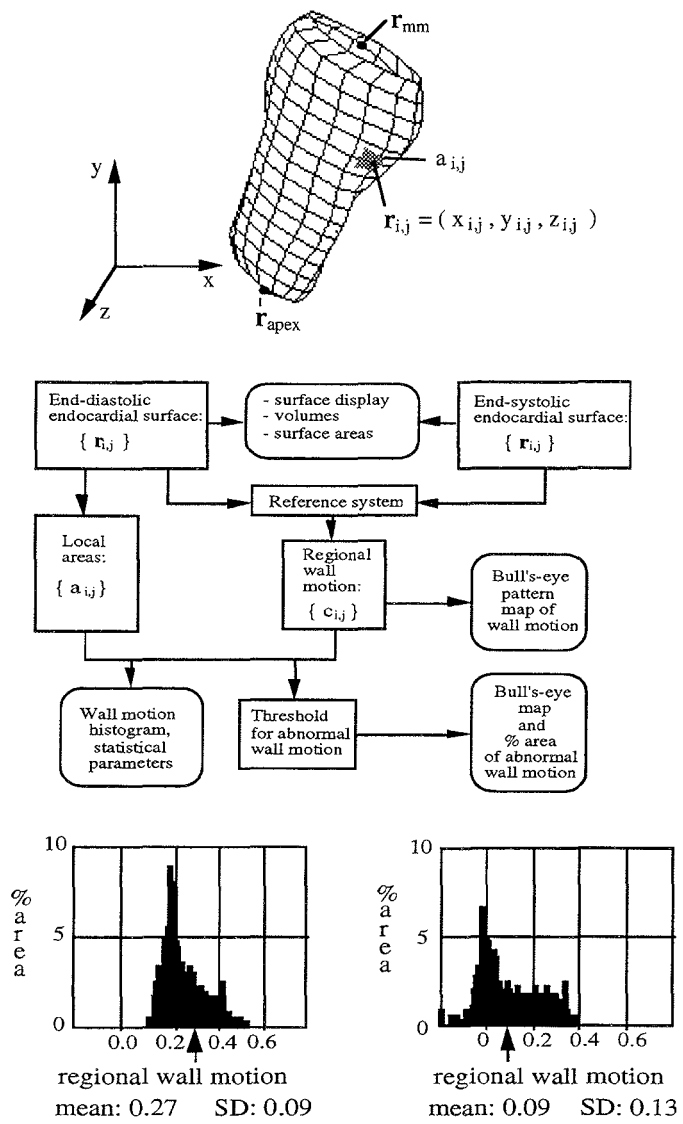

Figure A. *Upper panel:* Wire-frame display of the surface (low resolution for illustration) showing the mathematical description of the endocardial surface used for regional wall motion analysis; coordinates of the apex and the mitral midpoint, $\mathbf{r}_{apex}$ and $\mathbf{r}_{mm}$, and the points $\{ \mathbf{r}_{i,j} \}$ at the mesh corners; $a_{i,j}$ refer sto the portion of the subdivided endocardial surface area associated with point $\mathbf{r}_{i,j}$. This area is composed of 4 parallelograms defined by half of the distance along the straight lines connecting the point to its adjacent points. *Middle panel:* Flow-chart illustrating the analysis of left ventricular function based on a mathematical description of the endocardial surface at end-diastole and end-systole. *Lower panel:* Wall motion histograms obtained by analysis using reference system b) (center of major axis). The histogram displays the portion of the endocardial surface (in % of the end-diastole endocardial surface area) as vertical bars at different levels of wall motion (relative systolic shortening) at the horizontal axis, the calculated mean value of wall motion is indicated with arrow. *Left:* control subject no. 14, Table 1. *Right:* patient with previous myocardial infarction, subject no. 1, Table 1.

Left Ventricular Dimensions and Shape by Three-Dimensional Echocardiography: How Many Apical Imaging Views Should be Used for Reconstruction of Endocardial Short Axis Borders by Cubic Spline Interpolation?

Abstract

Objectives: The aim of this study was to assess how many sample points that were needed on a short axis endocardial border for determination of geometric indices of left ventricular (LV) function. **Background:** We have previously presented a method for three-dimensional (3D) reconstruction which is based on reconstruction of endocardial short axis borders by cubic spline interpolation. The accuracy in estimates of volume, surface area, and regional wall motion by this method therefore depends on the accuracy of reconstructed short axis borders.

Method: Manually drawn end-diastolic and end-systolic midventricular short axis endocardial borders from 10 subjects (with and without myocardial infarction) were analyzed. Endocardial borders were reconstructed by use of cubic spline interpolation through points (4-24) on the original borders, and then compared with the original borders with respect to cross-sectional area and length of circumference. Global shape difference and maximal local distance between reconstructed and original borders were calculated with the centerline method.

Results: The mean ± SD of percent error for all indices was significantly reduced when the number of points for interpolation was increased from 4 to 6, and from 6 to 8. When 8 points were used, the 95 % confidence limits for the difference between reconstructed and original borders were -2.2 to 0.7 % for area, -2.1 to 0.1 % for circumference, and 3.4 to 8.4 % for the maximal local distance. **Conclusions:** Regional shape analysis and calculation of dimensions can be performed accurately from borders reconstructed by cubic spline interpolation through 8 points, corresponding to 4 apical views used for 3D reconstruction. Detection of minor abnormalities in shape is improved when the density of points increases, whereas dimensions can be determined with sufficient accuracy from 6 points corresponding to 3 apical views.

Keywords: echocardiography, left ventricular dimensions, left ventricular shape, 3D reconstruction, cubic spline interrpolation

Introduction

Two-dimensional (2D) real-time ultrasound imaging is a widespread method for assessment of left ventricular (LV) dimensions and shape. Quantitative descriptions of borders defining the LV endocardium and epicardium are desired for analysis of dimensions and shape, both for direct analysis of 2D planar contours [1], and for three-dimensional (3D) reconstruction of LV shape [2-5].

Cubic spline interpolation is commonly used for generation of smooth curves in computer graphics [6,7], and can be applied to cardiac borders by using a limited number of sampled points for definition of the complete border (Fig. 1).

Simplified three-dimensional reconstruction from only 3 apical views based on cubic spline interpolation (Fig. 1a), has previously been shown to determine both ventricular volume and endocardial surface areas accurately [8-10], and for illustration of regional systolic contraction by computerized wall motion analysis [11,12]. Accuracy in this 3D reconstruction method is highly dependent of the accuracy in reconstruction of 2D short-axis borders from interpolation on a limited number of points located on the apical borders.

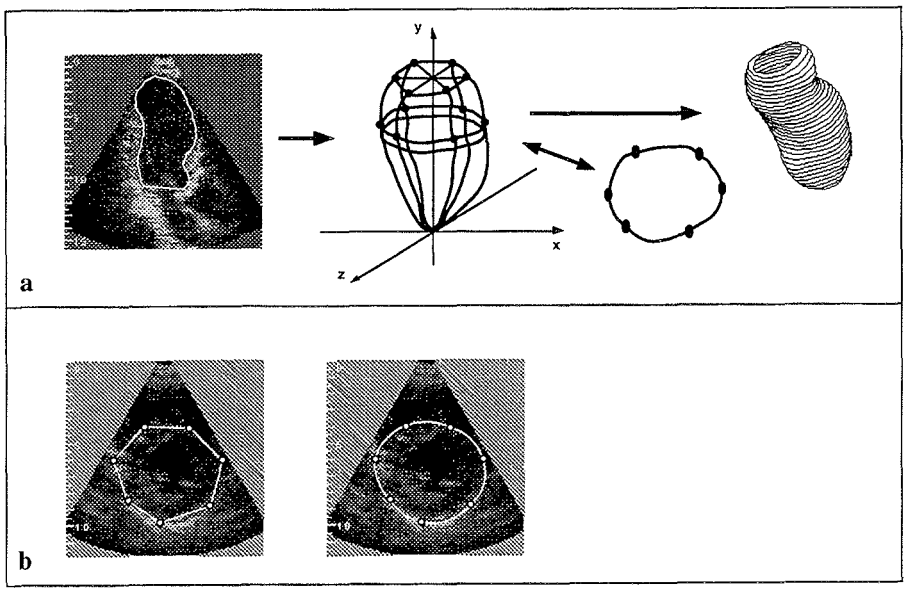

Fig. 1. **a)** Three dimensional LV reconstruction from endocardial borders in apical long axis views. The endocardial surface is generated as a smooth bicubic spline surface; the apical borders are described by cubic spline curves, and short axis are reconstructed by a closed cubic spline curve interpolating the apical borders.
b) Epicardial border defined from selected points and cubic spline interpolation.

The purpose of this study was to investigate how accurate LV endocardial short-axis borders could be reconstructed from a limited number of sampled points, and how the accuracy in reconstruction depends on the number of points used for cubic spline interpolation. Interpolated short-axis borders were compared with the original manually drawn borders, and the accuracy in reconstruction was assessed directly in terms of 2D or 3D geometrical indices with physiological impact: accuracy in 3D LV volume will be determined by accuracy of cross-sectional areas, accuracy of short-axis circumference is the dominant source of accuracy in 3D endocardial surface areas, and accuracy of both 2D and 3D regional wall motion and thickening calculations depend on the accuracy in reconstruction of shape globally and locally.

Methods

Study population. Ten subjects (8 men and 2 women), age 24 to 66 years, with (n=6) or without (n=4) LV regional wall motion abnormalities at rest due to previous myocardial infarction, were included in the study (Table 1). The subjects were selected due to high quality 2D ultrasound images, and all were in regular sinus rhythm.

Table 1 Study population and endocardial border dimensions

		area (cm2)		circumference (cm)		c.line normals (%)	
subject	RWMA	diastole	systole	diastole	systole	mean	SD
a	yes	30.8	21.0	21.0	17.8	18.9	5.2
b	yes	32.1	18.3	20.5	15.6	28.9	5.6
c	yes	28.3	18.2	19.2	15.6	23.1	5.8
d	yes	32.6	20.9	20.5	16.5	23.3	3.0
e	yes	22.8	15.2	17.6	14.2	21.3	9.2
f	yes	41.5	34.4	23.4	21.2	10.5	4.7
g	no	21.5	8.0	16.8	10.4	50.1	2.7
h	no	18.7	9.7	15.7	11.4	34.2	4.1
i	no	22.6	11.7	17.3	12.6	34.0	2.5
j	no	13.2	7.2	13.3	10.2	31.0	3.5

RWMA - regional wall motion abnormalities at rest; c.line - centerline.
Centerline normals are presented in percent of the radius calculated from the area within the centerline (the radius of a circle with the same area as the area within the centerline contour)

Echocardiography. An ultrasound scanner (Vingmed 750, Vingmed Sound, Horten, Norway) with a 3.25 MHz annular array transducer was used for all ultrasound imaging. Cineloops of the midventricular short axis were recorded by imaging from parasternal position, and the images were transferred as digital scanline data to a computer (Macintosh series II, Apple Computers, Cupertino, California) for further analysis. An electrocardiographic trace was recorded and stored together with the cineloop.

Detection of endocardial borders. A general program for handling of digital ultrasound data (EchoDisp 3.0, Vingmed Sound) was used. Endocardial borders were traced by an experienced clinician with a mouse driven cursor on the computer screen in end-diastolic and end-systolic frames excluding papillary muscles [1]. The process of border detection was optimized by adequate contrast setting, by zooming, and by repeatedly comparing the trace with the true endocardium in cineloop replay. The manually drawn endocardial borders were represented by polygons in an integer xy-format defined by computer screen pixels. In order to reduce high frequency noise introduced by manual tracing, these borders were resampled to be represented by 200 points equally spaced along the original polygon outline and smoothed by using a 5 point symmetric kernel {1,2,3,2,1}.

The end-diastolic and end-systolic endocardial borders in each subject were compared using the centerline method, after realignment using the center of area inside the borders as reference in order to compensate for cardiac translation (Fig. 2). Left ventricular (original) cross-sectional areas, circumferences, and length of centerline normals (mean ± SD) were calculated from these borders (Table 1).

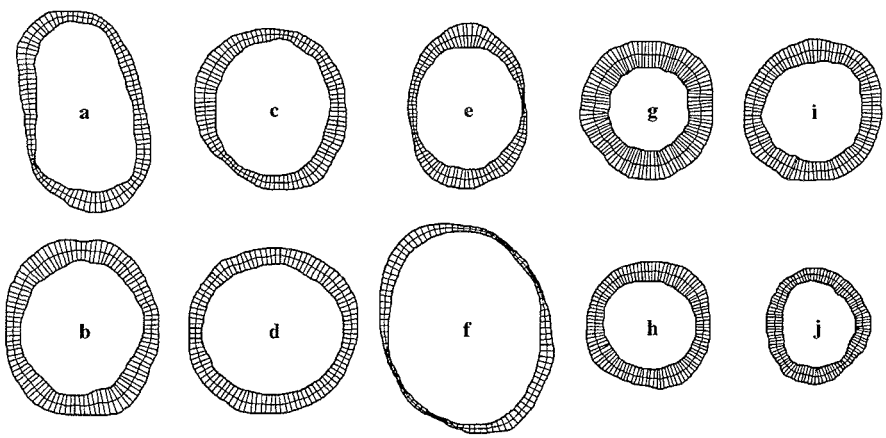

Fig. 2. Original borders for analysis from subjects a-j (see Table 1) in this study; manually drawn end-diastolic and end-systolic endocardial borders with centerline contour and normals.

Cubic spline interpolation. Special software was developed for further analysis and implemented in so-called ECARs (EchoDisp Custom Analysis Routines, Vingmed Sound), a system allowing specified routines to be applied with the EchoDisp program. The following procedure was repeated for end-diastolic and end-systolic borders in all subjects:

i) the coordinates of the center of area were calculated

ii) straight lines (2-12) were drawn through the center of area so that equal angles between adjacent lines were obtained (Fig. 3)

iii) the points of intersection (4-24) between the lines and the border were calculated, and a closed cubic spline curve [appendix A] was constructed interpolating these points.

Steps ii) and iii) were repeated with 2, 3, 4, 5, 6, 7, 8, 9, 10, 11 and 12 lines mimicking positions of apical imaging planes, thus 4, 6, 8, 10, 12, 14, 16, 18, 20, 22 and 24 points for interpolation were produced, respectively (Fig.4).

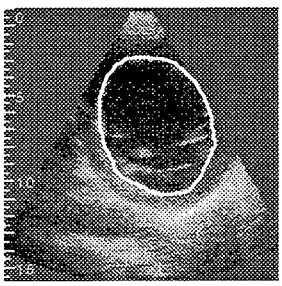

cross-sectional area: 41.4 cm^2
circumference: 23.4 cm

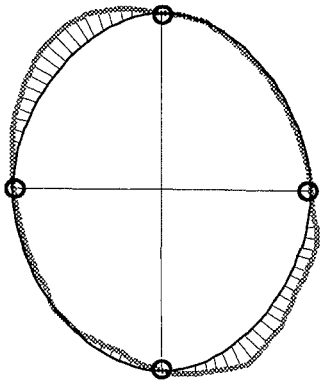

Fig. 3. Example of comparison of reconstructed and original endocardial borders. - Left panel: original manually drawn border in end-diastolic frame in (subject f, Table 1). - Right panel: original border (thick line), cubic spline curve (thin line) obtained from interpolation on 4 points, and centerline normals used for determination of shape differences.

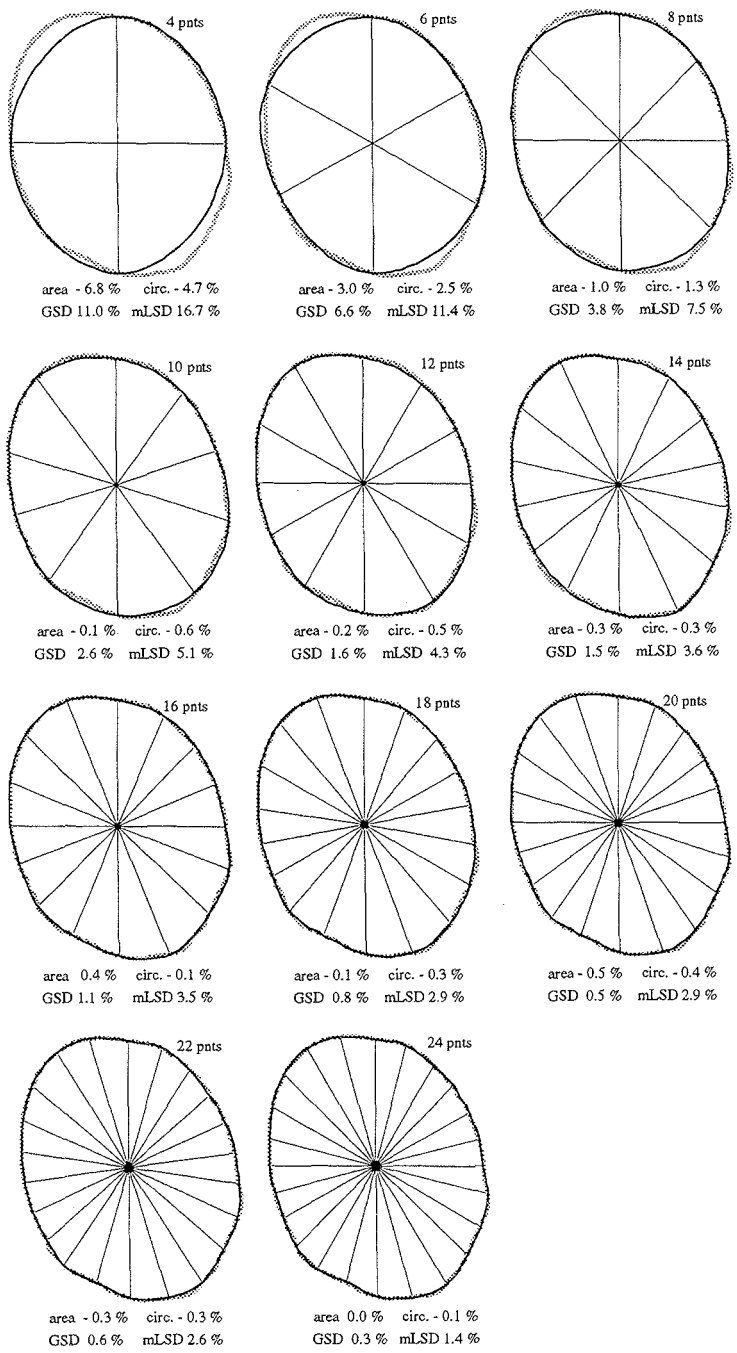

Fig. 4. Comparison of reconstructed (thin line) and original (thick line) borders of the same patient as in Fig.3 at different number of points used for cubic spline interpolation. All values (in %) - area, circ. (circumference), GSD = global shape difference, and mLSD = max. local shape difference - are calculated using definitions given in text.

Comparison of reconstructed and original borders. Left ventricular cross-sectional area and circumference of the reconstructed border were compared with the values from the corresponding original border and the differences were calculated in percent by

$$\%\ \text{error in area} = 100\ \frac{\text{area within reconstructed border - area within original border}}{\text{area within original border}}$$

$$\%\ \text{error in circumference} = 100\ \frac{\text{circumference of reconstructed border - circumference of original border}}{\text{circumference of original border}}$$

Areas were calculated using the polygon format of the borders, and circumference was calculated as length of polygon outline. The reconstructed borders (spline curves initially represented by continuous real functions) were converted to polygons with 200 equidistant points on the cubic spline curve for subsequent drawing and calculations.

The difference in shape between the reconstructed and the original borders was assessed by use of the centerline method [13], whereas the lengths of 100 normals to the centerline between the 2 borders were determined. Global difference in shape was calculated as the area of the region between the two borders and expressed as a percentage of the area within the original border by

$$\%\ \text{global shape difference} = 100\ \frac{\text{average of centerline normals x centerline contour}}{\text{area within original border}}$$

The maximum local difference in shape was determined by the maximum length of centerline normals, and it was expressed as a percentage of the radius defined from the area within the original border (the radius of a circle with the same area as the within the border). This difference was calculated by

$$\%\ \text{max. local difference} = 100\ \frac{\text{max. length of centerline normals}}{\text{square root (area within original border / } \pi \text{)}}$$

Statistical analysis. Values are presented as mean ± standard deviation (SD) for the complete set of borders, and in subgroups comprising all borders from end-diastolic frames, all borders from end-systolic frames, all borders from patients with wall motion abnormalities, and

all borders from normals. Confidence limits are calculated by standard method for the complete set of borders. Results obtained using one number of points for interpolation were compared with those obtained with two points less with the unpaired (2-tailed) t-Test for sample mean, and with the F-test for variance. Probability less than 0.05 was considered statistically significant.

Results

Mean ± SD of differences for all measurements are listed in Tables 2 - 5. At low density of points for reconstruction, the accuracy improved each time the number of points for interpolation was increased with two; from 4 to 6 points and from 8 to 10 points the mean value of difference changed significantly, and from 6 to 8 points the accuracy improved significantly in terms of variance. By group comparison the results indicates an overall tendency at low density of points that end-diastolic borders were more accurately reconstructed than end-systolic borders, and that borders from control subjects were more accurately reconstructed than those from patients with myocardial infarction.

Accuracy in cross-sectional areas. Individual results and 95 % confidence limits are displayed in Fig. 5. Accuracy was improved by successive increase in the density of points, however only small and not significant improvements in accuracy were found when the number of points exceeded 10. With 6 points for interpolation the 95 % confidence limits for difference in area was -7.7 to 3.6 %, whereas 8 points improved accuracy to a 95 % confidence limits of -2.2 to 0.7 %. The areas were underestimated except at the highest density of 24 points.

Accuracy in circumferences. Individual results and 95 % confidence limits are displayed in Fig. 6. Accuracy improved by increasing number of points in the same manner as for areas. At low density of points the percent error in circumference was smaller than for areas (95 % confidence limits - 5.4 to 1.8 % for 6 points, and - 2.1 to 0.1 to % for 8 points). For more than 10 points the area estimates were more accurate with a larger negative bias in circumferences.

Accuracy in shape. Individual results and 95 % confidence limits for the global and max. local difference in shape are displayed in Fig. 7 and Fig.8. Shape differences are illustrated in Fig. 4, and the magnitude of max. local difference are in same scale, and thus comparable with results from centerline method applied to the original borders (Table 1).

The accuracy in shape reconstruction improves each time the number of points for interpolation was increased. The greatest improvements occurred when the number was increased from 6 to 8, and from 8 to 10. By using 8 points for reconstruction the 95 % confidence limits were 3.4 to 8.4 % for the maximum local difference in shape.

Discussion

Cubic spline interpolation produced highly probable shapes representing endocardial borders from a limited number of selected points. The aim of the present study was to evaluate how the accuracy of a 3D bicubic spline description of the LV endocardium depends of the number of apical views used for reconstruction. Our results indicate that 3 apical planes (6 points for reconstruction of cross-sectional borders) are sufficient for determination of LV volumes and endocardial surface areas, and that 4 views (8 points) improves the accuracy and enables quantitative analysis of regional shape. Furthermore, the results of this study describes spatial variations in LV shape, and thus indicates the sample density that should be applied for quantitative purposes by use of imaging techniques in general.

Cubic spline representation of cardiac borders. Different types of splines has become standard tools in computer graphics for modelling of curves and surfaces, and provide a mathematical tool for easy drawing and adjustments of curves [6,7,14], e.g. representing cardiac borders. For reconstruction of LV endocardial and epicardial borders, cubic spline interpolation yields for continuity of the borders, as well for continuity of direction and curvature through the interpolation points [appendix A]. Furthermore, the cubic spline curve will yield optimal smoothness by the property of minimal variation in (mean squared) curvature of all possible borders through given points [6]. In our experience, this produces realistic estimates of ventricular borders which are not well visualized.

Cubic spline interpolation produces curves that represent the endocardium in regions with edge dropout or by suboptimal imaging in 2D echocardiography [15]. Nonuniform cubic splines as being used in the present study [appendix A], take into account different spacing between points for interpolation so that a higher density of points could be used in regions with good image quality or regions with irregular shape of the border, e.g. for inclusion of papillary muscles or for detection of right ventricular borders.

Determination of LV dimensions. The LV cavity volume is an important index of global function. In general, the accuracy of volumes improves with the amount of spatial data

used for calculation; by standard 2D echocardiography the biplane disc summation method is recommended in comparison with single plane or M-mode methods [1,16], whereas 3D methods that avoid assumptions of idealized geometry are superior to the conventional 2D and M-mode methods. The present results agree well with previous studies comparing 2D and 3D calculations of volumes [8,9,17]. Three-dimensional volume determination from 3 imaging planes has shown improved accuracy compared to the biplane method [8,9]. The biplane method corresponds to short axis reconstruction from 4 points assuming elliptic shaped cross-sections. Although the cubic spline not exactly reproduces ellipses, the accuracy of biplane method is reflected in the error of LV cross-sectional areas by 4 points for interpolation (cross-sectional areas were approx. 3 % lower when cubic spline curves were generated from 4 points on ellipsis).

Echocardiographic underestimation of volumes by biplane or single plane methods is reported from in vitro studies [17]. Underestimation in cross-sectional areas in the present study (Fig. 5, Table 2), strongly indicates that low spatial sampling, here by a small number of apical imaging planes, causes underestimation of LV volumes, and that both the negative bias and the variance of error decrease by increasing the number of spatial samples. The negative bias in reconstructed areas is likely to express deviation in real LV shape from the ideal smooth shape obtained by cubic spline interpolation. In terms of spatial frequency the deviation from ideal shape should be contained in relative high frequency components that are not recovered at a low density of points for reconstruction [appendix B]. Fourier analysis applies also to explain a positive bias at the highest density of points, thus aliasing from high frequency noise due to manual tracing and digital format of borders may cause overestimation in cross-sectional areas.

The endocardial surface area is a potentially important index for assessment of LV function after myocardial infarction [18,19]. Small error in circumference of reconstructed borders indicates good estimates of the endocardial surface areas from a small number of apical views (3-5). Using a low density of sampled points for interpolation, accuracy of circumferences is better than for areas. While longitudinal variations in shape do not affect volume estimates by disc summation it will, however, affect surface area estimates [10]. Underestimation of reconstructed circumferences can be explained from the use of cubic spline interpolation, thus variations in local curvature will be diminished due to the property of optimal smoothness [appendix A].

For 3D reconstruction, inaccuracy will be added by errors in border detection, off-axis imaging, and deviations in assumed angular position of apical imaging planes. Recent studies

have shown that volumes obtained by biplane disk summation area not affected significantly by correcting the position of the imaging planes [20], and that cross-sectional areas and circumferences only to a small extent are affected by errors in assumed angular positions of imaging planes [8,10].

Analysis of regional shape. Three-dimensional wall motion analysis based on 3 apical planes is feasible in patients with extensive myocardial infarctions [12,21]. Compared to 2D single plane methods, 3D analysis calculates regional wall motion in the whole endocardium, and facilitates estimation of the total and the infarcted part of the endocardial area. The present results indicate only small errors from original shape are seen by using 8 points for reconstruction of endocardial borders, however, increasing the density of points should assure higher precision in description of minor shape abnormalities.

Limitation and future work. The accuracy of reconstructed cross-sectional borders is a major determinant for the accuracy of LV shape and dimensions obtained from a limited number of apical imaging views. Assuming that endocardial borders are correctly defined and correctly realigned in 3D (Fig 1a), the present results describe the accuracy in 3D reconstruction of the mid-ventricular portion of the endocardium. The present method should be repeated using data including basal and apical cross-sections, and representing various cardiac diseases. Furthermore, direct 3D in vitro studies should be performed for assessment of accuracy in LV volumes and endocardial surface areas due to the number of apical imaging planes used for reconstruction.

The reconstructed borders obtained with the present method may vary due to the position of the center of radial lines relative to the original border, and due to different angular increment between these lines (Fig. 4). By using the center of area and equal angle increment, the points for interpolation will be evenly dispersed on the original border, thus, optimal agreement between original and reconstructed borders can be expected. This situation will not be reproduced exactly in 3D reconstruction by apical rotation, however, use of nonuniform cubic spline interpolation will produce probable borders unaware of great differences in spacing between points for interpolation [appendix A].

The impact of the errors in reconstructed shape on wall motion analysis is illustrated by the calculations of global and maximum shape differences (Fig. 7 -8). These errors can be more directly assessed by comparison of regional wall motion analysis obtained from reconstructed and from original borders.

The papillary muscles were excluded from the endocardial borders in the present study,

and their inclusion presumably requires a higher density is of points for reconstruction. In canine experimental studies the spatial content of endocardial borders including papillary muscles is covered by the first seven harmonics of the Fourier transform [22], indicating that at least 14 points are needed for adequate reconstruction of borders. Future investigations should compare accuracy of the presented indices with the spatial frequency spectre obtained by Fourier transform [appendix B], both with and without inclusion of papillary muscles. Fourier analysis is an actual approach as the spatial frequency spectre contains information of expected smoothness of cardiac shapes [22-27], and thus provide information of the necessary density of points needed for reconstruction. Furthermore, Fourier analysis applies for studying influence by high spatial frequency components from trabecular web and from noise due to manual drawing and digital format of borders.

Regional curvature is a major determinant of regional wall stress, and several studies have been performed using endocardial curvature for characterizing global and regional LV function [27-33]. Studies should be performed evaluating accuracy of curvature determined from cubic spline curves, and evaluating how accuracy in regional curvature depends of the density of points used for interpolation.

Further work should also include reconstruction of epicardial borders to assess analysis of wall thickening and LV mass calculation [34,1]. Epicardial edges are often poorly visualized by ultrasound, however, these edges are normally smooth and should therefore be reconstructable from a limited number of selected points (Fig. 1b).

Conclusions. Cubic spline interpolation provides an effective and accurate mean for definition of smooth LV borders. Simplified 3D reconstruction from a small number of apical imaging views is time effective and can supplement routine echocardiography for display of 3D shape and for quantifying indices of global and regional LV function.

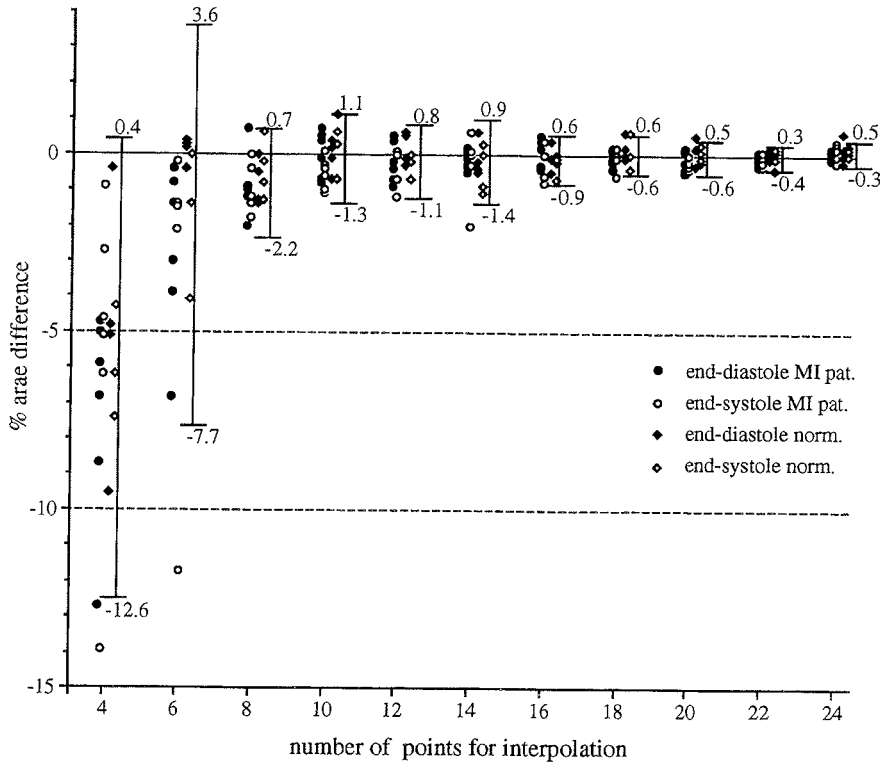

Fig. 5. Plot of % area difference between reconstructed and original borders at different number of points for interpolation. All individual results and 95 % confidence limits are displayed.

Table 2 Area difference between interpolated and original endocardial borders (%)

no. of pnts	end-diastole (10)	end-systole (10)	MI patients (12)	normals (8)	all (20)
4	-6.4 ± 3.3	-5.8 ± 3.4	-6.4 ± 3.8	-5.5 ± 2.6	-6.1 ± 3.3
6	-1.6 * ± 2.3	-2.5 * ± 3.4	-2.9 * ± 3.3	-0.8 * ± 1.5	-2.1 * ± 2.9
8	-0.9 ± 0.8 †	-0.7 ± 0.7 †	-0.9 ± 0.8 †	-0.6 ± 0.7	-0.8 ± 0.7 †
10	-0.0 * ± 0.6	-0.2 ± 0.7	-0.3 * ± 0.6	0.1 ± 0.6	-0.1 * ± 0.6
12	-0.1 ± 0.5	-0.3 ± 0.4	-0.3 ± 0.5	-0.1 ± 0.4	-0.2 ± 0.5
14	-0.1 ± 0.4	-0.4 ± 0.8	-0.2 ± 0.6	-0.3 ± 0.6	-0.2 ± 0.6
16	-0.1 ± 0.4	-0.2 ± 0.4 †	-0.1 ± 0.4	-0.2 * ± 0.4	-0.1 ± 0.4
18	0.0 ± 0.3	-0.0 ± 0.3	-0.1 ± 0.2	0.1 ± 0.3	-0.0 ± 0.3
20	-0.0 ± 0.3	-0.1 ± 0.2	-0.2 ± 0.2	0.1 ± 0.3	-0.1 ± 0.3
22	-0.1 ± 0.2 †	-0.1 ± 0.2	-0.1 ± 0.2	-0.0 ± 0.2	-0.1 ± 0.2
24	0.1 * ± 0.2	0.1 * ± 0.2	0.1 * ± 0.2	0.2 ± 0.2	0.1 * ± 0.2

Mean ± SD of % area difference. Numbers in parenthesis give the amount of borders for analysis in the subgroup.

* $p < 0.05$ t-Test for mean, † $p < 0.05$ F-test for variance.

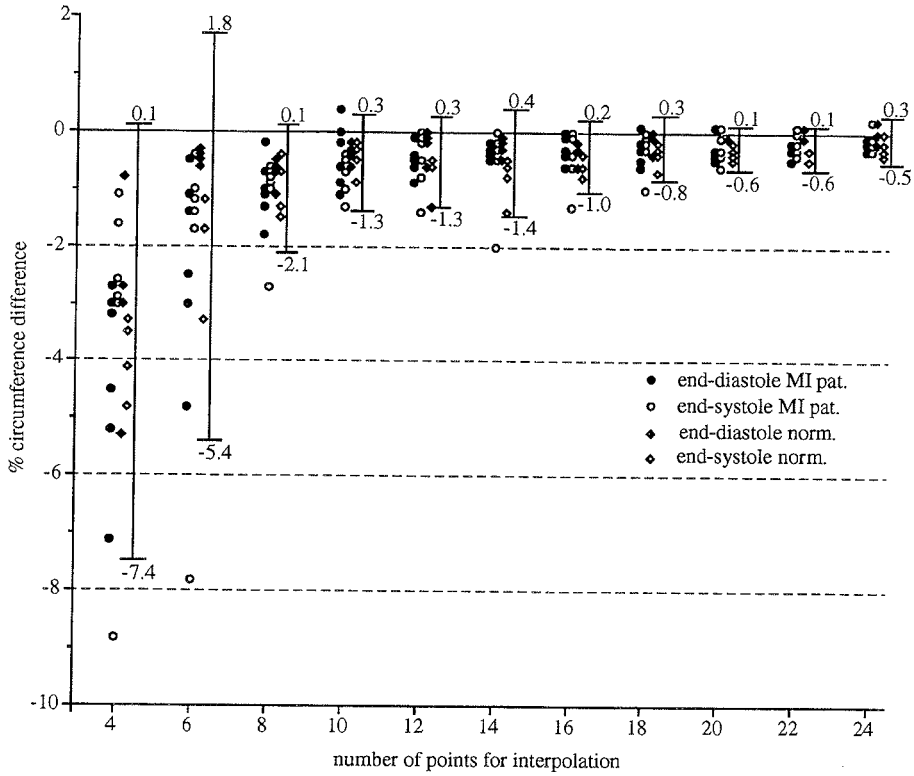

Fig. 6. Plot of % circumference difference between reconstructed and original borders at different number of points for interpolation. All individual results and 95 % confidence limits are displayed.

Table 3 Difference in circumference between interpolated and original endocardial borders (%)

no. of pnts	end-diastole (10)	end-systole (10)	MI patients (12)	normals (8)	all (20)
4	-3.8 ± 1.8	-3.6 ± 2.1	-3.8 ± 2.3	-3.4 ± 1.4	-3.7 ± 1.9
6	-1.5 * ± 1.5	-2.1 ± 2.1	-2.2 ± 2.1	-1.2 * ± 1.0	-1.8 * ± 1.8
8	-0.9 ± 0.5 †	-1.1 ± 0.7 †	-1.1 ± 0.7 †	-0.9 ± 0.4 †	-1.0 ± 0.6 †
10	-0.4 * ± 0.4	-0.6 ± 0.3	-0.6 * ± 0.5	-0.4 * ± 0.2	-0.5 * ± 0.4
12	-0.4 ± 0.3	-0.6 ± 0.5	-0.5 ± 0.4	-0.5 ± 0.4	-0.5 ± 0.4
14	-0.3 ± 0.1 †	-0.7 ± 0.6	-0.5 ± 0.5	-0.6 ± 0.4	-0.5 ± 0.5
16	-0.3 ± 0.2	-0.5 ± 0.4	-0.4 ± 0.4	-0.5 ± 0.2	-0.4 ± 0.3
18	-0.2 ± 0.2	-0.3 ± 0.3	-0.3 ± 0.3	-0.3 ± 0.2	-0.3 ± 0.3
20	-0.2 ± 0.2	-0.3 ± 0.2	-0.3 ± 0.2	-0.2 ± 0.2	-0.3 ± 0.2
22	-0.2 ± 0.2	-0.3 ± 0.2	-0.3 ± 0.2	-0.2 ± 0.2	-0.2 ± 0.2
24	-0.1 ± 0.2	-0.1 ± 0.2	-0.1 * ± 0.2	-0.1 ± 0.2	-0.1 * ± 0.2

Mean ± SD of % difference in circumference. Numbers in parenthesis give the amount of borders for analysis in the subgroup.
* $p < 0.05$ t-Test for mean, † $p < 0.05$ F-test for variance.

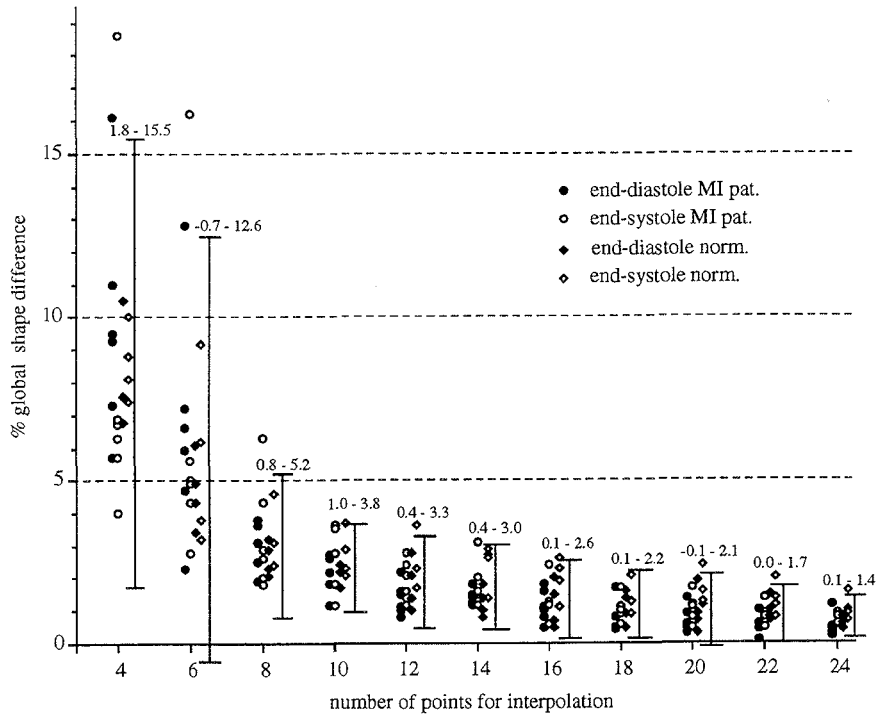

Fig. 7. Plot of % global shape difference (see text) between reconstructed and original borders at different number of points for interpolation. All individual results and 95 % confidence limits are displayed.

Table 4 Global shape difference between interpolated and original endocardial borders (%)

no. of pnts	end-diastole (10)	end-systole (10)	MI patients (12)	normals (8)	all (20)
4	9.1 ± 3.0	8.3 ± 4.0	8.9 ± 4.4	8.3 ± 1.4	8.7 ± 3.5
6	5.8 * ± 2.9	6.1 ± 4.0	6.5 ± 4.0	5.1 * ± 2.0	6.0 * ± 3.4
8	2.7 * ± 0.7 †	3.2 ± 1.4 †	3.1 * ± 1.3 †	2.9 * ± 0.8 †	3.0 * ± 1.1 †
10	2.2 ± 0.5	2.6 ± 0.9	2.3 ± 0.8	2.4 ± 0.6	2.4 * ± 0.7
12	1.6 * ± 0.6	2.1 ± 0.7	1.6 * ± 0.6	2.2 ± 0.8	1.9 * ± 0.7
14	1.4 ± 0.3 †	2.0 ± 0.7	1.6 ± 0.5	1.8 ± 0.8	1.7 ± 0.6
16	1.2 ± 0.5	1.6 ± 0.7	1.2 ± 0.5	1.6 ± 0.8	1.4 ± 0.6
18	1.0 ± 0.5	1.3 ± 0.5	1.0 ± 0.5	1.4 ± 0.6	1.2 ± 0.5
20	0.8 ± 0.5	1.3 ± 0.5	0.9 ± 0.4	1.3 ± 0.7	1.0 ± 0.6
22	0.7 ± 0.4	1.0 ± 0.5	0.7 * ± 0.3	1.2 ± 0.4	0.9 ± 0.4
24	0.6 ± 0.3	0.9 ± 0.3	0.7 ± 0.3	0.9 * ± 0.4	0.7 ± 0.3

Mean ± SD of % global shape difference. Numbers in parenthesis give the amount of borders for analysis in the subgroup.
* $p < 0.05$ t-Test for mean, † $p < 0.05$ F-test for variance.

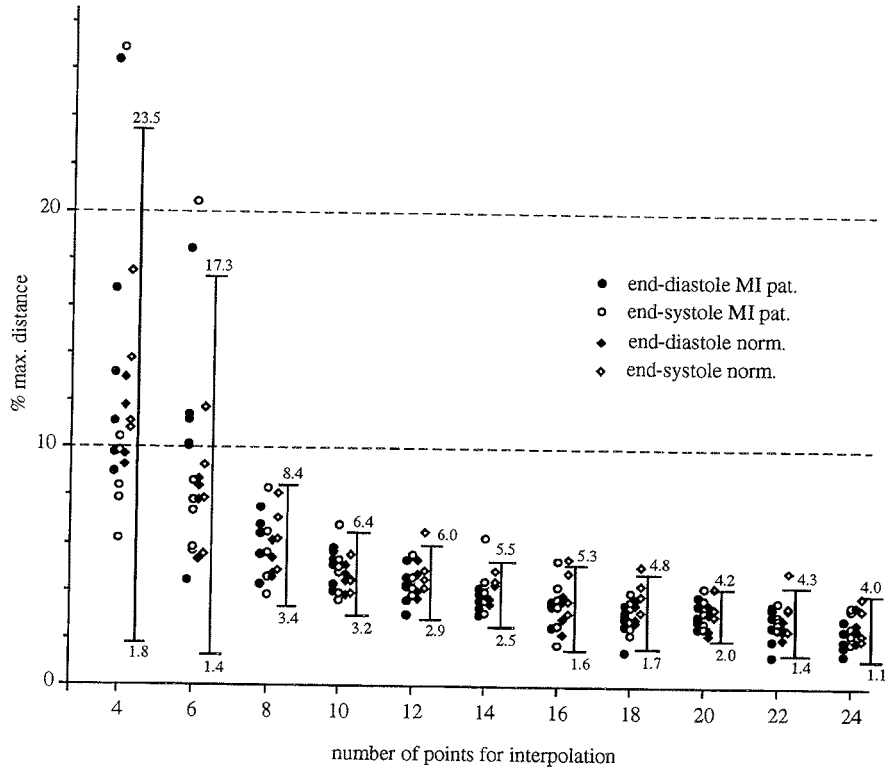

Fig. 8. Plot of % max. local difference (see text) between reconstructed and original borders at different number of points for interpolation. All individual results and 95 % confidence limits are displayed.

Table 5 Maximal local shape difference between interpolated and original endocardial borders (%)

no. of pnts	end-diastole (10)	end-systole (10)	MI patients (12)	normals (8)	all (20)
4	13.0 ± 5.3	12.3 ± 6.0	13.0 ± 6.9	12.1 ± 2.7	12.7 ± 5.5
6	9.6 ± 3.9	9.0 ± 4.4	10.1 ± 4.9	8.1 * ± 2.1	9.3 * ± 4.1
8	5.8 * ± 1.1 †	6.0 ± 1.5 †	5.9 * ± 1.4 †	5.9 * ± 1.2	5.9 * ± 1.3 †
10	4.8 * ± 0.7	4.8 ± 1.0	5.0 ± 0.9	4.5 * ± 0.6	4.8 * ± 0.8 †
12	4.3 ± 0.7	4.6 ± 0.8	4.3 ± 0.7	4.7 ± 0.9	4.5 ± 0.8
14	3.6 * ± 0.3 †	4.4 ± 0.9	3.9 ± 0.9	4.1 ± 0.6	4.0 ± 0.8
16	3.2 * ± 0.6	3.8 ± 1.2	3.3 ± 0.9	3.7 ± 1.0	3.5 ± 1.0
18	3.0 ± 0.6	3.5 ± 0.9	2.9 ± 0.7	3.7 ± 0.8	3.2 ± 0.8
20	3.0 ± 0.5	3.3 ± 0.6	3.2 ± 0.5	3.1 ± 0.6	3.1 ± 0.6
22	2.6 ± 0.7	3.1 ± 0.8	2.7 ± 0.6	3.0 ± 0.9	2.8 ± 0.7
24	2.3 ± 0.7	2.9 ± 0.7	2.4 ± 0.7	2.8 ± 0.7	2.6 ± 0.7

Mean ± SD of % max. local shape difference. Numbers in parenthesis give the amount of borders for analysis in the subgroup.
* $p < 0.05$ t-Test for mean, † $p < 0.05$ F-test for variance.

Appendix

Appendix A. Cubic spline interpolation

Mathematical function and properties. Given a set of points $\mathbf{p}_0, \mathbf{p}_1, \mathbf{p}_2 \cdots, \mathbf{p}_n$ in the xy-plane. Cubic spline interpolation will then produce a smooth curve passing these points, and that preserves both direction and curvature through the sample points $\mathbf{p}_i$. The mathematical form of the curve is

$$\mathbf{c} = (x(t), y(t)) \qquad \text{for } 0 < t < 1$$

where the functions x(t) and y(t) are composed of piecewise cubic polynoms that can be written on the form

$$x_i(t) = a_{i,0} + a_{i,1}\, t + a_{i,2}\, t^2 + a_{i,3}\, t^3$$

and $$y_i(t) = b_{i,0} + b_{i,1}\, t + b_{i,2}\, t^2 + b_{i,3}\, t^3$$

defined for $t_i < t < t_{i+1}$. The polynoms, x_i and y_i, represents the corresponding curve segment connecting points $\mathbf{p}_i$ and $\mathbf{p}_{i+1}$.

These polynoms fulfil the requirement for continuity of the function and its first and second derivative (e.g. x(t), x'(t), and x''(t)) through the interval ends t_i. The cubic spline interpolant will be optimal smooth as it, of all curves fulfilling the given requirements, will be the curve of minimum mean squared curvature. The cubic spline curve thereby represents an optimal shape as the minimum mean squared curvature corresponds to minimum strain energy of a flexible rod forced to interpolate the given data points [6]. By cubic spline interpolation in two directions, e.g axial and cross-sectional for 3D reconstruction of endocardial surfaces (Fig. 1a), a smooth bicubic spline surface is obtained.

A cubic spline curve is uniquely determined from the choice of end-conditions and parametrization.

End-conditions. For the endocardial surface reconstruction (Fig. 1a) two types of end-condition have been used:

1. The Bessel end-condition have been used for the cubic spline representation of the apical borders in the algorithm for 3D reconstruction of the endocardial surface (Fig. 1a); the end derivatives (x'(t=0) and x'(t=1) in Fig. A1) equals those of parabolas interpolating the 3

first and the 3 last data points respectively.

2. The closed cubic spline was the natural choice for reconstruction of short-axis contours (Fig. 1a & 1b) requiring smoothness all around the curve; the first and last data point coincides, and the 1. and 2. derivatives are continuous through this point (e.g. $x(t=0) = x(t=1)$, $x'(t=0) = x'(t=1)$, and $x''(t=0) = x''(t=1)$ in (Fig A2).

Parametrization. Spline curves are characterized as uniform or nonuniform. Uniform splines uses equal length of intervals (t_i, t_{i+1}) for effective calculations, but with reduced ability to reproduce smooth curves by interpolation through points with unequal spacing. Nonuniform cubic splines have therefore been chosen for the cardiac borders by chord-length parametrization:

the length of the intervals (t_i, t_{i+1}) are proportional to the distance between the respective data points $\mathbf{p}_i$ and $\mathbf{p}_{i+1}$.

Implementation of algorithms for cubic spline interpolation was partially based on reference [6].

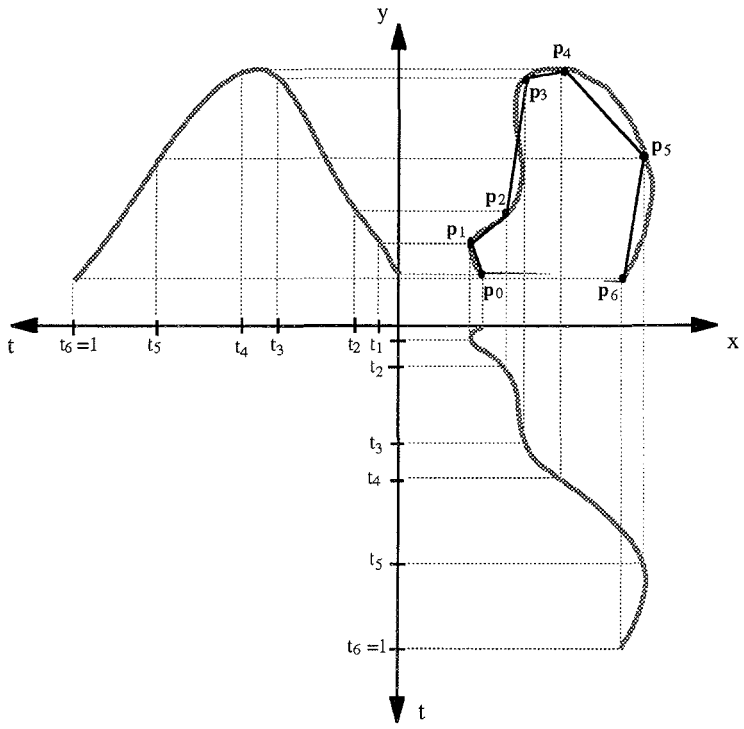

Fig. A1. Cubic spline curve interpolating points $\mathbf{p}_0$ to $\mathbf{p}_6$. The curve is composed by separate components, x(t) and y(t), displayed below and to the right.

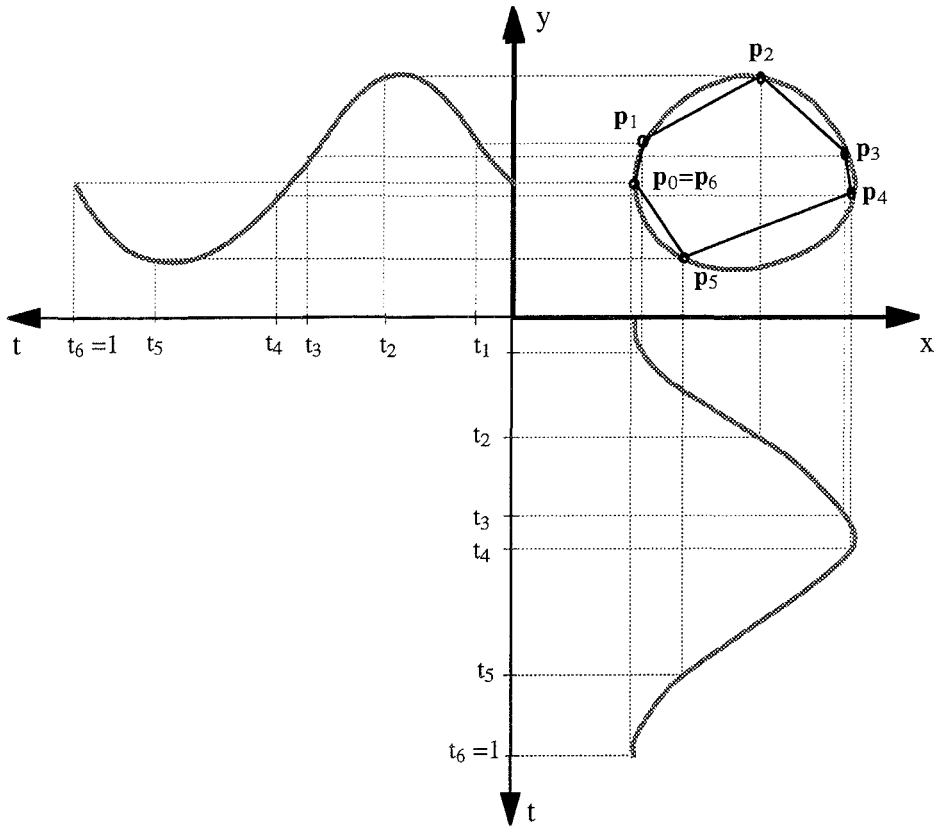

Fig. A2. Example of a closed cubic spline curve, and its components x(t) and y(t).

Appendix B. Fourier description of a closed contour and area calculation

A planar closed curve can be described in polar form as a function $r = r(\theta)$, expressing radial distance to an origin as a function of angle (Fig. B). With the requirement that r is uniquely defined for all angles, the area A of the enclosed region can be calculated by the integral

$$A = \frac{1}{2}\int_0^{2\pi} r^2(\theta)d\theta \qquad \text{(B1)}$$

The function $r(\theta)$ will be periodic with period 2π, thus it can be presented by the Fourier series

$$r(\theta) = R_o + \sum_{k=1}^{\infty} R_k \cos(k\theta - \gamma_k) \qquad \text{(B2)}$$

with coefficients given by the Fourier integrals

$$R_0 = \frac{1}{2\pi}\int_0^{2\pi} r(\theta)d\theta \qquad A_k = \frac{1}{\pi}\int_0^{2\pi} r(\theta)\cos(k\theta)d\theta \qquad B_k = \frac{1}{\pi}\int_0^{2\pi} r(\theta)\sin(k\theta)d\theta$$

$$R_k = \sqrt{A_k^2 + B_k^2}$$

$$\tan\gamma_k = \frac{B_k}{A_k}$$

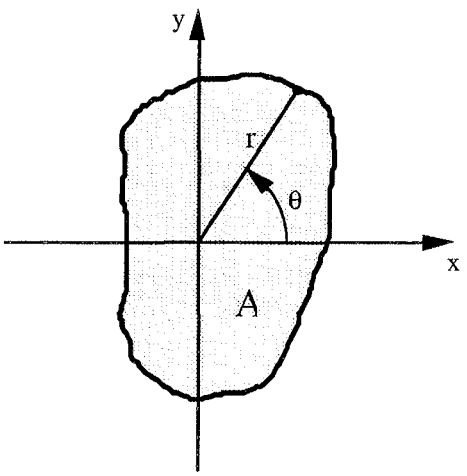

Fig. B. Example of a planar closed contour in polar form.

By using the Fourier series (B2) in formula (B1) the area can be calculated by

$$A = \pi R_0^2 + \frac{\pi}{2}\sum_{k=1}^{\infty} R_k^2 \qquad \text{(B3)}$$

The sequence { R_k^2 } is recognized as the components of the spatial power spectrum of a contour, and the range of nonzero components R_k^2 corresponds to the bandwidth of the contour. A continuous smooth contour (e.g describing the left ventricular endocardium in short axis) will be of limited bandwidth, with a finite number of frequency components, thus the area can be calculated accurately by a finite sum of n components by

$$A = \pi R_0^2 + \frac{\pi}{2}\sum_{k=1}^{n} R_k^2 \qquad \text{(B4)}$$

The simplest example is the circle with the center in the origin of the coordinate system: all coefficient R_k will become zero except R_0 which equals the radius of the circle.

By sampling of the radial distance $r(\theta)$ in a limited number of directions with equal angular increment, the coefficient in the Fourier series can be calculated by the discrete Fourier transform (DFT). The sampling theorem states the number of samples must at least be twice the number (the Nyquist limit) of nonzero components in the spatial power spectrum of the contour. Undersampling may cause error in calculated areas in both directions with:

- underestimation when relative high frequency power components are not recovered from a low density of sampled points
- overestimation by aliasing from high frequency components from noise (e.g. from manual drawing or digital format of cardiac border).

Acknowledgement

Svend Aakhus, MD, at Dept. of medicine, Section of Cardiology, University of Trondheim, has provided echocardiographic data for this study.

References

1. Schiller NB, Shah PM, Crawford M, DeMaria A, Devereux R, Feigenbaum H, Gurgesell H, Reichek N, Sahn D, Schnittger I, Silvermann NH, Tajik AJ. Recommendations for quantitation of the left ventricle by two-dimensional echocardiography. J Am Soc Echocardiogr 1989;2:358-367.

2. Ghosh A, Nanda NC, Maurer G. Three-dimensional reconstruction of echocardiographic images using the rotation method. Ultrasound Med Biol 1982;8:655-661.

3. Bjoernstad K, Maehle J, Aakhus S. Quantitative computerized analysis of left ventricular wall motion. In Domenicucci S, Roelandt J, Pezzano A (Eds.), Computerized Echocardiography, Torino: Centro Scientifico Editore, 1993;41-55.

4. Fine DG, Sapoznikov D, Mosseri M, Gotsman MS. Three-dimensional echocardiographic reconstruction: qualitative and quantitative evaluation of ventricular function. Computer Methods and Programs in Biomedicine 1988;26:33-44.

5. Janicki J, Weber KT, Gochman RF,.Shroff S, Geheb FJ. Three-dimensional myocardial and ventricular shape: a surface representation. Am J. Physiol 1981;241(Heart Circ Physiol 10):H1-H11.

6. Farin G. Curves and surfaces for computer aided geometric design - A practical guide, 3. ed. Academic press Inc., Boston, 1993.

7. Foley JD, van Dam A, Feiner SK, Hughes JF. Computer graphics - principles and practice, 2. ed. Addison Wesley publishing company, Reading, Massachusetts, 1990.

8. Aakhus S, Mæhle J, Bjoernstad K. A new method for echocardiographic computerized three-dimensional reconstruction of left ventricular endocardial surface: In vitro accuracy and clinical repeatability of volumes. J Am Soc Echocardiogr 1994;7:571-581.

9. Mele D, Mæhle J, Pratola C, Pedini I, Alboni P, Levine RA. Application in patient of a new simplified system for 3D-echo reconstruction of the left ventricle. J Am Soc Echocardiogr 1995;8:343 (abstract).

10. Mæhle J. Reconstruction and analysis of left ventricular surfaces by three-dimensional echocardiography. I. Quantitation of the endocardial surface area. 1996; art. C in thesis.

11. Bjørnstad K, Mæhle J, Aakhus S, Torp H. Evaluation of reference systems for describing regional left ventricular wall motion abnormalities by using 3-dimensional endocardial surface reconstruction. Eur Heart J 1995;16 (abstract suppl.):205.

12. Mæhle J. Reconstruction and analysis of left ventricular surfaces by three-dimensional echocardiography. II. New indices for global and regional systolic function in patients with myocardial infarction.1996; art. D in thesis..

13. Bolson EL, Kliman S, Sheehan F, Dogde HT. Left ventricular segmental wall motion - A new method using local direction information. Comput Cardiol 1980;1980:245-248.

14. de Boor C. A practical guide to splines, Springer -Verlag, New York, 1978.

15. Sklenar J, Jayaweera AR, Kaul S. A computer-aided approach for the quantitation of regional left ventricular function using two-dimensional echocardiography. J Am Soc Echocardiogr 1992;5:33-40.

16. Himelman RB, Cassady MM, Landzberg JS, Schiller NB. Reproducibility of quantitative two-dimensional echocardiography. Am Heart J 1988;115:425-431.

17. Sapin PM, Schroeder KD, Smith MD, DeMaria AN, King DL. Three-dimensional echocardiographic measurement of left ventricular volume in vitro: Comparison with two-dimensional echocardiography and cineventriculography. J Am Coll Cardiol 1993;22:1530-1537.

18. Guyer DE, Gibson TC, Gillam LD, King ME, Wilkins GT, Guerrero JL, Weyman AE. A new echocardiographic model for quantifying three-dimensional endocardial surface area. J Am Coll Cardiol 1986;8:819-29.

19. Picard MH, Wilkins GT, Ray PA, Weyman AE. Natural history of left ventricular size and function after acute myocardial infarction - assessment an prediction by echocardiographic endocardial surface mapping. Circulation 1990;82:484-494.

20. Sapin PM, Schröeder KL, Gopal AS, Smith MD, King DL. Three-dimensional echocardiography: Limitation of apical biplane imaging for measurement of left ventricular volume. J Am Soc Echocardiogr 1995; 8:576-84.

21. Bjørnstad K, Mæhle J, Aakhus S, Torp HG, Hatle LK, Angelsen BAJ. Evaluation of reference systems for describing regional wall motion from three-dimensional endocardial surface reconstruction. An echocardiographic study in subjects with and without myocardial infraction. submitted 1996; art. E in thesis.

22. Thomas JD, Hagege AA, Choong C.Y, Wilkins GT, Newell JB, Weyman AE. Improved accurancy of echocardiographic endocardial borders by spatiotemporal filtered Fourier reconstruction: description of the method and optimization of filter cutoffs. Circulation 1988;77:415-428.

23. Kass DA, Traill TA, Keating M, Alteri PI, Maugham WL. Abnormalities of dynamic ventricular shape change in patients with aortic and mitral valvular regurgitation: assessment by fourier shape analysis and global geometric indexis. Circulation Research 1988;62:127-138.

24. Jouan A. Analysis of sequences of cardiac countours by fourier descriptors for plane closed curves. IEEE trans. on Medical Imaging 1987;6:176-180.

25. Linker DT, Pearlman AS. A mathematical basis for the quantitative comparison of cardiac borders: criteria for selection of descriptors and an analysis of two methods. Comput Cardiol 1983; 1983:169-172.

26. Linker DT, Pearlman AS, Bolson EL, Huntsman LH, Moritz WE. Right ventricular spatial frequency: implications for reconstruction and volume estimation. Comput Cardiol 1982;1982:25-30.

27. Fantini F, Barletta G, Voegelin MR, Fantini A, Maioli M, Donato M. Abnormalities of left ventricular shape in patients with stable angina. Int J Cardiol 1990;27:107-116.

28. Mancini GBJ, Bates ER, Deboe SF, McGillem MJ. Quantitative regional curvature analysis - a prospective evaluation of ventricular shape of ventricular shape and wall motion measurements. Am Heart J 1988, 116, 1616-1621.

29. Mancini GBJ, Deboe SF, Anselmo E, LeFree MT. A comparison of traditional wall motion assessment and quantitative shape analysis: a new method for characterizing left ventricular function in humans. Am Heart J 1987;114:1183-1191.

30. Marcus E, Harzahav Y, Lorente P, Battler A, Beyar R, Adam D, Barta E, Rath S, Sideman S. Characterization of regional left-ventricular contraction by curvature difference analysis. Basic research in cardiology 1988;A:486-500.

31. Mitchell GF, Lamas GA, Vaughan DE, Pfeffer MA. Left ventricular remodeling in the year after first anterior myocardial infarction: A quantitative analysis of contractile segment lengths and ventricular shape. J Am Coll Cardiol 1992;19:1136-1144.

32. Reisner SA, Azzam Z, Halman M, Rinkevich D, Sideman S, Markiewicz W, Beyar R. Septal/free wall curvature ratio: a noninvasive index of pulmonary arterial pressure. J Am Soc Echocardiogr 1994;7:27-35.

33. Duncan JS, Forrester AL, Smeulders AWM, Zaret BL. A bending energy model for measurement of cardiac shape deformity. IEEE trans. Medical Imaging 1991;10:307-320.

34. McGillem MJ, Mancini GBJ, DeBoe SF, Buda AJ. Modification of the centerline method for assessment of echocardiographic wall thickening and motion: A comparison with area of risk. J Am Coll Cardiol 1988;11:861-866.